THE MOTION OF VORTEX LAYERS AND VORTEX FILAMENTS

by

Manhar Ramji Dhanak

A Thesis submitted for the Degree of Doctor

of Philosophy of the University of London

Department of Mathematics

Imperial College of Science and Technology

London 1980

ABSTRACT

The work in this thesis is devoted to the study of the motion of vortex layers and vortex filaments in fluids which are regarded as either inviscid or as having a small viscosity.

The first part of the thesis is concerned with the motion and stability of vortex layers in two dimensions. The growth of waves on a vortex sheet may be suppressed if the sheet is being stretched. The influence on this result of regarding the vortex sheet as having a finite thickness is examined. Also in Part I, the generalisation of Birkhoff's equation of motion of a vortex sheet to a thin layer of arbitrary vorticity distribution is considered. Hence an equation of motion of an instantaneously created vortex sheet undergoing viscous diffusion is obtained and is used to study growth of long waves on a Rayleigh layer. Higher order approximations to the equation of motion of a layer of uniform vorticity in an inviscid fluid are obtained.

The second part of the thesis deals with the motion of vortex filaments in three-dimensional flow. Two problems are considered. Firstly, the evolution of a vortex ring of elliptic configuration is determined numerically and the results are compared with those of quantitative experiments performed with smoke rings. The calculations suggest a break up of vortex rings of large initial eccentricities and this is verified by the experiments. Secondly, the interaction between an infinitely long straight vortex filament and an approaching rigid sphere is considered. The evolution of the vortex when the sphere is sufficiently far away from it is determined from linear theory and is followed up numerically for subsequent times.

ACKNOWLEDGEMENTS

I would like to express my gratitude to Professor D.W. Moore for his continual guidance and invaluable assistance throughout the course of this work. I am also indebted to Dr. B. de Bernardinis for his part in the experiments with vortex rings.

CONTENTS

CHAPTER I: GENERAL INTRODUCTION

In recent years a considerable interest has been shown in the motion and behaviour of vortices. The interest has in part been motivated by the concern over the persistence of trailing vortices behind large aircraft which constitute a hazard to other aircraft. Thus an understanding of the formation and properties of the trailing vortex system behind an aircraft is needed and has led to several studies of vortex formation and vortex interactions. A recent survey of such studies has been given by Saffman & Baker (1979).

Many unsteady fluid flows of interest, of the kind mentioned above, are characterized by low viscosity and the presence of distinct regions of high vorticity imbedded in an otherwise irrotational flow. Jets, wakes, free-shear layers and vortex rings are a few more examples of such flows. The usual source of vorticity in flows of this type is through viscous interaction with a solid boundary and subsequent ejection from the boundary in the form of a shear-layer or vortex sheet. Generally, this sheet may break up through Kelvin-Helmholtz instability or evolve in unsteady manner and roll up into a vortex filament. In any case, the vorticity away from the boundary is confined to narrow regions in the form of vortex layers or vortex filaments.

It is customary in such flows to neglect viscosity and replace the vortex layer or filament by a vortex sheet or line vortex respectively and calculate the induced flow kinematically using the Biot-Savart law. However, before this can be done, the position and shape of the layer or filament has to be determined.

The present study is concerned with the motion of vortex layers and vortex filaments. Throughout, the fluid is regarded as homogeneous and incompressible. It is also regarded as either inviscid or as having a small viscosity.

The work presented here is divided into two parts. Chapters 2-4 deal with the motion and stability of vortex layers while in Chapters 5-7, the motion of vortex filaments is considered.

The theme of the work on vortex layers in Part I has been to examine the effect on the motion and stability of a vortex sheet if it is regarded as having a finite thickness, in flow situations where the corresponding results for a sheet of zero thickness are known. A survey of calculations of the motion of a vortex sheet of zero thickness has been given by Fink & Soh (1974).

In Chapter 2, the effect of finite thickness on the stability of a stretching vortex sheet is examined by considering a simple flow model.

In Chapter 3, the generalisation of the equation of motion of a vortex sheet, as given by Birkhoff (1962), to a thin layer of arbitrary vorticity distribution is considered (in the case of a layer of uniform vorticity this has been achieved by Moore (1978)). Hence an equation of motion, valid for small times, of an instantaneously created vortex sheet undergoing viscous diffusion is obtained and used to study growth of long waves on a Rayleigh layer.

Higher order approximations to the equation of motion of a thin layer are obtained in Chapter 4 in the case of a uniform vorticity distribution in the layer. Hence an improvement to Moore's equation is obtained.

The motion of vortex filaments in Part II is studied using the 'cut-off' approximation of Crow (1970) for the velocity at a vortex. This has been successfully used before by, among others, Moore (1972) and Leonard (1974) and has been rigorously justified by Moore & Saffman (1972). The equation of motion of the filament based on this approximation is discussed in Chapter 5.

The equation is used in Chapter 6 to numerically follow the evolution of an elliptic vortex ring. Calculations are presented for various eccentricities of the initial ellipse. The results are compared with those from quantitative experiments in which the vortex rings were produced by puffing air through elliptical orifices.

In Chapter 7, the evolution of an infinitely long straight vortex filament in the presence of an approaching rigid sphere is considered. The shape of the vortex filament when the sphere is sufficiently far away from the vortex is determined approximately using linear theory. The subsequent evolution of the vortex from this shape is followed numerically. The interaction between a point source and a vortex is also discussed using the linearized form of the equation given in Chapter 5.

PART I: MOTION OF VORTEX LAYERS IN TWO-DIMENSIONS

CHAPTER 2: THE STABILITY OF AN EXPANDING CIRCULAR VORTEX LAYER

§1 Introduction

It is well known that a plane uniform vortex sheet of constant strength in an inviscid fluid is unstable; the strength of the vortex sheet is the discontinuity of tangential velocity across the sheet. Small disturbances on the vortex sheet grow exponentially with time, the ones with the shortest wavelength growing the fastest.

This violent instability can be significantly suppressed in real fluids by two possible mechanisms. One is viscous diffusion which tends to thicken the vortex sheet. The effect of finite thickness on the stability of a vortex sheet was examined by Lord Rayleigh (1896) who considered the growth of infinitesimal perturbations on a straight layer of uniform vorticity ω in an inviscid fluid. He showed that disturbances of wavenumber k grow like $\exp(\sigma t)$ where

$$\sigma^2 = \frac{\omega^2}{4}\left(\exp(-2kb) - (1-kb)^2\right) \qquad (2.1.1)$$

Here b is the thickness of the layer. The right hand side of (2.1.1) is negative if $kb > (kb)_c \approx 1.28$. Thus short waves of wavelength $\lambda = \frac{2\pi}{k}$ such that $\lambda < \lambda_c \approx 4.85b$ are not amplified. For $\lambda > \lambda_c$ waves grow exponentially.

In unsteady flows such as a rolling up vortex sheet created at sharp leading and trailing edges of lifting surfaces, the vortex sheet may undergo stretching. Stretching implies that the strength of a vortex sheet decreases with time; if the sheet is thought of as a rectilinear distribution of discrete vortices of constant strength, so that the strength of the sheet is proportional to their number density,

then stretching implies separation of these vortices. Stretching of the vortex sheet has been shown by Moore & Griffith-Jones (1974) to have a stabilising effect on the vortex sheet. They examined the stability of a uniform circular vortex sheet, which is undergoing stretching, to small disturbances in the plane of flow. The sheet is considered to be stable if all disturbances which are bounded initially remain bounded for all time. It is shown that the sheet remains stable provided the stretching rate is faster than $(\text{time})^{-\frac{1}{2}}$. The results are consistent with Saffman's (1974) heuristic treatment of the effect of stretching on the stability of a vortex sheet. Later, Moore (1976) examined the stability to two-dimensional disturbances of an arbitrary vortex sheet and considered the effect of non-uniformity of the vortex sheet.

Zakharov (1977), unaware of the work of Moore and Griffith-Jones, re-examined the stability of a uniform circular vortex sheet which is undergoing stretching, for a particular stretching rate. He found that a point vortex introduced at the centre of the expanding vortex sheet has a stabilising influence on the vortex sheet.

Moore & Griffith-Jones, in their investigation, showed that even though the vortex sheet was stable for sufficiently fast stretching rate, the amplitude of short-wave disturbances was greatly amplified. However, it is possible that in a real fluid,viscosity, by thickening the vortex sheet, damps out these short waves.

The object of this chapter is to examine the effect of finite thickness on the stability of a stretching vortex sheet in an inviscid fluid. This is achieved by studying the flow model of Moore & Griffith-Jones with the vortex sheet replaced by a uniform vortex layer. Thus a uniform circular cylindrical layer of constant vorticity is considered. The layer undergoes a radial expansion which is driven by a concentric

line source. Since the total amount of vorticity in the layer is constant, the cross-sectional area of cylindrical vortex layer must remain constant so that the thickness of the layer decreases with increase in radius.

The surfaces of the vortex layer are perturbed by small disturbances which do not vary in a direction parallel to the vortex lines so that the vortex lines are not distorted.

In §2, the equations governing the disturbances are obtained. It has not been possible to obtain exact solutions of these equations and in §3 a short-wave approximation is developed in the case when the thickness of the layer is comparable with the wavelength of the disturbances.

It is interesting to note certain observations made by Crow & Barker (1977) in an experiment to generate a vortex pair. For each vortex, they observed amplified disturbances on the rolling-up vortex sheet; the disturbances originate at the sharp edge where the sheet is created and grow on the outer portions of the vortex spiral. It was found that the wavelength of the disturbance was 2.6δ where $\delta = 4(\nu t)^{\frac{1}{2}}$. If the vortex sheet at the sharp edge was thickened, the appearance of the instability was delayed and the wavelength of the disturbance was 4.7δ. That this effect may be partly due to the stretching which the vortex sheet undergoes is revealed by a certain feature of the results obtained in §3 and is discussed there.

§2 Basic flow and stability analysis

Plane polar coordinates (r,θ) with $r = 0$ at the centre of the expanding layer and θ pointing in a fixed direction are chosen. At time t, let $R(t)$, $R_+(t)$ denote the inner and outer radii of the layer, respectively. If $\bar{u}_r$ and $\bar{u}_\theta$ are the radial and azimuthal velocity components, the equations to be satisfied by the unperturbed flow at time t are

$$\frac{1}{r}\frac{\partial}{\partial r}(r\bar{u}_\theta) = \begin{cases} \omega & R(t) < r < R_+(t) \\ 0 & \text{otherwise} \end{cases} \qquad (2.2.1)$$

and $$\frac{\partial}{\partial r}(r\bar{u}_r) = 0 \qquad r \neq 0 .$$

where ω is the constant vorticity in the layer, so that if Γ is the total circulation

$$\Gamma = \pi\omega A \qquad (2.2.2)$$

where $A = R_+^2(t) - R^2(t)$. Thus the area πA of the layer is conserved. The expansion of the layer can be considered to be due to a line source of variable strength at the origin.

The unperturbed velocity field is then given by

$$\bar{u}_r = \frac{\dot{R}R}{r} = \frac{\dot{R}_+R_+}{r}$$

$$\bar{u}_\theta = \begin{cases} 0 & r \leq R(t) \\ \Gamma(r^2-R^2)/2\pi Ar & R(t) \leq r \leq R_+(t) \\ \Gamma/2\pi r & r \geq R_+(t) \end{cases} \qquad (2.2.3)$$

where a dot denotes differentiation with respect to time. There is, of course, no discontinuity in velocity at the two surfaces of the layer.

The disturbed shapes of inner and outer surfaces of the vortex layer are taken to be of the form which preserves the area of the vortex layer, viz.,

$$\begin{aligned} r \equiv \tilde{R}(\theta,t) &= R(t)(1 + \varepsilon(t)e^{is\theta}) \\ r \equiv \tilde{R}_+(\theta,t) &= R_+(t)(1 + \mu(t)e^{is\theta}) \end{aligned} \tag{2.2.4}$$

respectively. Here, ε and μ are complex functions with $|\varepsilon|, |\mu| \ll 1$ and s is a positive integer whose values distinguish between the different modes; a general disturbance can be represented by a sum of these modes.

As the vorticity is uniform in the layer, the vorticity at any point within the layer remains unchanged and the perturbation velocity field is irrotational within the layer, the disturbance merely shifting the vortex lines in the layer. Hence the perturbation velocity field is irrotational everywhere and can be expressed by a velocity potential of the form

$$\tilde{\phi} = \begin{cases} a_1(t)r^{-s}e^{is\theta} & r > \tilde{R}_+ \\ a_2(t)r^{-s}e^{is\theta} + a_3(t)r^{s}e^{is\theta} & \tilde{R} < r < \tilde{R}_+ \\ a_4(t)r^{s}e^{is\theta} & r < \tilde{R} \end{cases} \tag{2.2.5}$$

where a_i $(i = 1,4)$ are complex functions of time. This choice of the potential ensures that the perturbation velocity field is regular everywhere.

The total velocity at a field point is then $\underline{\bar{u}} + \nabla\tilde{\phi}$ where $\nabla = \frac{\partial}{\partial r}\hat{\underline{r}} + \frac{1}{r}\frac{\partial}{\partial\theta}\hat{\underline{\theta}}$ and $\underline{\bar{u}}$ may be the analytic continuation of the basic flow from its original circular domains (as defined in (2.2.3)) into the wavy domains of the perturbed flow (as defined in (2.2.5)). The analytic continuation may be Taylor series expansions of the basic flow about points on the boundaries of the original domains.

The disturbed flow must satisfy the exact boundary conditions

$$\frac{D}{Dt}\left(r - R(t)(1 + \varepsilon(t)e^{is\theta})\right) = 0 \qquad (2.2.6)$$

and

$$\underline{u}\ (\equiv(u_r, u_\theta)) \quad \text{continuous} \qquad (2.2.7)$$

at the disturbed inner surface, with two similar conditions at the disturbed outer surface. The second condition ensures that the disturbances do not cause either a vortex sheet or a source distribution to appear at the surface, as these would violate the vorticity or the continuity equations. It ensures that the pressure is continuous across the surface, as can be seen by examining the unsteady Bernoulli equation.

Neglecting terms of order higher than $O(|\varepsilon|)$ in (2.2.6) gives

$$u_r = \dot{R} + (\dot{\varepsilon}R + \dot{R}\varepsilon + is\bar{u}_\theta(R)\varepsilon)e^{is\theta} \qquad (2.2.8)$$

But

$$u_r = \bar{u}_r(R) + (r-R)\frac{\partial \bar{u}_r(R)}{\partial r} + \ldots\ldots \left.\frac{\partial \tilde{\phi}}{\partial r}\right|_{r=R} + \ldots.$$

and $\bar{u}_r(R) = \dot{R}$

so that substituting into (2.2.8) and linearizing the equation gives

$$\left.\frac{\partial \tilde{\phi}}{\partial r}\right|_{r=R} = (R\dot{\varepsilon} + \dot{R}\varepsilon + is\bar{u}_\theta(R)\varepsilon - R\frac{\partial \bar{u}_r(R)}{\partial r}\varepsilon)e^{is\theta} \qquad (2.2.9)$$

Now, to $O(\varepsilon)$, in view of (2.2.8), u_r is continuous across the disturbed surface so that the boundary condition (2.2.7) implies the continuity of

$$u_\theta = \bar{u}_\theta(R) + R\frac{\partial \bar{u}_\theta(R)}{\partial r}\varepsilon e^{is\theta} + \frac{1}{R}\frac{\partial \tilde{\phi}}{\partial \theta}$$

But since

$$\frac{1}{r}\frac{\partial}{\partial r}(r\bar{u}_\theta) = \begin{cases} \omega & r = R + 0 \\ 0 & r = R - 0 \end{cases}$$

and $\bar{u}_\theta$ is continuous across $r = R$, we have

$$\frac{1}{R}\{\frac{\partial\tilde{\phi}}{\partial\theta}(R + 0) - \frac{\partial\tilde{\phi}}{\partial\theta}(R - 0)\} = -R\varepsilon\omega e^{is\theta} \qquad (2.2.10)$$

and from (2.2.9)

$$\frac{\partial\tilde{\phi}}{\partial r}(R \pm 0) = (R\dot{\varepsilon} + \dot{R}\varepsilon + is\bar{u}_\theta(R)\varepsilon - R\frac{\partial\bar{u}_r(R)}{\partial r}\varepsilon) \qquad (2.2.11)$$

A similar analysis at the disturbed outer surface gives three further equations, corresponding to (2.2.10)-(2.2.11), in $\tilde{\phi}$ and μ. Then substituting for $\tilde{\phi}$ from (2.2.5) and eliminating a_i $(i = 1,4)$ gives

$$\begin{aligned} &\dot{\varepsilon} + \frac{i\omega}{2}\varepsilon - \frac{i\omega}{2}(\frac{R}{R_+})^s\mu = 0 \\ &\dot{\mu} - (\frac{i\omega}{2} - \frac{i\Gamma s}{2\pi R_+^2})\mu + \frac{i\omega}{2}(\frac{R}{R_+})^s\varepsilon = 0 \end{aligned} \qquad (2.2.12)$$

Equations (2.2.12) reduce to known results in three cases,

(i) putting $R_+ = a$, a constant and $R = 0$ in the second of these equations gives the equation for a two-dimensional disturbance of a circular cylindrical vortex (Lamb, 1932, p.231).

(ii) by eliminating μ, say, from (2.2.12) and transforming the resulting equation by the substitution

$$\varepsilon(t) = \eta(t)\exp(-\frac{is\Gamma}{4\pi}\int_0^t \frac{dt'}{R_+^2(t')}) \qquad (2.2.13)$$

gives

$$\ddot{\eta} - \frac{2s\dot{R}v}{R}\dot{\eta} + \eta\left[\frac{\omega^2}{4}\left((1-vs)^2 - (1-2v)^s\right) + \frac{i\omega v^2\dot{R}}{R}s(s-2)\right] = 0 \qquad (2.2.14)$$

where $v = \dfrac{A}{2R_+^2}$.

By taking the limit $R \to R_+$ in (2.2.14), the equation governing perturbations on a uniform expanding vortex sheet, as given by Moore & Griffith-Jones is recovered.

(iii) If $\dot{R} = 0$, then (2.2.14) reduces to the equation governing small perturbations on a non-stretching uniform circular vortex layer and is in agreement with the result obtained for this case by Zakharov (1977).

From (2.2.12), it can be shown that

$$\mu = \pm\eta^* \exp\left(-\frac{is\Gamma}{4\pi}\int_0^t \frac{dt'}{R_+^2(t')}\right) \qquad (2.2.15)$$

where the asterisk denotes complex conjugate. Thus, in view of (2.2.4), the disturbed surfaces are given by

$$r = R\left(1 + |\eta|\exp\left[is\left(\theta - \frac{\Gamma}{4\pi}\int_0^t \frac{dt'}{R_+^2(t')}\right) + i\alpha(t)\right]\right)$$

$$r = R_+\left(1 \pm |\eta|\exp\left[is\left(\theta - \frac{\Gamma}{r\pi}\int_0^t \frac{dt'}{R_+^2(t')}\right) - i\alpha(t)\right]\right) \qquad (2.2.16)^\dagger$$

Thus, since $\dot{\theta} = 0$ at the inner surface and $\dot{\theta} = \Gamma/2\pi R_+^2$ at the outer surface, it follows that the disturbances on the two surfaces travel in opposite direction with equal phase speed.

---

†Here $e^{i\alpha(t)} = \eta/|\eta|$

It may be noted from (2.2.14) that when s = 2, so that the surfaces of the vortex layer are distorted into ellipses of small eccentricity, a motion in which this shape rotates with angular velocity $\Gamma/4\pi R_+^2$ is possible. A similar result was obtained by Moore & Griffith-Jones for the expanding vortex sheet. The result is analogous to Kirchoff's well-known solution for a rotating elliptical vortex core.

It has not been possible to find an analytic solution of (2.2.14) for $s \neq 2$, even in the case where the radius is a function of time of the form considered by Moore & Griffith-Jones, viz.,

$$R(t) = R_0(1 + at)^n \qquad (2.2.17)$$

where $R_0(>0)$ is the initial radius and a and n are arbitrary constants assumed positive for an expanding radius which does not become zero for $t \geq 0$.

However, in the case of short waves of wavelength comparable to the thickness of the layer, it is possible to obtain an approximate solution to (2.2.14) for a general R(t) using the WKB method. This is developed in §3.

§3 Short waves of wavelength comparable to initial layer thickness

For a layer of thickness $b(t) = R_+(t) - R(t)$ small compared with $R_1(t) = \frac{1}{2}(R_+ + R_-)$, it is proposed to solve (2.2.14) approximately in the case when the wavelength of the disturbance $2\pi R_1(t)/s$ is of the same order as $b(t)$. To be specific let

$$\begin{aligned} s &= ms_1 \\ b(t) &= b_1(t)/m \end{aligned} \tag{2.3.1}$$

where m is a large parameter and R_1/b_1 is of the same order as s_1 so that

$$\beta(t) = \frac{sb(t)}{R_1(t)} = \frac{s_1 b_1(t)}{R_1(t)} = O(1) \tag{2.3.2}$$

Then, in (2.2.14)

$$v = \frac{R_1 b}{(R_1 + b/2)^2} = \frac{\beta}{ms_1}\left(1 - \frac{\beta}{ms_1} + O\left(\frac{1}{m^2 s_1^2}\right)\right)$$

and

$$(1-2v)^s = \left(1 - \frac{2\beta}{ms_1}\right)^{ms_1} = e^{-2\beta}\left(1 + \frac{\beta^2}{ms_1} + O\left(\frac{1}{m^2 s_1^2}\right)\right)$$

so that (2.2.14) is approximately given by

$$\ddot{\eta} - \frac{2\dot{R}_1\beta}{R_1}\dot{\eta} + \eta[m^2 s_1^2 \Phi_0 + O(m s_1)] = 0 \tag{2.3.3}$$

where

$$\Phi_0 = \frac{\Gamma^2}{16\pi^2 R_1^4 \beta^2}\left((1-\beta)^2 - e^{-2\beta}\right) \tag{2.3.4}$$

An approximate solution to (2.3.4) for large m is then given by the WKB method as

$$\eta \sim \frac{C}{\Phi_0^{\frac{1}{4}}} \exp\left(is \int_0^t \Phi_0^{\frac{1}{2}}(t')dt' \right) + \frac{D}{\Phi_0^{\frac{1}{4}}} \exp\left(-is \int_0^t \Phi_0^{\frac{1}{2}}(t')dt' \right) \quad (2.3.5)$$

where $s = ms_1$ is now written. The expression Φ_0 is analogous to the dispersion relation (2.1.1) governing the growth of waves on a straight uniform non-stretching vortex layer; indeed if $\dot{R} = 0$, (2.1.1) is recovered in the above approximation.

The approximate solution (2.3.5) is valid only if

$$s^2 >> \Phi_0^{-\frac{3}{4}} \frac{d^2}{dt^2} \Phi_0^{-\frac{1}{4}} \quad (2.3.6)$$

(Olver (1961)). Thus, in general (2.3.5) is true for a restricted range of values of t. In particular, it is not valid at such times as when Φ_0 vanishes.

As remarked in §1, Φ_0 vanishes when $\beta = \beta_c \simeq 1.28$, i.e. when the wavelength of the disturbance is 4.85 times the thickness of the layer. For an expanding vortex layer, $\beta(t)$ is a monotonically decreasing function so that if $\beta(0) > \beta_c$, Φ_0 will vanish at a finite time $t = t_c$, such that $\beta(t_c) = \beta_c$, and (2.3.5) will not be valid near $t = t_c$. Also since Φ_0 is positive for $t < t_c$ and negative for $t > t_c$, the essential character of the solution (2.3.5) for $t << t_c$ and $t >> t_c$, when it is valid, will differ. The connection formulae relating the solution in these two ranges of time can be obtained and the transition solution near $t = t_c$ determined by standard methods.

Thus for $\beta(0) > \beta_c$

$$\eta \sim \begin{cases} \dfrac{c}{(\Phi_0)^{\frac{1}{4}}} \cos\left(s \int_t^{t_c} (\Phi_0(t'))^{\frac{1}{2}} dt' + \dfrac{\pi}{4} - \alpha\right) & t << t_c \\ c\left(\dfrac{s\pi^3}{\dot{\Phi}_0(t_c)}\right)^{1/6} \left\{\cos(\alpha) B_i(z) + \sin(\alpha) A_i(z)\right\} & t \sim t_c \\ \dfrac{c}{(-\Phi_0)^{\frac{1}{4}}} \left\{\cos(\alpha) \exp\left(s \int_{t_c}^{t} (-\Phi_0(t'))^{\frac{1}{2}} dt'\right) + \sin(\alpha) \exp\left(-s \int_{t_c}^{t} (-\Phi_0(t'))^{\frac{1}{2}} dt'\right)\right\} & t >> t_c \end{cases} \tag{2.3.7}$$

where c and α are arbitrary constants, $-\pi < \alpha \leq \pi$, A_i and B_i are the Airy functions and

$$z = (s\dot{\Phi}_0)^{2/3}(t - t_c) \tag{2.3.8}$$

The approximate solution (2.3.7) holds provided (2.3.6) is satisfied.

For $\beta(0) < \beta_c$, the approximate solution for η is given by

$$\eta(t) \sim \frac{D}{(-\Phi_0)^{\frac{1}{4}}} \cosh\left(\int_0^t s(-\Phi_0(t'))^{\frac{1}{2}} dt' + \alpha_1\right) \tag{2.3.9}^{\dagger}$$

which holds provided (2.3.6) is satisfied.

In the power law case (2.2.17), the right hand side of (2.3.6) is uniformly bounded for $t > t_c$ only if $n \leq \frac{1}{2}$. Accordingly, (2.3.7) for $t >> t_c$ and (2.3.9) will hold for a restricted range of values of t if $n > \frac{1}{2}$. However, for large t the thickness of the vortex layer is very small and the motion may be modelled by replacing the vortex layer by a vortex sheet and Moore & Griffith-Jones have shown that in this case for $n > \frac{1}{2}$ the perturbations on the sheet grow algebraically.

In view of (2.3.7) and (2.3.9), the final amplitude of the disturbance as $t \to \infty$ is greater than the amplitude at $t = T$, where $T = 0$ if $\beta(0) < \beta_c$ and $T = t_c$ if $\beta(0) > \beta_c$, by a factor of order

---

†Here D and α_1 are arbitrary constants.

$$\exp\left[\frac{s\Gamma}{4\pi}\int_{T}^{\infty}\frac{1}{R_1^2\beta}\left(e^{-2\beta}-(1-\beta)^2\right)^{\frac{1}{2}}dt'\right] . \qquad (2.3.10)$$

This is an extension to the corresponding result obtained by Moore & Griffith-Jones and allows for the thickness of the vortex layer.

The solutions (2.3.7) for $t \gg t_c$ and (2.3.9) can be expressed as in Moore & Griffith-Jones in a way which enables it to be applied more generally. If U(t) is the jump in tangential velocity across the layer of uniform vorticity ω at time t, and there are $p/2\pi$ complete waves on a length of the vortex containing unit circulation, then to leading order the amplitude of the disturbance is proportional to

$$\exp\left[\frac{\omega}{2}\int_{T}^{t}\left(e^{-pU^2(t')/\omega}-\left(1-\frac{pU^2(t')}{\omega}\right)^2\right)^{\frac{1}{2}}dt'\right] \qquad (2.3.11)$$

where T is as in (2.3.10). This result is valid only for waves on a circular uniform vortex layer of non-constant strength when the wavelength of the waves is comparable to U/ω. However, it is possible that the result is true for any uniform vortex layer. When the vortex layer is not uniform (2.3.11) will require modification in view of the results obtained by Moore (1976) for waves on a non-uniform vortex sheet. In particular the vorticity ω would need to be determined at each instant of time.

It is interesting to note that Φ_0 in (2.3.7, 9) is a maximum at $t = t_m$ when $\beta = \beta_m \simeq 0.634$. Since the area of the vortex layer remains constant, $b(t) = b_0R_0/R_1(t)$, where b_0 and R_0 are initial values of b and R_1, so that $\beta(t) = sb_0R_0/R_1^2(t)$. Thus at $\beta = \beta_m$, the wavelength of the disturbance $\lambda_m = 2\pi R_1(t_m)/s$ is

$$\lambda_m = \frac{2\pi R_0}{\beta_m R_1(t_m)}\, b_0$$

If the initial thickness was fb_0, where $f > 1$, then

$$\lambda_m = \frac{2\pi R_0 f}{\beta_m R_1(t_m)} b_0$$

so that the ratio λ_m/b_0 is greater in this case. Also, the value of t_m in this case will be greater. If we assume that, in experiments, the waves on a stretching vortex layer are first observed when they have a wavelength λ_m, then these results would partly explain the observations of Crow & Barker (1977) described in §1, although the vorticity distribution in the layer is not uniform in the experiments nor is the flow laminar when the vortex layer is thickened.

CHAPTER 3: EQUATION OF MOTION OF A THIN VORTEX LAYER

§1 Introduction

Many incompressible fluid flows at high Reynolds number are characterized by thin vortex layers, surrounded by irrotational flow. It is usual in such flows to neglect viscosity and replace the vortex layer by a vortex sheet. If the instantaneous position of the vortex sheet can be determined, then the flow can be calculated using the Biot-Savart line integral.

A convenient formulation of the motion of a vortex sheet in an inviscid fluid in two-dimension has been given by Birkhoff (1962). If Γ denotes the net vorticity between one end of the sheet and a point, with complex coordinate z, on the sheet, then the equation of motion, can be written in parametric form as $z = z(\Gamma,t)$ where z satisfies

$$\frac{\partial z^*}{\partial t}(\Gamma,t) = -\frac{i}{2\pi} \fint_0^{\Gamma_e} \frac{d\Gamma'}{z(\Gamma,t) - z(\Gamma';t)} \qquad (3.1.1)$$

where $\fint$ denotes Cauchy principal value integral and Γ_e is the total circulation in the sheet. Equation (3.1.1) reduces the problem of calculating the position of the vortex sheet to a marching problem in time and would therefore seem suitable for numerical treatment. However, invariably chaotic behaviour results and the solutions are sensitive to time step and discretization procedures used. It is possible that this behaviour is a manifestation of the Helmholtz instability of the vortex sheet discussed in Chapter 2.

Recently Moore (1978) (henceforth referred to as (M)) has generalised the Birkhoff equation to a thin vortex layer of uniform vorticity in the hope (unrealized) that this may overcome the difficulty.

In this chapter the case when the vorticity is non-uniform is considered. The vorticity is required to decay exponentially away from the centroid line C (defined in §2) of the distribution. The free vortex layer is regarded as a double-sided boundary layer on an evolving space curve C whose equation of motion is sought.

The method of solution is as in (M). Thus an 'outer' problem based on flow at a large distance from C due to a vortex sheet at C is posed. The solution to this is matched to an 'inner' solution for the flow in the vicinity of C. An expansion in terms of the small ratio(ϵ) of a typical vortex layer thickness to a typical radius of curvature of C is developed.

In §2 the intrinsic coordinate system used is described and the equations of motion established. In §3, assuming that the vorticity distribution $\bar{\omega}$ is instantaneously known, an inner approximation to the flow field is obtained in terms of $\bar{\omega}$.

In evaluating the outer flow only the mean properties of the vortex layer, such as the curvature of C and the circulation density of the equivalent vortex sheet are required and the actual details of the vorticity distribution do not matter. Hence the outer solution is identical to that found in (M) and the results are summarised in §4.

In §5, the outer solution is matched to the inner solution to obtain an equation of motion of C in terms of the unknown vorticity distribution $\bar{\omega}$.

The determination of $\bar{\omega}$ is discussed in §6. It is found that for the leading order correction to Birkhoff equation (3.1.1), the equation for $\bar{\omega}$ reduces to the boundary layer equation and does not lead to any further simplification. Thus, in general, the determination of $\bar{\omega}$ remains an unsolved problem. In §7, the equations obtained in §§5,6 are used to study growth of long waves on an initially straight vortex layer of arbitrary vorticity distribution in an inviscid fluid; the

results are in agreement with Drazin & Howard (1962) and provide a useful check for the equations.

In §8, a solution for $\bar{\omega}$, valid for small times, is found for the case of an instantaneously created arbitrary vortex sheet undergoing viscous diffusion. Hence an equation of motion for such a sheet is obtained. The equation is used to study long waves on a Rayleigh layer.

Wherever possible, the notation used in (M) is retained.

The equation of motion of the vortex layer in terms of the unknown vorticity distribution $\bar{\omega}$ is given by (3.5.19). The equation retains the simplicity of the vortex sheet model, while incorporating finite thickness effects approximately. In §9, a simple interpretation of the equation in terms of forces acting on an element of the vortex layer is given (the reader may wish to consider this interpretation first).

A modification to Kirchoff's invariant for a vortex sheet is obtained in Appendix C; it allows for viscous dissipation.

§2 Preliminaries

In this section the equations of motion for the flow in the immediate vicinity of the vortex layer are established. The intrinsic coordinate system to be used here was introduced in (M) and is briefly described below.

Let s be the arc-distance measured along a plane curve C; C will be identified with the centroid line of the vorticity distribution. Let P be a point close enough to C for there to be a unique normal from P to C. Let the normal meet C at O. Then, in a frame $\overline{OXY}$, fixed relative to flow at infinity, the position of P at time t is given by

$$\underline{r}(P) = \underline{R}(s,t) + n\hat{\underline{n}}(s,t) \tag{3.2.1}$$

where $\underline{R}(s,t)$ refers to the point O, n is the distance OP and $\hat{\underline{n}}(s,t)$ is the unit normal at O; $\hat{\underline{n}}(s,t)$ points to the left as C is traversed in the increasing s direction (n is positive in the positive $\hat{\underline{n}}(s,t)$ direction).

Differentiation of (3.2.1) and use of Serret-Frenet formulae for plane curves leads to

$$\underline{dr} = \hat{\underline{s}}(1 - \frac{n}{\rho})ds + \hat{\underline{n}}dn \tag{3.2.2}$$

where $\rho(s,t)$ is the radius of curvature of C at O and

$$\hat{\underline{s}} = \frac{\partial \underline{R}}{\partial s} , \tag{3.2.3}$$

$\hat{\underline{s}}(s,t)$ is the unit tangent at O. Hence the coordinate system is orthogonal with line elements $h_1 ds$ and $h_2 dn$ where

$$\begin{aligned} h_1 \equiv h &= 1 - \frac{n}{\rho} \\ h_2 &= 1 \end{aligned} \tag{3.2.4}$$

If $\underline{\bar{u}}(P)$ is the fluid velocity in $\overline{OXY}$ frame at P at time t, then define relative velocity (u,v) in (s,n) system by

$$\underline{\bar{u}}(P) = \frac{\partial \underline{R}}{\partial t} + n \frac{\partial \hat{\underline{n}}}{\partial t} + u\hat{\underline{s}} + v\hat{\underline{n}} \tag{3.2.5}$$

and since

$$\frac{\partial \hat{\underline{n}}}{\partial t}(s,t) = -\Omega(s,t)\hat{\underline{s}} , \tag{3.2.6}$$

where $\Omega(s,t)$ is the angular velocity of the frame $(\hat{\underline{s}},\hat{\underline{n}})$ at a point with fixed s, (3.2.5) can be written

$$\underline{\bar{u}}(P) = (\hat{\underline{s}} \cdot \frac{\partial \underline{R}}{\partial t} - \Omega n + u)\hat{\underline{s}} + (\hat{\underline{n}} \cdot \frac{\partial \underline{R}}{\partial t} + v)\hat{\underline{n}} \tag{3.2.7}$$

From (M 2.7-2.9), the continuity equation in the (s,n) coordinates is

$$\frac{\partial u}{\partial s} + \frac{\partial}{\partial n}(hv) = n \frac{\partial \Omega}{\partial s} \tag{3.2.8}$$

and the vorticity is given by

$$\text{curl } \underline{\bar{u}} = \frac{\hat{\underline{z}}}{h}(\frac{\partial v}{\partial s} - \frac{\partial}{\partial n}(hu)) + 2\Omega\hat{\underline{z}} , \tag{3.2.9}$$

where $\hat{\underline{z}}$ is the unit vector normal to the plane of flow.

Let

$$\text{curl } \underline{\bar{u}} = \bar{\omega}(\bar{x},\bar{y},\bar{t})\hat{\underline{z}} \tag{3.2.10}$$

in a coordinate system $\overline{Oxy}$ fixed with respect to flow at infinity. Then $\bar{\omega}$ satisfies

$$\frac{\partial \bar{\omega}}{\partial \bar{t}} + (\underline{\bar{u}}.\hat{\underline{x}})\frac{\partial \bar{\omega}}{\partial \bar{x}} + (\underline{\bar{u}}.\hat{\underline{y}})\frac{\partial \bar{\omega}}{\partial \bar{y}} = \bar{\nu}(\frac{\partial^2 \bar{\omega}}{\partial \bar{x}^2} + \frac{\partial^2 \bar{\omega}}{\partial \bar{y}^2}) \tag{3.2.11}$$

where $\hat{\underline{x}}$, $\hat{\underline{y}}$ are unit vectors in the $\overline{OX}$, $\overline{OY}$ directions and $\bar{\nu}$ is the kinematic viscosity. To make the transformation to s,n,t variables, we note that if

$$\underline{r} = (\bar{x},\bar{y}),$$

then it follows from (3.2.1) that

$$\begin{aligned} \bar{x} &= \hat{\underline{x}}.\underline{R}(s,t) + n\hat{\underline{x}}.\hat{\underline{n}} \\ \bar{y} &= \hat{\underline{y}}.\underline{R}(s,t) + n\hat{\underline{y}}.\hat{\underline{n}} \\ \bar{t} &= t \end{aligned} \tag{3.2.12}$$

so that the Jacobian of the transformation is

$$\begin{aligned} J &= h((\hat{\underline{x}}.\hat{\underline{n}})(\hat{\underline{y}}.\hat{\underline{s}}) - (\hat{\underline{y}}.\hat{\underline{n}})(\hat{\underline{x}}.\hat{\underline{s}})) \\ &= -h \end{aligned}$$

After substituting for $\bar{\underline{u}}$ from (3.2.7), the transformed vorticity equation becomes

$$\frac{\partial\bar{\omega}}{\partial t} + \frac{u}{h}\frac{\partial\bar{\omega}}{\partial s} + v\frac{\partial\bar{\omega}}{\partial n} = \frac{\bar{\nu}}{h}\left(\frac{\partial}{\partial n}\left(h\frac{\partial\bar{\omega}}{\partial n}\right) + \frac{\partial}{\partial s}\left(\frac{1}{h}\frac{\partial\bar{\omega}}{\partial s}\right)\right) \tag{3.2.13}$$

or, on using the continuity equation (3.2.8),

$$\frac{\partial\bar{\omega}}{\partial t} + \frac{1}{h}\left(\frac{\partial}{\partial s}(\bar{\omega}u) + \frac{\partial}{\partial n}(h\bar{\omega}v) - \bar{\omega}n\frac{\partial\Omega}{\partial s}\right) = \frac{\bar{\nu}}{h}\left(\frac{\partial}{\partial n}\left(h\frac{\partial\bar{\omega}}{\partial n}\right) + \frac{\partial}{\partial s}\left(\frac{1}{h}\frac{\partial\bar{\omega}}{\partial s}\right)\right) \tag{3.2.14}$$

The plane curve C given by

$$\underline{r} = \underline{R}(s,t)$$

in the fixed frame $\overline{Oxy}$ will now be defined. We have

$$\bar{\omega}(s,n,t) = \bar{\omega}(\underline{R}(s,t) + n\hat{\underline{n}}(s,t),t)$$

$\underline{R}(s,t)$ is chosen so that uniformly in s and t, $\bar{\omega}$ decays exponentially as $n \to \pm\infty$ and

$$\int_{-\infty}^{\infty} \bar{\omega} n dn = 0 \tag{3.2.15}$$

This choice of C ensures that most of the vorticity lies in a thin layer containing C. The crucial advantage of this choice becomes apparent when the circulation in the layer is considered.

For the circulation in the layer between the normal through a typical point O(s,t) on C and the end s = 0 of the layer is

$$\Gamma(s,t) = \int_0^s \int_{-\infty}^{\infty} \bar{\omega} h dn ds$$

i.e., on substituting for h from (3.2.4)

$$\Gamma(s,t) = \int_0^s \int_{-\infty}^{\infty} \bar{\omega} dn ds - \int_0^s \int_{-\infty}^{\infty} \frac{\bar{\omega} n}{\rho(s,t)} dn ds$$

so that in view of (3.2.15)

$$\Gamma(s,t) = \int_0^s \int_{-\infty}^{\infty} \bar{\omega} dn ds \tag{3.2.16}$$

Hence, the circulation density is

$$\gamma(s,t) = \frac{\partial \Gamma}{\partial s} = \int_{-\infty}^{\infty} \bar{\omega} dn \tag{3.2.17}$$

An equation of $\gamma(s,t)$ can be obtained by multiplying (3.2.14) by h and integrating across the width of the layer. For

$$\frac{\partial}{\partial t} \int_{-\infty}^{\infty} \bar{\omega}(1 - \frac{n}{\rho}) dn + \frac{\partial}{\partial s} \int_{-\infty}^{\infty} (dn \bar{\omega} u) - \{ \frac{\partial \Omega}{\partial s} - \frac{\partial}{\partial t} (\frac{1}{\rho}) \} \int_{-\infty}^{\infty} \bar{\omega} n dn$$

$$- \bar{\nu} \frac{\partial}{\partial s} \int_{-\infty}^{\infty} (dn(1 - \frac{n}{\rho})^{-1} \frac{\partial \bar{\omega}}{\partial s}) + [(1 - \frac{n}{\rho}) \bar{\omega} v - \bar{\nu} h \frac{\partial \bar{\omega}}{\partial n}]_{-\infty}^{\infty} = 0$$

where h has been substituted by the expression (3.2.4). Now $\bar{\omega}$ and $\frac{\partial\bar{\omega}}{\partial n}$ vanish at $\pm\infty$ so that on using equation (3.2.15),

$$\frac{\partial\gamma}{\partial t} + \frac{\partial}{\partial s}(U_c\gamma) = \bar{\nu}\frac{\partial}{\partial s}\int_{-\infty}^{\infty}(1-\frac{n}{\rho})^{-1}\frac{\partial\bar{\omega}}{\partial s}\,dn \qquad (3.2.18)$$

provided

$$U_c\int_{-\infty}^{\infty}\bar{\omega}dn = \int_{-\infty}^{\infty}\bar{\omega}udn \qquad (3.2.18a)$$

where U_c is the convection velocity. Equations (3.2.18), (3.2.18a) generalise equation (3.2.32) in (M) to the non-uniform vorticity case. Note that for the inviscid case, the right hand side of (3.2.18) vanishes and we have a conservation equation for $\gamma(s,t)$.

Further, we need an invariant of motion based on the definition of the centroid line, (3.2.15),

$$0 = \frac{\partial}{\partial t}\int_{-\infty}^{\infty}\bar{\omega}ndn$$

$$= \int_{-\infty}^{\infty} n\frac{\partial\bar{\omega}}{\partial t}\,dn$$

so that on substituting for $\frac{\partial\bar{\omega}}{\partial t}$ from (3.2.14),

$$0 = -\int_{-\infty}^{\infty}\{\frac{n}{h}(\frac{\partial}{\partial s}(\bar{\omega}u) + \frac{\partial}{\partial n}(h\bar{\omega}v) - \bar{\omega}n\frac{\partial\Omega}{\partial s} - \bar{\nu}(\frac{\partial}{\partial n}(h\frac{\partial\bar{\omega}}{\partial n}) + \frac{\partial}{\partial s}(\frac{1}{h}\frac{\partial\bar{\omega}}{\partial s}))\,dn.$$

i.e., after integrating by parts,

$$0 = \int_{-\infty}^{\infty}\{\frac{n}{h}(\frac{\partial}{\partial s}(\bar{\omega}u) - \bar{\omega}n\frac{\partial\Omega}{\partial s} - \bar{\nu}\frac{\partial}{\partial s}(\frac{1}{h}\frac{\partial\bar{\omega}}{\partial s})) - \frac{\bar{\omega}v}{h} - \frac{\overline{\nu\omega}}{\rho h^2}\}dn \qquad (3.2.19)$$

where $\rho(s,t)$ is the local radius of curvature of C. For a layer with a straight centroid line C and $h \to 1$, (3.2.19) reduces to

$$0 = \frac{\partial}{\partial s}(\int_{-\infty}^{\infty}\bar{\omega}undn) - \int_{-\infty}^{\infty}\bar{\omega}vdn \qquad (3.2.20)$$

using $\rho = \infty$ and $\frac{\partial \Omega}{\partial s} = 0$. The viscous terms vanish in view of (3.2.15).

If at any time t, the vorticity distribution $\bar{\omega}(s,n,t)$ is known everywhere, then equations (3.2.8), (3.2.9), (3.2.18) and (3.2.19) enable us to determine the flow in the neighbourhood of the centroid line C. The details are pursued in §3 for a given vorticity distribution $\bar{\omega}(s,n,t)$.

§3 The inner flow

In this section the velocity field in the neighbourhood of the centroid line C will be determined, given that the instantaneous vorticity distribution is $\bar{\omega}(s,n,t)$.

We assume that $\bar{\omega}$ decays at least as fast as

$$\exp\left(-\left|\frac{n}{\beta_{\pm}}\right|\right) \qquad \text{as } n \to \pm\infty \quad , \tag{3.3.1}$$

so that the scale of $\beta_{\pm}(s,t)$ gives a measure of the thickness of the vortex layer. To ensure that the layer is thin, we must have, uniformly in s,

$$|\beta_{\pm}(s,t)/\rho(s,t)| \leq \varepsilon \tag{3.3.2}$$

where ρ is the radius of curvature of C at position s and $\varepsilon \ll 1$.

It is proposed to determine the flow velocities as an expansion in powers of ε.

The flow in the vicinity of the curve C will be referred to as the inner flow. To study the inner flow, it is suitable to use the scaled variables

$$x = s, \qquad y = \varepsilon^{-1} n \tag{3.3.3}$$

Then, the procedure is to expand the unknown fluid velocity $\underline{\bar{u}}$ in powers of ε. The expansion will hold in the immediate vicinity of the curve C, i.e. for $|n| \ll |\rho|$.

However the velocity of the centroid line C is not known, so we must introduce the expressions

$$\begin{aligned} \frac{\partial \underline{R}}{\partial t}(s,t) \equiv \underline{W}(s,t) &= \underline{W}_0(x,t) + \varepsilon \underline{W}_1(x,t) + \ldots\ldots \\ -\frac{\partial \underline{\hat{n}}}{\partial t}(s,t) \equiv \Omega(s,t)\underline{\hat{s}} &= (\Omega_0(x,t) + \varepsilon\Omega_1(x,t) + \ldots\ldots)\underline{\hat{s}} \end{aligned} \tag{3.3.4}$$

as well as

$$u(s,n,t) = u_0(x,y,t) + \varepsilon u_1(x,y,t) + \varepsilon^2 u_2(x,y,t) + \ldots\ldots$$

and (3.3.5)

$$v(s,n,t) = \varepsilon v_1(x,y,t) + \varepsilon^2 v_2(x,y,t) + \ldots\ldots$$

The absence of v_0 reflects the fact that, to leading order, the layer is straight. We define a scaled vorticity by

$$\varepsilon^{-1}\omega(x,y,t) = \bar{\omega}(s,n,t) \tag{3.3.6}$$

On substituting the velocity expansions into the kinematic vorticity equation and comparing terms of order ε^{-1}, ε^0, ε, ... gives

$$\begin{aligned} -\frac{\partial u_0}{\partial y} &= \omega(x,y,t) \\ -\frac{\partial u_1}{\partial y} &= -(2\Omega_0 + \frac{u_0}{\rho}) \\ \frac{\partial v_1}{\partial x} - \frac{\partial u_2}{\partial y} &= -(2\Omega_0 + \frac{u_1}{\rho} + \frac{y}{\rho 2}\, u_0) \\ &- - - - - - - - - - - - - - - - - - \end{aligned} \tag{3.3.7}$$

Hence,

$$u_0 = -\int_{-\infty}^{y} \omega dy + \bar{u}_0(x,t) \tag{3.3.8}$$

and

$$u_1 = (2\Omega_0 + \frac{\bar{u}_0}{\rho})y - \frac{1}{\rho}\int_{-\infty}^{y} dy_1 \int_{-\infty}^{y_1} \omega dy_2 + \bar{u}_1 \tag{3.3.9}$$

where $\bar{u}_0(x,t)$, $\bar{u}_1(x,t)$ are arbitrary, to be determined later on by matching. Taking the lower limit of the integrals in (3.3.8), (3.3.9) and in (3.3.11) below, is justified in view of the exponential decay of the integrand as $y \to -\infty$. Further terms of order ε^2 and higher are not calculated here since it is intended to obtain only a first order correction to Birkhoff's equation to allow for the vorticity distribution.

On expressing the continuity equation in terms of the scaled variables and substituting the velocity expansions (3.3.5) in, gives

$$\frac{\partial u_0}{\partial x} + \frac{\partial v_1}{\partial y} = 0$$

$$\frac{\partial u_1}{\partial x} + \frac{\partial v_2}{\partial y} = y\frac{\partial \Omega_0}{\partial x} + \frac{v_1}{\rho} - \frac{y}{\rho_0}\frac{\partial u_0}{\partial x} \qquad (3.3.10)$$

- - - - - - - - - - - - - - - - - - -

Here, v is only required to leading order so that using the expression for u_0 from (3.3.9),

$$v_1 = \int_{-\infty}^{y} dy_1 \frac{\partial}{\partial x}\int_{-\infty}^{y_1} \omega dy_2 - y\frac{\partial \bar{u}_0}{\partial x} + \bar{v}_1(x,t) \qquad (3.3.11)$$

$\bar{v}_1$ will be determined below. Note that $\bar{u}_0$, $\bar{u}_1$ and $\bar{v}_1$ are terms independent of y in the expression for the relative velocity at $-\infty$ and therefore differ from the corresponding functions in (M).

On rewriting equation (3.2.19) in terms of the scaled variables and substituting the expansions (3.3.5) and expressions (3.3.6), (3.3.7) in $O(\varepsilon)$ terms give,

$$0 = \frac{\partial}{\partial x}\int_{-\infty}^{\infty} yu_0\omega dy - \int_{-\infty}^{\infty} \omega v_1 dy \qquad (3.3.12)$$

which is the same as (3.2.20), as it must be since to leading order the centroid line of the vortex layer is straight.

Inserting the expressions for u_0, v_1 from (3.3.8) and (3.3.11) into (3.3.12) gives

$$0 = \frac{\partial}{\partial x}\int_{-\infty}^{\infty} \omega y\{-\int_{-\infty}^{y} \omega dy_1 + \bar{u}_0(x,t)\}dy - \int_{-\infty}^{\infty} \omega\{\int_{-\infty}^{y} dy_1 \frac{\partial}{\partial x}\int_{-\infty}^{y_1} \omega dy_2$$

$$- y\frac{\partial \bar{u}_0}{\partial x} + \bar{v}_1(x,t)\}dy$$

so that, since

$$\int_{-\infty}^{\infty} \omega y dy = 0$$

(c.f. (3.2.15)),

$$\bar{v}_1 \gamma = -\frac{\partial}{\partial x} \int_{-\infty}^{\infty} \omega y \int_{-\infty}^{y} \omega dy_1 dy - \int_{-\infty}^{\infty} dy \omega \int_{-\infty}^{y} dy_1 \frac{\partial}{\partial x} \int_{-\infty}^{y_1} \omega dy_2 \qquad (3.3.13)$$

where

$$\gamma(x,t) = \int_{-\infty}^{\infty} \omega dy \ ,$$

as defined in (3.2.17). After a little algebra,

$$\bar{v}_1 = -\frac{1}{\gamma(x,t)} \frac{\partial}{\partial x} \int_{-\infty}^{\infty} \Delta(\gamma(x,t) - \Delta) dy \qquad (3.3.14)$$

where

$$\Delta(x,y,t) = \int_{-\infty}^{y} \omega dy$$

The relative flow velocities, to $O(\varepsilon)$, near the curve C are now determined except for the arbitrary functions $\bar{u}_0$, $\bar{u}_1$; these would be determined, once the boundary conditions as $y \to \pm\infty$ are made available. In §4 an 'outer' flow, valid for $|n| >> |\beta_{\pm}(s,t)|$, is obtained. By matching the outer flow solution in the limit $n \to 0_{\pm}$ with the inner solution in the limit $y \to \pm\infty$, the arbitrary functions of x and t which appear both in the inner and outer solutions are determined. This is done in §5.

For later use, an approximate expression for the velocity of convection of vorticity, U_c, will now be derived. From (3.2.18a), and using (3.3.3), (3.3.5) and (3.3.6)

$$\gamma U_c = \int_{-\infty}^{\infty} \bar{\omega} u dn$$

$$= \int_{-\infty}^{\infty} \omega \{u_0 + \varepsilon u_1 + \varepsilon^2 u_2 + \ldots\} dy$$

On substituting for u_0, u_1 from (3.3.8)-(3.3.9)

$$\gamma U_c = \int_{-\infty}^{\infty} \omega[- \int_{-\infty}^{y} \omega dy_1 + \bar{u}_0]dy + \varepsilon \int_{-\infty}^{\infty} \omega[(2\Omega_0 + \frac{\bar{u}_0}{\rho})y - \frac{1}{\rho} \int_{-\infty}^{y} dy_1 \int_{-\infty}^{y_1} \omega dy_2]dy$$

$$+ O(\varepsilon^2)$$

and after using (3.2.15) and integrating by parts,

$$U_c = (-\tfrac{1}{2}\gamma + \bar{u}_0) - \frac{\varepsilon}{\gamma\rho} \int_{-\infty}^{\infty} \Delta(\gamma-\Delta)dy + \varepsilon \bar{u}_1 + O(\varepsilon^2) \qquad (3.3.15)$$

where Δ is as in (3.3.14).

§4 The outer flow

In the outer region, i.e. for $|n| >> |\beta_{\pm}(s,t)|$, in view of the exponential decay (3.3.1), the vorticity is negligible and the flow is therefore effectively irrotational. It will be characterized by the mean properties of the vortex layer and will be insensitive to the actual details of the vorticity distribution. Hence, with the appropriate definitions of the position of the equivalent vortex sheet C and the circulation density $\gamma(s,t)$, the outer solution will be identical with that given in (M). The results obtained there are summarised below.

Let $Z(s,t)$ be the complex parametric equation of the centroid line C where

$$Z(s,t) = \underline{R}(s,t).\hat{\underline{x}} + i\underline{R}(s,t).\hat{\underline{y}} \tag{3.4.1}$$

with $\underline{R}(s,t)$ as in (3.2.1). Then, in terms of the intrinsic coordinates (s,n), points z', $z' = \bar{x}' + i\bar{y}'$, can be written

$$z' = Z(s',t) + in'e^{i\alpha'} \tag{3.4.2}$$

where $\alpha'(s',t)$ is the inclination of the tangent $\hat{\underline{s}}(s',t)$ to the $\overline{OX}$ direction. For each z' there is a unique α' provided $|n'| << \rho(s,t)$.

If now the flow in the outer region $|n| >> |\beta_{\pm}(s,t)|$ is regarded as being irrotational, the velocity at z can be expressed as an analytic complex function

$$q(z,t) = \bar{u}(\bar{x},\bar{y},t) - i\bar{v}(\bar{x},\bar{y},t) \tag{3.4.3}$$

where $\bar{u}$ and $\bar{v}$ are the components of $\underline{\bar{u}}$ in $\overline{Oxy}$ frame. Then

$$q(z,t) = \frac{-i}{2\pi}\int_0^{a(t)}\int \frac{\bar{\omega}'(1 - \frac{n'}{\rho'})dn'ds'}{z - (Z(s';t) + in'e^{i\alpha'})} \tag{3.4.4}$$

where ' means that the quantity is to be evaluated at (s',n') and where the range of the integration with respect to n' is extended over the

inner region.

Since

$$\frac{n'}{|z - Z'(s,t)|} < 1,$$

the integrand in the inner integral in (3.4.4) can be expanded and integrated term by term to get

$$q(z,t) = \frac{-i}{2\pi}\int_0^{a(t)} \frac{\int_{-\infty}^{\infty} \omega' dy' ds'}{z - Z'} - \frac{i\varepsilon}{2\pi}\int_0^{a(t)} \left\{ \frac{ie^{i\alpha'}}{(z - Z')^2} - \frac{1}{\rho'(z - Z')} \right\} \int_{-\infty}^{\infty} \omega' y' dy' ds' + + O(\varepsilon^2) \qquad (3.4.5)$$

where the inner variable $y = n/\varepsilon$ has been introduced and the limit of the y integration has been extended to $(-\infty,\infty)$ in the convention of boundary layer theory. The integrals in the $O(\varepsilon^2)$ term can be shown to remain bounded as $z \to Z(s,t)$ so that (3.4.5) is uniformly valid in z. Now, in view of the definition (3.2.15) of the centroid line C, the $O(\varepsilon)$ term vanishes. Hence the error introduced in replacing the vortex layer by an equivalent vortex sheet at C is $O(\varepsilon^2)$.

This is a familiar result in boundary layer theory where the effect of the boundary layer is taken care of by considering the surface to be at a distance δ_1 above its true position, δ_1 being the displacement thickness; the error introduced is $O((\delta_1/\ell)^2)$, ℓ being a typical length scale.

For z satisfying $|\beta_{\pm}| \ll |z - Z(s,t)| \ll \rho$, on writing

$$z = Z(x,t) + i\varepsilon y e^{i\alpha}, \qquad (3.4.6)$$

(3.4.5) becomes

$$q(z,t) = \frac{-i}{2\pi}\int_0^{a(t)} \frac{\gamma(x',t)dx'}{Z(x,t) + i\varepsilon y e^{i\alpha} - Z'} + O(\varepsilon^2) \qquad (3.4.7)$$

The integral on the right hand side is analytic for $y > 0$ and $y < 0$ but is discontinuous across C. The limits as $y \to 0_{\pm}$ can be obtained by making use of the Plemelj formulae. Hence the inner limit of the outer solution can be written

$$q(z,t) = Q_{\pm}(Z,t) + i\varepsilon y e^{i\alpha} \frac{\partial Q_{\pm}(Z,t)}{\partial Z} + O(\varepsilon^2) \qquad (3.4.8)$$

where

$$Q_{\pm}(Z,t) = \lim_{z \to Z} q(z,t) \quad \{\text{from } \pm \text{ side of C}\} \ .$$

From the Plemelj formulae,

$$Q_{\pm}(Z,t) = \frac{-i}{2\pi} \int\!\!\!\!\!\!- _0^{a(t)} \frac{\gamma(x',t)dx'}{Z(x,t) - Z(x',t)} \mp \tfrac{1}{2}\gamma(x,t)e^{-i\alpha(x,t)} \qquad (3.4.9)$$

where the slash denotes Cauchy principal value.

This is to be matched with the outer limit of the inner solution obtained in §3; the details are pursued in §5.

For latter use, the integrand in (3.2.18) may be expanded in powers of n/ρ and integrated term by term to give, in view of (3.2.15) and (3.2.17)

$$\frac{\partial \gamma}{\partial t} + \frac{\partial}{\partial s}(\gamma U_c) = \bar{\nu}\left(\frac{\partial^2 \gamma}{\partial s^2} + O(\varepsilon^2)\right) \qquad (3.4.10a)$$

where U_c is defined by (3.2.18a) and given in terms of the inner flow by (3.3.15). We now restrict ourselves to the cases where either $\bar{\nu}$ is zero or when the thickness of the layer is $O((\bar{\nu}T)^{\frac{1}{2}})$ where T is a characteristic time of the motion of the layer. This implies that right hand side of (3.4.10a) is $O(\varepsilon^2)$ so that

$$\frac{\partial \gamma}{\partial t} + \frac{\partial}{\partial s}(\gamma U_c) = O(\varepsilon^2) \qquad (3.4.10)$$

The restriction also implies that the vorticity equation (3.2.14) to leading order is

$$\frac{\partial \bar{\omega}}{\partial t} + \frac{\partial (u\bar{\omega})}{\partial s} + \frac{\partial (v\bar{\omega})}{\partial n} = \bar{\nu} \frac{\partial^2 \bar{\omega}}{\partial n^2} \tag{3.4.11}$$

Equation (3.4.11) imply that for flow at high Reynolds number, the boundary layer equations determine $\bar{\omega}$ to leading order in ε.

§5 The equation of motion of the layer

From equation (3.2.7), the velocity in the vicinity of C ($|n| << \rho(s,t)$) is given by

$$\underline{u} = \frac{\partial \underline{R}}{\partial t} + (u - \Omega n)\hat{\underline{s}} - v\hat{\underline{n}} \tag{3.5.1}$$

In complex notation this is

$$q^I(z,t) = \frac{\partial Z^*}{\partial t} + (u - \Omega n)e^{-i\alpha} - ive^{-i\alpha} \tag{3.5.2}$$

As in (3.3.4), the unknown time derivative of Z^* is expanded in powers of ε,

$$\frac{\partial Z^*}{\partial t} = \Pi_0^* + \varepsilon\Pi_1^* + \ldots \tag{3.5.3}$$

Then in terms of inner variables, and expansions (3.3.4)-(3.3.5),

$$q^I(z,t) = \Pi_0^* + u_0 e^{-i\alpha} + \varepsilon\{\Pi_1^* + (u_1 - \Omega_0 y - iv_1)e^{-i\alpha}\} + O(\varepsilon^2) \tag{3.5.4}$$

In the limit $y \to \pm\infty$, equations (3.3.8), (3.3.9) and (3.3.11) yield

$$u_0(x,\pm\infty,t) = \begin{cases} -\gamma + \bar{u}_0 \\ \\ \bar{u}_0 \end{cases} \tag{3.5.5},$$

$$u_1(x,\pm\infty,t) = (2\Omega_0 + \frac{\bar{u}_0}{\rho})y + \bar{u}_1 - \begin{cases} \frac{\gamma y}{\rho} \\ 0 \end{cases} \tag{3.5.6}$$

and

$$v_1(x,\pm\infty,t) = -y\frac{\partial \bar{u}_0}{\partial x} + \bar{v}_1 + \begin{cases} y\frac{\partial \gamma}{\partial x} \\ 0 \end{cases} \tag{3.5.7}$$

In (3.5.6) and (3.5.7), the terms proportional to y are those which would be present in the irrotational flow in the vicinity of a vortex sheet. It is expected that the terms independent of y arise due to the distribution of vorticity in a layer.

Substituting expressions (3.5.5)-(3.5.7) into (3.5.4), we require that for fixed y $q^I(z,t)$ must coincide with (3.4.8) as $\varepsilon \to 0$.

The O(1) matching gives

$$\Pi_0^* + (-\tfrac{1}{2}\gamma + \bar{u}_0)e^{-i\alpha} = -\frac{i}{2\pi}\int_0^{a(t)} \frac{\gamma(s',t)ds'}{Z(s,t) - Z(s',t)} \qquad (3.5.8)$$

This is as in (M); note, however, that the definition of $\bar{u}_0$ is different here.

In the O(ε) matching, as may be expected, the terms proportional to y reveal no new information. However, for consistency, these must be matched and this is checked in Appendix A. Matching of terms independent of y gives

$$\Pi_1^* + (\bar{u}_1 - i\bar{v}_1)e^{-i\alpha} = 0 \qquad (3.5.9)$$

Hence, from (3.5.3),

$$\frac{\partial Z^*}{\partial t} = -\frac{i}{2\pi}\int_0^{a(t)} \frac{\gamma(s',t)ds'}{Z(s,t) - Z(s',t)} - \{-\tfrac{1}{2}\gamma + \bar{u}_0 + \varepsilon(\bar{u}_1 - i\bar{v}_1)\}e^{-i\alpha} + O(\varepsilon^2) \qquad (3.5.10)$$

It is convenient to introduce Birkhoff's circulation coordinate Γ. Suppose $s(\Gamma,t)$ is the arc distance along C to a normal section which has constant net vorticity Γ between it and the end $s = 0$ for $t \geq 0$. Then

$$\Gamma(s,t) = \int_0^s \gamma(s',t)ds' \qquad (3.5.11)$$

so that

$$0 = \gamma(s,t)\left(\frac{\partial s}{\partial t}\right)_\Gamma + \int_0^s \frac{\partial \gamma'}{\partial t}\, ds' \qquad (3.5.12)$$

Now from the circulation density equation (3.4.10),

$$\frac{\partial \gamma}{\partial t} = -\frac{\partial}{\partial s}(U_c \gamma)$$

On substituting for $\partial\gamma/\partial t$ in (3.5.12) gives

$$0 = \gamma(s,t)\left(\frac{\partial s}{\partial t}\right) - U_c\gamma(s,t) \qquad (3.5.13)$$

so that, since $\gamma(s,t) \neq 0$ for $s \neq 0$, $a(t)$,

$$\left(\frac{\partial s}{\partial t}\right)_\Gamma = U_c \qquad (3.5.14)$$

Hence if Γ,n,t are the new independent variables and we write

$$\begin{aligned} z(\Gamma,t) &= Z(s,t) \\ U(\Gamma,t) &= \gamma(s,t) \\ \hat{\Delta}(\Gamma,t) &= \Delta(s,t) \end{aligned} \qquad (3.5.15)$$

then

$$\left(\frac{\partial}{\partial t}\right)_\Gamma = \frac{\partial}{\partial t} + U_c \frac{\partial}{\partial s} \qquad (3.5.16)$$

The function $\bar{u}_0 + \varepsilon\bar{u}_1$ can be eliminated from (3.5.10) by introducing U_c from (3.3.15) so that on substituting for $\bar{v}_1$ from (3.3.14), (3.5.10) becomes

$$\frac{\partial Z^*}{\partial t} + U_c e^{-i\alpha} = -\frac{i}{2\pi}\int_0^{a(t)} \frac{\gamma(s',t)ds'}{Z(s,t)-Z(s',t)} - \frac{e^{-i\alpha}}{\gamma}\left[\frac{1}{\rho}\int_{-\infty}^{\infty} \Delta(\gamma-\Delta)dn + i\frac{\partial}{\partial x}\int_{-\infty}^{\infty}\Delta(\gamma-\Delta)dn\right] + O(\varepsilon^2) \qquad (3.5.17)$$

or in terms of Γ,n,t, on noting that

$$\frac{\partial \alpha}{\partial s} = \frac{1}{\rho}\,, \quad \frac{\partial Z}{\partial s} = e^{i\alpha} \quad \text{and} \quad \frac{\partial}{\partial s} = U\frac{\partial}{\partial \Gamma} \qquad (3.5.18)$$

$$\frac{\partial z^*}{\partial t}(\Gamma,t) = -\frac{i}{2\pi}\int_0^{\Gamma_e}\frac{d\Gamma'}{z(\Gamma,t)-z(\Gamma',t)} - i\frac{\partial}{\partial\Gamma}\left[U\frac{\partial z^*}{\partial\Gamma}\int_{-\infty}^{\infty}\hat{\Delta}(U-\hat{\Delta})dn\right] + O(\varepsilon^2) \tag{3.5.19}$$

Now from (3.5.18), it follows that

$$e^{i\alpha} = U\frac{\partial z}{\partial\Gamma}$$

where $\alpha(s,t)$ and $U(\Gamma,t)$ are real so that

$$1 = U\left|\frac{\partial z}{\partial\Gamma}\right| \quad . \tag{3.5.20}$$

Thus $U(\Gamma,t)$ can be determined from the instantaneous configuration of $z(\Gamma,t)$.

The function $\int_{-\infty}^{\infty}\hat{\Delta}(U-\hat{\Delta})dn$ characterises the distribution of vorticity in a layer so that the instantaneous value of $\overline{\omega}$ or $\hat{\Delta}$ needs to be known before it can be determined. In the next section an equation for $\hat{\Delta}$ is derived.

If all the vorticity were concentrated in a sheet at C, the term in [ ] in (3.5.19) vanishes and we recover Birkhoff's equation of motion of a vortex sheet. It may be noted that the correction term can be written as

$$-i\frac{\partial}{\partial\Gamma}\left[\delta_2 U^3\frac{\partial z^*}{\partial\Gamma}\right] \tag{3.5.21}$$

where

$$\delta_2 = \int_{-\infty}^{\infty}\frac{\hat{\Delta}}{U}\left(1-\frac{\hat{\Delta}}{U}\right)\,dn \tag{3.5.22}$$

δ_2 can be identified with the momentum thickness of the layer if we define the momentum thickness as

$$\delta_2 = \int_{-\infty}^{\infty}\frac{(U_2-u)(U_1-u)}{(U_1-U_2)^2}\,dn$$

where U_1, U_2 are respectively the "streamwise" velocities at $\pm\infty$ and u is the local component of velocity tangential to C. In appendix B it is shown that δ_2 satisfies the boundary-layer type energy equation.

Moore (M) has shown that linear and angular impulse are conserved by the solutions of the modified Birkhoff equation in the case of a uniform distribution of vorticity. His argument can be used to show that these still hold good for solutions of (3.5.19) when the vorticity distribution is non-uniform. Moore also derives a modification to Kirchoff's invariants for the uniform vorticity case. In Appendix C this has been extended to the non-uniform vorticity case. The final result is (C3.8)

$$\frac{d}{dt}\left(\tilde{W}_0 - \frac{\rho_0}{2}\int_0^{\Gamma_e} U\delta_2 d\Gamma\right) = -\bar{\mu}\int_0^{\Gamma_e}\frac{1}{U}\int_{-\infty}^{\infty}\bar{\omega}^2 dn d\Gamma + O(\varepsilon^2)$$

where

$$\tilde{W}_0 = -\frac{\rho_0}{8\pi}\int_0^{\Gamma_e}\int_0^{\Gamma_e}\log|z(\Gamma,t) - z(\Gamma',t)|d\Gamma d\Gamma'$$

ρ_0 being the density of the fluid and $\bar{\mu} = \rho_0\bar{\nu}$. Hence an invariance is obtained if $\bar{\nu} = 0$.

Finally, for later use, the circulation density equation (5.4.10) can be written in terms of Γ,t variables as

$$\frac{\partial U}{\partial t} + \frac{U^2\partial}{\partial\Gamma}\left(-\tfrac{1}{2}U + \hat{u}_0\right) = O(\varepsilon) \qquad (3.5.23)$$

where $\hat{u}_0(\Gamma,t) = \bar{u}_0(s,t)$.

§6 Equation for $\hat{\Delta}(\Gamma,n,t)$

Before (3.5.10) can be used to evaluate the instantaneous position of a point on the centroid line corresponding to Γ, the instantaneous value of $\bar{\omega}(\Gamma,n,t)$ or $\hat{\Delta}(\Gamma,n,t)$ must be determined. Since $\bar{\omega}$ appears in the $O(\varepsilon)$ term in (3.5.10), it is only required to leading order in ε. As remarked in §4, $\bar{\omega}$ to this order is given by the boundary layer equation for vorticity (3.4.11), viz.

$$\frac{\partial\bar{\omega}}{\partial t} + \frac{\partial}{\partial s}(u\bar{\omega}) + \frac{\partial}{\partial n}(v\bar{\omega}) = \bar{\nu}\frac{\partial^2\bar{\omega}}{\partial n^2} \tag{3.6.1}$$

where the leading order terms in u and v are implied.

Integrating (3.6.1) across the layer gives

$$\frac{\partial\Delta}{\partial t} + \frac{\partial}{\partial s}\int_{-\infty}^{n} u\bar{\omega}\,dn' + v\bar{\omega} = \bar{\nu}\frac{\partial\bar{\omega}}{\partial n} \tag{3.6.2}$$

using $\bar{\omega} = \frac{\partial\bar{\omega}}{\partial n} = 0$ at $n = -\infty$. The constant of integration is zero in view of the circulation density equation (3.4.10). Then substituting for u and v by the leading order terms in (3.3.8) and (3.3.11) and using (3.3.14) gives

$$\frac{\partial\Delta}{\partial t} - \tfrac{1}{2}\frac{\partial\Delta^2}{\partial s} + \frac{\partial}{\partial s}(\bar{u}_0\Delta) + \frac{\partial\Delta}{\partial n}\left[\frac{\partial}{\partial s}\int_{-\infty}^{n}\Delta\,dn' - n\frac{\partial\bar{u}_0}{\partial s} - \frac{1}{\gamma}\frac{\partial}{\partial s}\delta_2\right] = \bar{\nu}\frac{\partial^2\Delta}{\partial n^2} \tag{3.6.3}$$

where δ_2 is given by (3.5.22).

Thus, writing in terms of Γ,n,t variables and using the circulation density equation (3.5.23) gives

$$\frac{\partial\hat{\Delta}}{\partial t} + \tfrac{1}{2}U\frac{\partial}{\partial\Gamma}(\hat{\Delta}(U-\hat{\Delta})) - \frac{\hat{\Delta}}{U}\frac{\partial U}{\partial t} + \frac{\partial\hat{\Delta}}{\partial n}\left[U\frac{\partial}{\partial\Gamma}\int_{-\infty}^{n}\hat{\Delta}\,dn' + \frac{n}{U}\left(\frac{\partial U}{\partial t} - \frac{U^2}{2}\frac{\partial U}{\partial\Gamma}\right) - \frac{\partial}{\partial\Gamma}\delta_2\right]$$

$$= \bar{\nu}\frac{\partial^2\hat{\Delta}}{\partial n^2} \tag{3.6.4}$$

Since $U = \left|\frac{\partial z}{\partial \Gamma}\right|^{-1}$,

$$\frac{\partial U}{\partial t} = -U^3 \, \mathrm{Re}\left(\frac{\partial z}{\partial \Gamma} \frac{\partial^2 z}{\partial t \partial \Gamma}\right)$$

so that, in view of (3.5.10),

$$\frac{\partial U}{\partial t} = -U^3 \, \mathrm{Re}\left(\frac{\partial z}{\partial \Gamma} \frac{\partial I}{\partial \Gamma}\right) + O(\varepsilon) \tag{3.6.5}$$

where

$$I = -\frac{i}{2\pi} \oint_0^{\Gamma_e} \frac{d\Gamma'}{z(\Gamma,t) - z(\Gamma',t)}$$

Hence (3.6.4) becomes

$$\frac{\partial \hat{\Delta}}{\partial t} + \tfrac{1}{2} U \frac{\partial}{\partial \Gamma}(\hat{\Delta}(U-\hat{\Delta})) + \frac{\partial \hat{\Delta}}{\partial n}\left(U \frac{\partial}{\partial \Gamma} \int_{-\infty}^{n} \hat{\Delta} dn' - \frac{nU}{2} \frac{\partial U}{\partial \Gamma} - \frac{\partial \delta_2}{\partial \Gamma}\right)$$

$$= \bar{\nu} \frac{\partial^2 \hat{\Delta}}{\partial n^2} - U^2 \, \mathrm{Re}\left(\frac{\partial z}{\partial \Gamma} \frac{\partial I}{\partial \Gamma}\right)\left(\hat{\Delta} - n \frac{\partial \hat{\Delta}}{\partial n}\right) \tag{3.6.6}$$

The boundary conditions are:

(a) $\hat{\Delta} \to U(\Gamma,t)$ as $n \to \infty$, $\hat{\Delta} \to 0$ as $n \to -\infty$.

(b) $\hat{\Delta} \to 0$ as $\Gamma \to 0, \Gamma_e$

(c) $\frac{\partial \hat{\Delta}}{\partial n} = O(\exp(-|n|/|\beta_{\pm}(\Gamma,t)|))$ as $n \to \pm\infty$.

Thus for a given initial distribution, $\hat{\Delta}(\Gamma,n,0) = \hat{\Delta}_0(\Gamma,n)$, equation (3.6.6) and the above boundary conditions specify $\hat{\Delta}(\Gamma,n,t)$. In general, the problem of evaluating $\hat{\Delta}(\Gamma,n,t)$ is a formidable task and would have to be solved numerically.

In §7, equations (3.5.19) and (3.6.4) are linearized to consider perturbations on a straight vortex layer of arbitrary steady velocity profile for the case $\bar{\nu} = 0$.

In §8, the equation of motion of a vortex sheet undergoing viscous diffusion is obtained and growth of small perturbations on a Rayleigh layer is studied.

Meanwhile, it may be noted that if $\bar{\omega} = \bar{\omega}_0$, a constant for $-H(\Gamma,t) < n < H(\Gamma,t)$, $\bar{\omega} = 0$ otherwise and $\bar{\nu} = 0$, then

$$\Delta = \bar{\omega}_0(n + H) \qquad \text{and} \qquad H = \frac{U}{2\bar{\omega}_0}$$

On substituting this into (3.5.19), we recover Moore's equation (M(4.20)) for the motion of a thin vortex layer of constant vorticity.

§7 Growth of long waves on a straight vortex layer in an inviscid fluid

In this section instability of an initially straight and steady vortex layer in non-viscous fluid to disturbances of wave-numbers k, $k/k_1 \ll 1$ (where k_1 is as defined below), is considered using the equations derived in §§5,6. The results for the growth rate are compared with Drazin & Howard (1962).

The vorticity distribution in the unperturbed layer is taken to be $\omega_0(y)$, where (x,y) denotes position in Cartesian coordinate system OXY with the centroid line C along OX for $t < 0$. In view of equation (3.3.1), it is assumed that $\omega_0(y) \to 0$ as $y \to \pm\infty$ at least as fast as $\exp(-k_1|y|)$. Suppose the streamwise velocities at $y = \pm\infty$ are $\mp V/2$. Then the perturbed centroid line can be written,

$$z(\Gamma,t) = V^{-1}\Gamma + f(\Gamma,t) \tag{3.7.1}$$

where $|\partial f/\partial\Gamma| \ll V^{-1}$. The integrated vorticity function $\hat{\Delta}$ is taken to be

$$\hat{\Delta}(\Gamma,y,t) = \Delta_0(y) + \Delta'(\Gamma,y,t) \tag{3.7.2}$$

where $\Delta_0(y) = \int_{-\infty}^{y} \omega_0(y_1)dy_1$ and $|\Delta'| \ll |\Delta_0|$, uniformly in y.

On substituting (3.7.1) and (3.7.2) into (3.5.19) and (3.6.4), with $\bar{\nu} = 0$, gives on linearizing

$$\frac{\partial f^*}{\partial t} = \frac{iV^2}{2\pi}\int_{-\infty}^{\infty} \frac{[f(\Gamma,t)-f(\Gamma',t)]d\Gamma'}{(\Gamma-\Gamma')^2} + \frac{iV}{2}M_0\{\frac{\partial^2 f}{\partial\Gamma^2} - \frac{\partial^2 f^*}{\partial\Gamma^2}\} - iM' \tag{3.7.3}$$

$$\frac{\partial\Delta'}{\partial t} + (\tfrac{1}{2}V^2 - V\Delta_0)\frac{\partial\Delta'}{\partial\Gamma} + \frac{\partial\Delta_0}{\partial y}[V\int_{-\infty}^{y}\frac{\partial\Delta'}{\partial\Gamma}dy_1 + M'] = V(y\frac{\partial\Delta_0}{\partial y} - \Delta_0) \times$$

$$\times (\frac{\partial}{\partial t} - \frac{V^2}{2}\frac{\partial}{\partial\Gamma})\,\mathrm{Re}[\frac{\partial f}{\partial\Gamma}] \tag{3.7.4}$$

where

$$M_0 = \int_{-\infty}^{\infty}\Delta_0(V-\Delta_0)dy \quad , \qquad M' = 2\int_{-\infty}^{\infty}(V-\Delta_0)\frac{\partial\Delta'}{\partial\Gamma}\,dy$$

In order to consider sinusoidal disturbances, f and Δ' are chosen to be

$$f(\Gamma,t) = e^{\sigma t}(a_+ e^{ik\Gamma/V} + a_- e^{-ik\Gamma/V})$$

$$\Delta'(\Gamma,t) = e^{\sigma t}(\Delta_+(y)e^{ik\Gamma/V} + \Delta_-(y)e^{-ik\Gamma/V}) \qquad (3.7.5)$$

where $a_\pm$, $\Delta_\pm$ have complex values, $a_\pm$ being constants.

On substituting (3.7.5) into (3.7.3) and evaluating the principal value integral by contour integration, terms proportional to $e^{\sigma t \mp ik\Gamma/V}$ can be equated to yield,

$$\sigma a_+^* = \frac{(w_1-w_2)}{2} a_- - \frac{k}{2}\left[\int_{-\infty}^{\infty} \frac{(w_1-w)(w-w_2)}{w_1-w_2}\, dy\right](a_- - a_+^*) - \left[\frac{2k}{(w_1-w_2)} \int_{-\infty}^{\infty} (w_1-w)\Delta_- dy\right] \qquad (3.7.6)$$

$$\sigma a_-^* = \frac{(w_1-w_2)}{2} a_+ - \frac{k}{2}\left[\int_{-\infty}^{\infty} \frac{(w_1-w)(w-w_2)}{w_1-w_2} dy\right](a_+ - a_-^*) + \left[\frac{2k}{(w_1-w_2)} \int_{-\infty}^{\infty} (w_1-w)\Delta_+\, dy\right] \qquad (3.7.6a)$$

while from (3.7.4),

$$w\Delta_- - w'\left[\int_{-\infty}^{y} \Delta_-(y_1)dy_1 + 2\int_{-\infty}^{\infty} \frac{(w_1-w)}{(w_1-w_2)}\Delta_- dy_1\right] = \frac{w_1}{2}(w-w_2-yw')(a_+^* + a_-) \qquad (3.7.7)$$

$$(2\sigma-w)\Delta_+ + w'\left[\int_{-\infty}^{y} \Delta_+(y_1)dy_1 + 2\int_{-\infty}^{\infty} \frac{(w_1-w)}{(w_1-w_2)}\Delta_+(y_1)dy_1\right]$$

$$= -\frac{w_2}{2}(w-w_2-yw')(a_-^*+a_+) \qquad (3.7.7a)$$

Here

$$w(y) = \sigma - ik(\frac{V}{2} - \Delta_0(y))$$

$$w_1 \equiv w(\infty) = \sigma + ik\frac{V}{2} \qquad (3.7.8)$$

$$w_2 \equiv w(-\infty) = \sigma - ik\frac{V}{2}$$

and ' denotes differentiation with respect to y. This notation is consistent with that of Drazin and Howard.

On noting that

$$(2\sigma-w)^* = w, \quad w_1^* = w_2,$$

the complex conjugate of equation (3.7.7a) can be written

$$w\Delta_+^* - w'\left[\int_{-\infty}^{y} \Delta_+^* dy_1 + 2\int_{-\infty}^{\infty} \frac{(w_1-w)}{(w_1-w_2)}\Delta_+^* dy_1\right] = \frac{w_1}{2}(w-w_2-yw')(a_+^* + a_-) \qquad (3.7.7b)$$

which is identical with (3.7.7). Hence

$$\Delta_+^*(y) \equiv \Delta_-(y) \qquad (3.7.9)$$

is a solution.

The solution of (3.7.7) is straightforward and is given in Appendix D. If this solution is substituted into (3.7.6) and, in view of (3.7.9), into the complex conjugate of (3.7.6a), then after a little algebra,

$$\begin{pmatrix} \sigma - \frac{k}{(w_1-w_2)}(\frac{F_1}{2} + F_2) & -(\frac{w_1-w_2}{2} + \frac{k}{(w_1-w_2)}(F_2 - \frac{F_1}{2})) \\ \frac{w_1-w_2}{2} + \frac{k(F_2-\frac{F_1}{2})}{(w_1-w_2)} & \sigma + \frac{k}{(w_1-w_2)}(\frac{F_1}{2} + F_2) \end{pmatrix} \begin{bmatrix} a_+^* \\ a_- \end{bmatrix} = \underset{\sim}{0} \qquad (3.7.10)$$

where

$$F_1 = \int_{-\infty}^{\infty} (w-w_2)(w_1-w)dy$$

$$F_2 = \int_{-\infty}^{\infty} \frac{(w-w_1)(w-w_2)}{2w^2} (2(w_1+w_2)w + w_1w_2)dy$$

Then setting the determinant of the matrix in (3.7.10) to zero gives the dispersion relation

$$\sigma^2 + \frac{(w_1-w_2)^2}{4} + \frac{k}{2}\int_{-\infty}^{\infty} \frac{(w^2-w_1^2)(w^2-w_2^2)}{w^2} + k^2\left(\int_{-\infty}^{\infty} \frac{(w_1-w)(w-w_2)}{(w_1-w_2)^2}\right) \times$$

$$\times \int_{-\infty}^{\infty} \frac{(w-w_1)(w-w_2)}{w^2}(2(w_1+w_2)w + w_1w_2)dy = 0 \qquad (3.7.11)$$

The last term on the left hand side is evidently of the $O((\frac{k}{k_1})^2)$, since the coefficient of k^2 is $O(\delta_2{}^2)$, where δ_2 is the momentum thickness of the layer, and for consistency cannot be retained; terms of that order have been excluded from the governing equation (3.5.19) and (3.6.4). Hence, on noting that

$$\sigma^2 + \frac{(w_1-w_2)^2}{4} = \frac{w_1{}^2+w_2{}^2}{2} \quad ,$$

(3.7.11) becomes

$$\frac{(w_1{}^2+w_2{}^2)}{2} + \frac{k}{2}\int_{-\infty}^{\infty} \frac{(w^2-w_1{}^2)(w^2-w_2{}^2)}{w^2} = O(k^2\delta_2{}^2) \qquad (3.7.12)$$

This is in agreement with equation (2.9) of Drazin & Howard (1962).

§8 The equation of motion of a viscous vortex sheet

Here, the effect of viscous diffusion of vorticity on the motion of an instantaneously created arbitrary vortex sheet in flow at high Reynolds number is considered. A solution, valid for small times, for the vorticity distribution is derived and hence, using (3.5.19), an equation of motion of the sheet is determined. The equation is used to study the growth of long waves on a Rayleigh layer.

For flow at high Reynolds number, the equation for the vorticity $\bar{\omega}$ is given by the boundary layer approximation (3.6.1). However, it is convenient to express the equation in terms of Γ,n,t variables. Thus on differentiating (3.5.4) and using the continuity equation gives

$$\frac{\partial\bar{\omega}}{\partial t} + (\tfrac{1}{2}U^2 - U\hat{\Delta})\frac{\partial\bar{\omega}}{\partial\Gamma} + [U\frac{\partial}{\partial\Gamma}\int_{-\infty}^{n}\hat{\Delta}dn - nU^2\frac{\partial\hat{u}_0}{\partial\Gamma} - \frac{\partial}{\partial\Gamma}\delta_2]\frac{\partial\bar{\omega}}{\partial n} = \bar{\nu}\frac{\partial^2\bar{\omega}}{\partial n^2} \qquad (3.8.1)$$

where now $\bar{\omega} = \bar{\omega}(\Gamma,n,t)$, δ_2 is given by (3.5.22), $U,\hat{\Delta}$ are as in (3.5.15) and where the circulation density equation (3.5.23) has been used.

In view of (3.5.23) and (3.5.20), the circulation density $U(\Gamma,t)$, to leading order, depends on the configuration of the vortex sheet and external flow field. It is insensitive, to this order, to the details of local vorticity distribution. Thus $\bar{\omega}(\Gamma,n,t)$ may be written

$$\bar{\omega}(\Gamma,n,t) = U(\Gamma,t)\hat{\omega}(\Gamma,n,t) \qquad (3.8.2)$$

where

$$\int_{-\infty}^{\infty}\hat{\omega}dn = 1 + O(\varepsilon)$$

In (3.8.1) the rate of change of vorticity at a station Γ along the sheet is governed by viscous diffusion and convection relative to the vortex sheet. It is expected that initially, the influence of the former will far outweigh that of the latter. Thus the equation for $\hat{\omega}_1$, the first approximation to $\hat{\omega}$, is

$$\frac{\partial \hat{\omega}_1}{\partial t} = \bar{\nu} \frac{\partial^2 \hat{\omega}_1}{\partial n^2} \tag{3.8.3}$$

and the required solution is

$$\hat{\omega}_1 = \frac{e^{-\eta^2}}{2\sqrt{\pi \bar{\nu} t}}, \qquad \eta = \frac{n}{2\sqrt{\bar{\nu} t}} \tag{3.8.4}$$

This satisfies $\int_{-\infty}^{\infty} \hat{\omega}_1 = 1$ and $\hat{\omega}_1 \to 0$ $n \to \pm\infty$. To obtain the second approximation, put

$$\hat{\omega} = \hat{\omega}_1 + \hat{\omega}_2 \tag{3.8.5}$$

and substitute into (3.8.1). This gives

$$\frac{\partial \hat{\omega}_2}{\partial t} - \bar{\nu} \frac{\partial^2 \hat{\omega}_2}{\partial n^2} = \left(\frac{\partial U}{\partial t} + (\tfrac{1}{2}U^2 - U\hat{\Delta}_1) \frac{\partial U}{\partial \Gamma} \right) \hat{\omega}_1 +$$

$$+ \left[U \frac{\partial}{\partial \Gamma} \int_{-\infty}^{n} \hat{\Delta}_1 dn - nU^2 \frac{\partial \bar{u}_0}{\partial \Gamma} - \frac{\partial}{\partial \Gamma} \int_{-\infty}^{\infty} \hat{\Delta}_1 (U - \hat{\Delta}_1) dn \right] \frac{\partial \hat{\omega}_1}{\partial n} \tag{3.8.6}$$

where $\hat{\Delta}_1 = U \int_{-\infty}^{n} \hat{\omega}_1 dn$.

In view of (3.5.23) it can be shown that

$$\hat{\omega}_2 = \frac{tU}{2(\bar{\nu}t)^{\frac{1}{2}}} \frac{\partial U}{\partial \Gamma} \{ 2\sqrt{\pi}\, \eta \operatorname{erf} \eta (1 - \operatorname{erf} \eta) +$$

$$+ e^{-\eta^2} \left[\frac{4}{3} \left(\frac{2}{\pi} \right)^{\frac{1}{2}} \eta + \tfrac{1}{2}(\eta^2 - \tfrac{1}{2}) - \frac{\eta e^{-\eta^2}}{2\sqrt{\pi}} - (\eta^2 - \tfrac{1}{2}) \operatorname{erf} \eta \right] \}$$

$$- \frac{t}{2U(\bar{\nu}t)^{\frac{1}{2}}} \frac{\partial U}{\partial t} (\eta^2 - \tfrac{1}{2}) e^{-\eta^2} \tag{3.8.7}$$

This satisfies $\int_{-\infty}^{\infty} \hat{\omega}_2 = 0$ and $\hat{\omega}_2 \to 0$ when $n \to \pm\infty$. Thus, in view of (3.8.5),

$$\int_{-\infty}^{\infty} \hat{\Delta}(U - \hat{\Delta}) dn = \left(\frac{2\bar{\nu}t}{\pi} \right)^{\frac{1}{2}} U^2 \left(1 + \frac{t}{2U} \frac{\partial U}{\partial t} + O\left[tU \frac{\partial U}{\partial \Gamma} \right]^2 \right) \tag{3.8.8}$$

Then since, from (3.6.5)

$$\frac{\partial U}{\partial t} = -U^3 \, \mathrm{Re}\left(\frac{\partial z}{\partial \Gamma} \frac{\partial I}{\partial \Gamma}\right) + O(\varepsilon),$$

substituting (3.8.8) into (3.5.19) gives

$$\frac{\partial z^*}{\partial t}(\Gamma,t) = I - i\left(\frac{2\bar{\nu}t}{\pi}\right)^{\frac{1}{2}} \frac{\partial}{\partial \Gamma}\left(U^3 \frac{\partial z^*}{\partial \Gamma}\left[1 - tU^2 \mathrm{Re}\left(\frac{\partial z}{\partial \Gamma} \frac{\partial I}{\partial \Gamma}\right) + O\left(\left(tU \frac{\partial U}{\partial \Gamma}\right)^2\right)\right]\right) + O(\varepsilon^2) \tag{3.8.9}$$

where

$$I = -\frac{i}{2\pi} \int_0^{\Gamma_e} \frac{d\Gamma'}{z(\Gamma,t) - z(\Gamma',t)}$$

Equation (3.8.9) is the main result of this section. The rest of the section is devoted to considering the growth of long waves on a Rayleigh layer.

Suppose that instantaneously at $t = 0$ an infinitely long straight vortex sheet of constant strength V is created in a fluid of viscosity $\bar{\nu}$ so that if undisturbed its configuration would be given by $z = \Gamma V^{-1}$. Suppose now that at $t = 0$ the sheet is so disturbed as to assume an instantaneous shape

$$z(\Gamma,t) = \Gamma V^{-1} + f(\Gamma,t) \tag{3.8.10}$$

where $|\partial f/\partial \Gamma| \ll V^{-1}$. It is proposed to study a particular form of disturbance $f(\Gamma,t)$. If (3.8.10) is substituted into (3.8.9) and only terms linear in f are retained, then after a little algebra, we have

$$\frac{\partial f^*}{\partial t} = I_1 + iV^3\left(\frac{2\bar{\nu}t}{\pi}\right)^{\frac{1}{2}}\left(\frac{3}{2} \frac{\partial^2 f}{\partial \Gamma^2} + \frac{1}{2} \frac{\partial^2 f^*}{\partial \Gamma^2} + t \, \mathrm{Re}\left(\frac{\partial I_1}{\partial \Gamma}\right)\right) + O(\varepsilon^2) \tag{3.8.11}$$

where

$$I_1 = \frac{iV^2}{2\pi} \int_{-\infty}^{\infty} \frac{[f(\Gamma,t) - f(\Gamma',t)]}{(\Gamma - \Gamma')^2} \, d\Gamma'$$

$f(\Gamma,t)$ is chosen so that it represents a sinusoidal disturbance of spatial wavenumber k, viz.,

$$f(\Gamma,t) = ae^{ik\Gamma/V} + be^{-ik\Gamma/V} \tag{3.8.12}$$

where $a(t)$, $b(t)$ are complex valued. On substituting (3.8.12) into (3.8.11) and evaluating I_1 by contour integration, terms proportional to $e^{\mp ik\Gamma/V}$ can be equated to give

$$\begin{aligned}\frac{da^*}{dt} &= \frac{iVk}{2}\left(b - k\left(\frac{2\bar{\nu}t}{\pi}\right)^{\frac{1}{2}}\left[3b + a^* + \frac{iVk}{4}t(b - a^*)\right]\right)\\ \frac{db^*}{dt} &= \frac{iVk}{2}\left(a - k\left(\frac{2\bar{\nu}t}{\pi}\right)^{\frac{1}{2}}\left[3a + b^* + \frac{iVk}{4}t(a - b^*)\right]\right)\end{aligned} \tag{3.8.13}$$

The form of equations (3.8.13) suggests that a possible choice of solution is

$$a(t) \equiv b(t) = \alpha(t) + i\beta(t) \tag{3.8.14}$$

say. This choice is not unique (e.g. $a \equiv -b$ is also a solution) but it will suffice for our purpose.

Putting (3.8.14) into (3.8.13) and equating real and imaginary parts give

$$\dot{\alpha} = -\frac{Vk}{2}\left\{1 - 2k\left(\frac{2\bar{\nu}t}{\pi}\right)^{\frac{1}{2}}\right\}\beta \tag{3.8.15}$$

$$\dot{\beta} = -\frac{Vk}{2}\left\{1 - 4k\left(\frac{2\bar{\nu}t}{\pi}\right)^{\frac{1}{2}}\right\}\alpha - \frac{V^2k^3t}{4}\left(\frac{2\bar{\nu}t}{\pi}\right)^{\frac{1}{2}}\beta \tag{3.8.16}$$

where the dot denotes differentiation with respect to time.

It is convenient to express (3.8.15), (3.8.16) in non-dimensional form. Write

$$t = \frac{2}{Vk}t_1, \quad \alpha(t) = \alpha(0)\alpha_1(t_1), \quad \beta(t) = \alpha(0)\beta_1(t_1) \tag{3.8.17}$$

and define a Reynolds number $R = \pi V/\bar{\nu}k$. Then (3.8.22), (3.8.23) become

$$\dot{\alpha}_1 = -\{1 - 4(\frac{t_1}{R})^{\frac{1}{2}}\}\beta_1 \qquad (3.8.18)$$

$$\dot{\beta}_1 = -\{1 - 8(\frac{t_1}{R})^{\frac{1}{2}}\}\alpha_1 - \frac{2t_1^{3/2}}{R^{\frac{1}{2}}}\beta_1. \qquad (3.8.19)$$

The choice of the Reynolds number R above means that the approximation in ϵ leading to the governing equation (3.8.9) is valid for $t_1 << R$. The approximate solution to the vorticity equation is valid for $t_1 << 1$. Equations (3.8.18), (3.8.19) therefore hold when both conditions are satisfied.

The equations were integrated numerically for a range of values of the Reynolds number with initial conditions $\alpha_1(0) = 1$, $\beta_1(0) = 0$. The integrations were carried out up to $t_1 = 0.15R$ although the results are strictly true for $t_1/R << 1$. The results are displayed in Figs. 3.2, 3.3. Fig. 3.2 shows a plot of amplification rate $\dot{\alpha}/\alpha$ vs. $(t_1/R)^{\frac{1}{2}} = k(\frac{\bar{\nu}t}{2\pi})^{\frac{1}{2}}$ for R = 100, 500, 1000, 2000. The amplification rate achieves a maximum at $(t_1/R)^{\frac{1}{2}} = (t_1/R)^{\frac{1}{2}}_{max}$ which is quite outside the range of validity of the governing equations. However, it is interesting to note its dependence on R which is displayed in Fig. 3.3(b). $(t_1/R)^{\frac{1}{2}}_{max}$ decreases with 1/R and at R=2000 has a value 0.031. This implies that in fluids of small viscosity $\bar{\nu}$, the waves of wavelength λ on a Rayleigh layer grow fastest when $t = 0.00015\lambda^2/\bar{\nu}$. Also displayed in Fig. 3.3 is the dependence on Reynolds number of $(t_1/R)^{\frac{1}{2}}_c$, the value of $(t_1/R)^{\frac{1}{2}} > 0$ when $\dot{\alpha}$ vanishes although $(t_1/R)^{\frac{1}{2}}_c$ is outside the range of validity of the governing equations; $(t_1/R)^{\frac{1}{2}}_c$ decreases with 1/R and at R=2000 has a value 0.125. This implies that waves of wavelength λ stop growing on a Rayleigh layer of small viscosity $\bar{\nu}$ when $t = 0.002\lambda^2/\bar{\nu}$.

Figure 3.2 shows that for $(t_1/R)^{\frac{1}{2}} > (t_1/R)^{\frac{1}{2}}_c$, $\dot{\alpha}$ vanishes again when $(t_1/R)^{\frac{1}{2}} = 0.25$. This can be inferred from (3.8.18) where the right

hand side vanishes at this value of $(t_1/R)^{\frac{1}{2}}$. It is believed that this is a spurious effect and is a consequence of the truncation in the expansion in ε made in deriving the governing equation of motion of the layer. The effect corresponds to that found by Moore (M) in the uniform vorticity case when equations corresponding to (3.8.18), (3.8.19) for that case were used to study growth of long waves on a straight layer. As Moore points out, the appearance of this spurious effect means that any attempt to integrate the modified integro-differential equation (3.8.9) will be faced with a serious difficulty. For, even though the value of $(t_1/R)^{\frac{1}{2}} = k(\bar{\nu}t/2\pi)^{\frac{1}{2}}$ at which the spurious growth appears is quite outside the range of validity of (3.8.9), short wave disturbances, which will be excited in any numerical calculation, will be amplified. A possible remedy to the situation is to obtain a higher order correction than $O(\varepsilon)$ to the governing equation; hopefully this would suppress the spurious behaviour. The matter is pursued in the next chapter.

§9 An interpretation of equation of motion (3.5.19)

A simple interpretation of the modified Birkhoff equation (3.5.19) can be given as follows.

Consider an element of the layer with local radius of curvature $\rho(s)$, where s (defined below) is associated with the particular element chosen, and let Q(s) be the local centre of curvature. Let P(s) be the centroid of the vorticity distribution $\bar{\omega}(s,y)$ in the element. The surfaces AC and BD (see Fig. 3.1) are chosen so that the vorticity there is effectively zero; this is always possible in view of the exponential decay of vorticity (cf (3.3.1)) as QP is traversed away from P. Let the distance from P to AC, and from P to BD measured along QP be δ_-^+ respectively. The element is assumed to have length ds (see the figure); s being identified with the arc-distance measured along the line joining the centroid of each element.

If y is the distance, measured along QP, from P, then

$$\int_{-\infty}^{\infty} \bar{\omega} y dy = 0 \qquad (3.9.1)$$

Suppose the jump in the tangential velocity across the element is $-\gamma(s)$. Then for flow at great distances from P, the element can be represented by a point vortex of strength $\gamma(s)ds$ at P. If in a coordinate frame fixed with respect to flow at infinity the position of P is given by

$$\underline{x} = \underline{R}(s)$$

then in the absence of any distribution of vorticity (i.e. if we have a vortex sheet),

$$\frac{\partial \underline{R}}{\partial t}(s) = \underline{V}_0 \equiv (U_0, V_0) \qquad (3.9.2)$$

where $\underline{V}_0$ is the velocity induced by the other elements of the layer together with the velocity with which P is convected along the sheet.

(3.9.2) is essentially Birkhoff's equation (3.1.1).

Suppose that when the vorticity is distributed in a layer, the velocity contribution from all the other elements of the layer to the element at s can be regarded as due to an appropriate distribution of point vortices. Then the distribution of vorticity in the element at s will give rise to an extra velocity at P(s), given by

$$(U_1,V_1) = \frac{\partial \underline{R}}{\partial t} - (U_0, V_0) \qquad (3.9.3)$$

It is asserted that the existence of this extra velocity produces a force on the element given by the Kutta lift and the local pressure gradient,

$$\gamma ds(U_1,V_1) \wedge \underline{k} - ds\left(\frac{\partial p}{\partial s}, 0\right) \equiv (F,G)ds \qquad (3.9.4)$$

assuming that the fluid has unit density and that the pressure p remains sensibly constant across the layer (see below). Then, provided (F,G) and $\frac{\partial p}{\partial s}$ can be found, (U_1,V_1) is determined.

If the fluid velocity in the neighbourhood of P is (u,v) relative to (U_0,V_0) and if $u \to \bar{u}_0(s)$ as $y \to -\infty$, then, since the jump in tangential velocity across the layer is $-\gamma(s)$, $u \to -\gamma(s) + \bar{u}_0(s)$ as $y \to +\infty$. Assuming that $\left|\frac{\partial}{\partial s}\right| << \left|\frac{\partial}{\partial y}\right|_{\delta}$, (u,v) satisfies the curved boundary layer type equations (which to $O(\frac{\pm}{\rho})$ are of course the same as that for a flat boundary layer). To $O(\frac{\pm}{\rho})$ the pressure in the layer is constant so that

$$-\frac{\partial p}{\partial s} = \frac{\partial \bar{u}_0}{\partial t} + \frac{1}{2}\frac{\partial \bar{u}_0^2}{\partial s} = \frac{\partial}{\partial t}(-\gamma + \bar{u}_0) + \frac{1}{2}\frac{\partial}{\partial s}(-\gamma + \bar{u}_0)^2 \qquad (3.9.5)$$

so that

$$\frac{\partial \gamma}{\partial t} + \frac{\partial}{\partial s}(\gamma(-\tfrac{1}{2}\gamma + \bar{u}_0)) = 0 \qquad (3.9.6)$$

which is the circulation density equation (cf. (3.4.10)).

For simplicity let $\bar{u}_0 \equiv 0$, so that $\frac{\partial P}{\partial s} = 0$. Then, using the Kármán type argument (Goldstein, p.131), it can be shown that the total rate of change of momentum in the tangential direction inside ACDB, considered as a fixed surface, is given by

$$\left[\int_{-\delta_-}^{\delta_+} \frac{\partial u}{\partial t} + \frac{\partial}{\partial s} \int_{-\infty}^{\infty} u(\gamma+u)dy - \frac{\partial \gamma}{\partial s} \int_{\delta_-}^{\delta_+} udy \right] ds \qquad (3.9.7)$$

This must be equated to F since the viscous forces give zero contribution. Since $\bar{u}_0 \equiv 0$ and $u \equiv -\Delta = \int_{-\infty}^{y} \bar{\omega}\, dy$, approximately, integrating the first and the last terms in (3.9.7) by parts and using (3.9.6) it can be shown that these terms cancel. Hence, from (3.9.4) and using $\frac{\partial P}{\partial s} = 0$,

$$V_1 = -\frac{1}{\gamma} \frac{\partial}{\partial s} \int_{-\infty}^{\infty} \Delta(\gamma-\Delta)dy \qquad (3.9.8)$$

In order to contain the momentum flux in the tangential direction and maintain the inward mass flux from BD in circular motion at tangential speed $-\gamma$, i.e. a net momentum flux, $-ds \int_{-\infty}^{\infty} \Delta(\gamma-\Delta)dy$, a force

$$-\frac{ds \int_{-\infty}^{\infty} \Delta(\gamma-\Delta)dy}{\rho} \qquad (3.9.9)$$

is required to act upon the element along PQ. This is provided by G so that from (3.9.4), we have

$$U_1 = \frac{1}{\gamma\rho} \int_{-\infty}^{\infty} \Delta(\gamma-\Delta)dy \qquad (3.9.10)$$

Both (3.9.8) and (3.9.10) are in agreement with the corresponding values in (3.5.17). It may be noted that the curvature affects only the tangential velocity whereas the net change in momentum flux along the tangent affects only the normal velocity.

APPENDIX A: Matching $O(\varepsilon)$ terms proportional to y

For consistency, terms of $O(\varepsilon)$ which are proportional to y in the outer solution (3.4.8) must be matched with those in (3.5.4).

Thus it is required that

$$ie^{i\alpha}\frac{\partial Q_+}{\partial Z} = (\Omega_0 + \frac{\bar{u}_0}{\rho} - \frac{1}{\rho}\gamma - i\frac{\partial}{\partial x}\gamma + i\frac{\partial \bar{u}_0}{\partial x})e^{-i\alpha} \qquad (A3.1)$$

and

$$ie^{i\alpha}\frac{\partial Q_-}{\partial Z} = \Omega_0 + \frac{\bar{u}_0}{\rho} + i\frac{\partial \bar{u}_0}{\partial x} \qquad (A3.2)$$

Since Q_+ is analytic, it can be differentiated in any direction so that

$$\frac{\partial Q_+}{\partial Z} = e^{-i\alpha}\frac{\partial Q_+}{\partial x} \qquad (A3.3)$$

Then from (3.4.9) and (3.5.8)

$$\frac{\partial Q_+}{\partial x} = \frac{\partial \Pi_0^*}{\partial x} + e^{-i\alpha}\frac{\partial}{\partial x}(-\gamma + \bar{u}_0) + i(\gamma - \bar{u}_0)\frac{\partial \alpha}{\partial x}e^{-i\alpha} \qquad (A3.4)$$

and since

$$\frac{\partial Z^*}{\partial x} = e^{-i\alpha}, \quad \frac{\partial \alpha}{\partial t} = \Omega_0, \quad \frac{\partial \alpha}{\partial x} = \frac{1}{\rho}, \qquad (A3.5)$$

$$\frac{\partial Q_+}{\partial x} = -i\Omega_0 e^{-i\alpha} + e^{-i\alpha}(\frac{\partial \bar{u}_0}{\partial x} - \frac{\partial \gamma}{\partial x} + i(\frac{\gamma}{\rho} - \frac{\bar{u}_0}{\rho})) \qquad (A3.6)$$

Multiplying (A3.6) by i and using (A3.3), it follows that the left hand side of (A3.1) agrees with the right hand side.

Similarly, (A3.2) is also true.

APPENDIX B: Energy equation

δ_2, as defined in (3.5.22), can be shown to satisfy the boundary layer type energy equation as follows.

Multiplying equation (3.6.3) by γ and integrating across the layer gives

$$\frac{\partial}{\partial t}\int \gamma\Delta - \frac{\partial}{\partial s}\int\gamma\Delta^2 + \frac{2\partial\bar{u}_0}{\partial s}\int\gamma\Delta + \bar{u}_0\frac{\partial}{\partial s}\int\gamma\Delta + [\gamma\Delta v]$$

$$- \{(\frac{\partial\gamma}{\partial t} + \bar{u}_0\frac{\partial\gamma}{\partial s})\int\Delta - \frac{\partial\gamma}{\partial s}\int\Delta^2\} = 0 \qquad \text{(B3.1)}$$

after an integration by parts and using (3.3.1) and (3.3.14). The integrals in (B3.1) are with respect to n and extend across the vortex layer. [ ] denote jump in value across the layer.

Similarly, on multiplying (3.6.3) by Δ and integrating across the layer gives

$$\frac{\partial}{\partial t}\int\Delta^2 - \frac{\partial}{\partial s}\int\Delta^3 + \frac{3\partial\bar{u}_0}{\partial s}\int\Delta^2 + \bar{u}_0\frac{\partial}{\partial s}\int\Delta^2 + [\Delta^2 v] = -2\bar{\nu}\int_{-\infty}^{\infty}\bar{\omega}^2 dn \qquad \text{(B3.2)}$$

On subtracting (B3.2) from (B3.1) and using the circulation density equation (3.4.10), gives

$$\frac{\partial}{\partial t}\int_{-\infty}^{\infty}\Delta(\gamma-\Delta)dn + \bar{u}_0\frac{\partial}{\partial s}\int_{-\infty}^{\infty}\Delta(\gamma-\Delta)dn + \frac{3\partial\bar{u}_0}{\partial s}\int_{-\infty}^{\infty}\Delta(\gamma-\Delta)dn - \frac{\partial\gamma}{\partial s}\int_{-\infty}^{\infty}\Delta(\gamma-\Delta)dn$$

$$- \frac{\partial}{\partial s}\int_{-\infty}^{\infty}\Delta^2(\gamma-\Delta)dn = 2\bar{\nu}\int_{-\infty}^{\infty}\bar{\omega}^2 dn \qquad \text{(B3.3)}$$

or introducing δ_2 and writing in terms of Γ,t variables

$$U^2\frac{\partial}{\partial t}(\frac{\delta_2}{U}) + \frac{1}{2}\frac{\partial}{\partial\Gamma}(U^3\delta_2) = \frac{\partial}{\partial\Gamma}(U^2\delta_3) + \frac{2\bar{\nu}}{U}\int_{-\infty}^{\infty}\bar{\omega}^2 dn \qquad \text{(B3.4)}$$

where the equation for circulation density has been used to eliminate $\frac{\partial u_0}{\partial s}$ and where δ_3 is given by

$$\delta_3 = \int_{-\infty}^{\infty} \frac{\Delta^2}{U^2} \left(1 - \frac{\Delta}{U}\right) \, dn$$

δ_3 corresponds to the energy thickness of the boundary layer theory.

APPENDIX C: Modification to Kirchoff's invariant

A modification to Kirchoff's invariant for a vortex sheet to allow for a uniform distribution in a layer of small thickness was obtained in (M). This is extended here to the case of a non-uniform vorticity distribution.

For a vortex sheet, Kirchoff's invariant is

$$\tilde{W}_0 = -\frac{\rho_0}{8\pi}\int_0^{\Gamma_e}\int_0^{\Gamma_e} \log|z(\Gamma,t) - z(\Gamma',t)|d\Gamma d\Gamma' \qquad (C3.1)$$

where ρ_0 is the density of the fluid.

A short calculation shows that

$$\frac{d\tilde{W}_0}{dt} = -\frac{\rho_0}{2\pi}\left[\mathrm{Re}\int_0^{\Gamma_e}\frac{\partial z}{\partial t}(\Gamma,t)\left\{\oint_0^{\Gamma_e}\frac{d\Gamma'}{z(\Gamma,t)-z(\Gamma',t)}\right\}d\Gamma\right] \qquad (C3.2)$$

Then from (3.5.19) and (3.5.21),

$$\frac{d\tilde{W}_0}{dt} = -\frac{\rho_0}{2\pi}\,\mathrm{Re}\int_0^{\Gamma_e}\left(2\pi i\,\frac{\partial z}{\partial t}\frac{\partial z^*}{\partial t} - 2\pi\,\frac{\partial z}{\partial t}\frac{\partial}{\partial \Gamma}\left(\delta_2 U^3\,\frac{\partial z^*}{\partial \Gamma}\right) + O(\varepsilon^2)\right)d\Gamma \qquad (C3.3)$$

where $\delta_2(\Gamma,t)$ is as in (3.5.21). The first term in the integrand, being pure imaginary, gives no contribution so that, integrating by parts,

$$\frac{d\tilde{W}_0}{dt} = -\frac{\rho_0}{2}\int_0^{\Gamma_e}\delta_2 U^3\left(\frac{\partial z^*}{\partial \Gamma}\frac{\partial^2 z}{\partial \Gamma \partial t} + \frac{\partial z}{\partial \Gamma}\frac{\partial^2 z^*}{\partial \Gamma \partial t}\right)d\Gamma + O(\varepsilon^2) \qquad (C3.4)$$

and since

$$U^2 = \left(\frac{\partial z}{\partial \Gamma}\frac{\partial z^*}{\partial \Gamma}\right)^{-1}$$

$$\begin{aligned}\frac{d\tilde{W}_0}{dt} &= \frac{\rho_0}{2}\int_0^{\Gamma_e}\frac{\delta_2}{U}\frac{\partial U^2}{\partial t}\,d\Gamma + O(\varepsilon^2)\\ &= \frac{\rho_0}{2}\int_0^{\Gamma_e}\left\{\frac{\partial}{\partial t}(\delta_2 U) - U^2\frac{\partial}{\partial t}\left(\frac{\delta_2}{U}\right)\right\}d\Gamma + O(\varepsilon^2)\end{aligned} \qquad (C3.5)$$

The second term in the integrand in (C3.5) can be eliminated by using (B3.4) to give

$$\frac{d}{dt}\left(\tilde{W}_0 - \frac{\rho_0}{2}\int_0^{\Gamma_e} U\delta_2 d\Gamma\right) = -\bar{\mu}\int_0^{\Gamma_e}\left(\frac{1}{U}\int_{-\infty}^{\infty}\bar{\omega}^2 dn\right)d\Gamma + O(\varepsilon^2) \qquad (C3.6)$$

where $\bar{\mu} = \rho_0\bar{\nu}$.

APPENDIX D: Solution of integral equation for Δ_- of §7

Equation (3.7.7) can be written

$$\frac{d}{dy}\left(\frac{1}{w}\int_{-\infty}^{y}\Delta_-\right) - \frac{2w'}{w^2}\int_{-\infty}^{\infty}\frac{(w_1-w)}{w_1-w_2}\Delta_- dy = \frac{w_1}{2}\frac{(w-w_2-yw')}{w^2}(a_+^* + a_-) \qquad (D3.1)$$

so that

$$\Delta_- = \frac{2w'}{w_2}\int_{-\infty}^{\infty}\frac{(w_1-w)}{w_1-w_2}\Delta_-(y_1)dy_1 + \frac{w_1}{2}(a_+^* + a_-)\frac{\partial}{\partial y}\left[w\int_{-\infty}^{y}\frac{(w-w_2-yw')}{w^2}\right] \qquad (D3.2)$$

(D3.2) is of the form

$$\Delta_-(y) = \int_{-\infty}^{\infty} K(y,y_1)\Delta_-(y_1)dy_1 + G(y) \qquad (D3.3)$$

with

$$K(y,y_1) = \frac{2w'(y)}{w_2}\frac{(w_1-w(y_1))}{w_1-w_2}$$

and

$$G(y) = \frac{w_1}{2}(a_+^* + a_-)\frac{\partial}{\partial y}\left[w\int_{-\infty}^{y}\frac{w-w_2-yw'}{w^2}dy\right]$$

Then $K(y,y_1)$ is degenerate and so if

$$\beta_1 = \int_{-\infty}^{\infty}(w_1-w(y_1))\Delta_-(y_1)dy ,$$

multiplying (D3.3) by $w_1-w(y)$ and integrating with respect to y gives

$$\beta_1\left(1 - \frac{2}{w_1-w_2}\int_{-\infty}^{\infty}w'(w_1-w)dy\right) = \int_{-\infty}^{\infty}(w_1-w(y))G(y)dy$$

Hence,

$$\Delta_-(y) = G(y) + \frac{2}{(w_1-w_2)(2w_2-w_1)}\int_{-\infty}^{\infty}(w_1-w(y))G(y)dy \qquad (D3.4)$$

CHAPTER 4: HIGHER ORDER APPROXIMATION TO THE EQUATION OF MOTION OF A VORTEX LAYER

§1 Introduction

The equation of motion of a vortex layer derived in Chapter 3 is valid provided the thickness of the layer is small compared with the radius of curvature of the centroid line. Thus (3.5.19) describes the motion of long waves on a vortex layer fairly well. It might be thought that with a suitable choice of vorticity distribution (e.g. uniform vorticity in a thin layer), (3.5.19) can be integrated numerically to study the evolution of such waves. However, in any numerical calculation short wave disturbances are bound to be excited numerically and it is necessary to determine the behaviour of these disturbances. The situation is similar to that of Kortweg-de Vries equation (Benjamin, et al. 1972) which is asymptotically valid for long waves, but which displays a spurious instability for short waves.

In the case of a non-viscous uniform vortex layer, Moore (1978; (M)) has used the modified equation corresponding to (3.5.19) to consider sinusoidal disturbances to an initially straight layer and has obtained the growth rate of such disturbances. This reveals that short waves are strongly amplified. From the analysis of Ch. 3, §8, it would appear that the same would be true in the case of a non-uniform vorticity distribution. Thus any numerical work involving the equation (3.5.19) would be faced with a serious difficulty.

From Moore's analysis it is apparent that the difficulty is purely an artefact of the truncation in the expansion in ε, made by neglecting terms of $O(\varepsilon^2)$. Hence a possible remedy is to obtain a higher order approximation to the governing equation in the hope that this would give a suitable growth rate for disturbances to the solutions of the

governing equation. This is pursued in the following sections of this chapter. For simplicity, the analysis is restricted to the case of a non-viscous vortex layer of uniform vorticity and finite thickness. Thus in this chapter the matching achieved in (M) is extended to include higher order terms; in fact, terms up to $O(\varepsilon^3)$ are included in the analysis.

The inner and outer solutions to $O(\varepsilon^3)$ are obtained in §2 and §3 respectively and are matched in §4 to obtain the equation of motion. The higher order terms are checked against known solutions of the equation.

In §5, the derived equation is used to obtain the growth rate of sinusoidal perturbations to an initially straight uniform vortex layer. The results, unfortunately, are discouraging; while for long waves, for which the governing equation is valid, the growth rate is in good agreement with Rayleigh's (1896, p.342) exact result, short waves are still strongly amplified. Hence the numerical difficulty mentioned above is not resolved by obtaining the equation of motion to a higher degree of approximation.

§2 The inner flow to $O(\varepsilon^3)$

Let C be the plane curve defined in Ch. 3, §2. For a layer of constant vorticity, C is identified with the centre line of the vortex layer. Thus in terms of the intrinsic coordinates (s,n) of Chapter 3, based on C, the non-viscous vorticity distribution can be expressed as

$$\bar{\omega}(s,n,t) = \begin{cases} \bar{\omega}_0 & -H(s,t) < n < H(s,t) \\ 0 & \text{otherwise} \end{cases} \tag{4.2.1}$$

where $n = \pm H(s,t)$ are the boundaries C_+ and C_- of the layer and $\bar{\omega}_0$ is a constant. In order to express (4.2.1) in terms of the inner variables x,y introduced in Ch. 3, §3, we write $H = \varepsilon H_1$ and $\bar{\omega}_0 = \omega/\varepsilon$.

In this section, the components u and v of fluid velocity in the (s,n) frame are determined to $O(\varepsilon^3)$ for the constant vorticity case. More precisely, in the notation of Ch. 3 §3, terms up to u_3 and v_3 in the expansions (3.3.5) are determined for $\bar{\omega}$ given by (4.2.1). The approximation to u is then used to obtain the convection speed U_c to $O(\varepsilon^3)$.

The boundary conditions at $y = \pm\infty$ are to be replaced by those at C_+ and C_-. Firstly, since $\underline{\bar{u}}$, the fluid velocity in a coordinate frame $\overline{OXY}$ fixed with respect to flow at infinity, is continuous across C_+ and C_-, it follows from (3.2.7) that u and v also are to be continuous across these curves.

Secondly, a kinematic condition is to be satisfied at each boundary. This can be shown (M §2) to be

$$v(s,H,t) = \frac{\partial H}{\partial t} + \left(1 - \frac{H}{\rho}\right)^{-1} u(s,H,t)\, \frac{\partial H}{\partial s} \tag{4.2.2}$$

at C_+ and

$$-v(s,-H,t) = \frac{\partial H}{\partial t} + (1 + \frac{H}{\rho})^{-1} u(s,-H,t) \frac{\partial H}{\partial s} \qquad (4.2.3)$$

at C_-.

For consistency with the expansions (3.3.4) for $\frac{\partial \underline{R}}{\partial t}$ and angular speed $\Omega(s,t)$ and (3.3.5) for u and v, the unknown time derivative $\frac{\partial H}{\partial t}$ must also be expanded in terms of ε. Thus

$$\frac{\partial H}{\partial t} \equiv \varepsilon \frac{\partial H_1}{\partial t} = \varepsilon(H_1(x,t) + \varepsilon H_2(x,t) + \varepsilon^2 H_3(x,t) + \ldots) \qquad (4.2.4)$$

Then with $\bar{\omega}$ as in (4.2.1), the set of equations (3.3.7), obtained from the kinematic vorticity equation, together with the above boundary conditions can be used to give $u_0, u_1, u_2, u_3, \ldots$. Thus from the first two equations of the set u_0 and u_1 can be determined. These are given by (M (2.19), (2.20)); note that in (M) $\bar{u}_0$, $\bar{u}_1$ (called A in (M)) refer to values of u_0, u_1 at y = 0 and therefore differ from $\bar{u}_0$, $\bar{u}_1$ as used in Ch. 3. For consistency, Moore's definition of these quantities will be used from henceforth.

If u_0, u_1 and v_1 (M (2.23), (2.28)) are substituted from (M) into the third equation of the set (3.3.7) and the equation integrated, then

$$u_2 = \begin{cases} J + \frac{\omega}{\rho^2}[-H_1 y^2 + \frac{1}{2}H_1^2 y] + \frac{\omega}{2}\frac{\partial^2 H_1}{\partial x^2} y^2 - \omega \frac{\partial}{\partial x}(H_1 \frac{\partial H_1}{\partial x})y + \bar{u}_{2+}(x,t) & y > H_1 \\ J + \frac{\omega y^3}{2\rho^2} + \bar{u}_2 & H_1 > y > -H_1 \\ J + \frac{\omega}{\rho^2}[H_1 y^2 + \frac{1}{2}H_1^2 y] - \frac{\omega}{2}\frac{\partial^2 H_1}{\partial x^2} y^2 - \omega \frac{\partial}{\partial x}(H_1 \frac{\partial H_1}{\partial x})y + \bar{u}_{2-}(x,t) & y < -H_1 \end{cases} \qquad (4.2.5)$$

where

$$J = 2\Omega_1 y + \frac{1}{\rho}(\Omega_0 y^2 + \bar{u}_1 y) - \tfrac{1}{2}\frac{\partial^2 \bar{u}_0}{\partial x^2} y^2 - \omega \frac{\partial}{\partial x}(H_1 \frac{\partial H_1}{\partial x})y + \frac{\bar{u}_0 y^2}{\rho^2}$$

and $\bar{u}_2$, $\bar{u}_{2+}$ and $\bar{u}_{2-}$ are independent of y. Since u_2 is required to be continuous across the boundaries C_+ and C_-, we must have

$$\bar{u}_{2+} = \bar{u}_2 + \frac{\partial^2}{\partial x^2}\left(\frac{\omega H_1^3}{6}\right)$$

$$\bar{u}_{2-} = \bar{u}_2 - \frac{\partial^2}{\partial x^2}\left(\frac{\omega H_1^3}{6}\right) \qquad (4.2.6)$$

$\bar{u}_2(x,t)$ is arbitrary and is to be determined by matching.

From the second of the equations (3.2.6), after substituting for u_0, u_1 and v_1 from (M) and integrating, we have

$$v_2 = \begin{cases} K + \frac{\omega}{\rho}\frac{\partial H_1}{\partial x}(y^2 - H_1 y) + \frac{1}{2}\frac{\partial}{\partial x}\left(\frac{\omega H_1}{\rho}\right)y^2 - \frac{1}{2}\frac{\partial}{\partial x}\left(\frac{\omega H_1^2}{\rho}\right)y + \bar{v}_{2+}(x,t) & y > H_1 \\ K + \frac{\omega}{6}\frac{\partial}{\partial x}\left(\frac{1}{\rho}\right)y^3 + \bar{v}_2(x,t) & H_1 > y > -H_1 \\ K - \frac{\omega}{\rho}\frac{\partial H_1}{\partial x}(y^2 + H_1 y) - \frac{1}{2}\frac{\partial}{\partial x}\left(\frac{\omega H_1}{\rho}\right)y^2 - \frac{1}{2}\frac{\partial}{\partial x}\left(\frac{\omega H_1^2}{\rho}\right)y + \bar{v}_{2-}(x,t) & y < -H_1 \end{cases} \qquad (4.2.7)$$

where

$$K = -\frac{1}{2}\frac{\partial}{\partial x}\left(\Omega_0 + \frac{\bar{u}_0}{\rho}\right)y^2 - \frac{1}{\rho}\frac{\partial \bar{u}_0}{\partial x}y^2 - \frac{\omega H_1}{\rho}\frac{\partial H_1}{\partial x}y - \frac{\partial \bar{u}_1}{\partial x}y$$

and $\bar{v}_{2+}$, $\bar{v}_2$ and $\bar{v}_{2-}$ are to be determined. For v_2 to be continuous across $y = \pm H_1$ we must have

$$\bar{v}_{2+}(x,t) = \bar{v}_2(x,t) + \frac{\partial}{\partial x}\left(\frac{\omega H_1^3}{6\rho}\right)$$

$$\bar{v}_{2-}(x,t) = \bar{v}_2(x,t) - \frac{\partial}{\partial x}\left(\frac{\omega H_1^3}{6\rho}\right) \qquad (4.2.8)$$

$\bar{v}_2$ will now be determined from the kinematic boundary condition which has to be satisfied. Expanding the kinematic condition (4.2.2) at C_+ and condition (4.2.3) at C_- in terms of ε and equating coefficients of powers of ε to zero leads, respectively, to the sets

$$\pm v_1(x,\pm H_1,t) = H_1 + u_0(x,\pm H_1,t)\frac{\partial H_1}{\partial x}$$

$$\pm v_2(x,\pm H_1,t) = H_2 + [u_1(x,\pm H_1,t) \pm u_0(x,\pm H_1,t)\frac{H_1}{\rho}]\frac{\partial H_1}{\partial x}$$

$$\pm v_3(x,\pm H_1,t) = H_3 + [u_2(x,\pm H_1,t) \pm u_1(x,\pm H_1,t)\frac{H_1}{\rho} + u_0(x,\pm H_1,t)\frac{H_1^2}{\rho^2}]\frac{\partial H_1}{\partial x}$$

. . . . . (4.2.9)

On substituting for u_0, u_1 and v_2 into the second pair of equations of the set (4.2.9), it is found that these are satisfied provided

$$\bar{v}_2 = 2H_1\frac{\partial H_1}{\partial x}(\Omega_0 + \frac{\bar{u}_0}{\rho}) + \frac{H_1^2}{2}[\frac{\partial}{\partial x}(\Omega_0 + \frac{\bar{u}_0}{\rho}) + \frac{2}{\rho}\frac{\partial \bar{u}_0}{\partial x}] \qquad (4.2.10)$$

and

$$H_2 + \frac{\partial}{\partial x}(H_1[\bar{u}_1 - \frac{\omega H_1^2}{6\rho}]) = 0 \qquad (4.2.11)$$

Equation (4.2.11) can also be obtained by expanding the circulation density equation and equating coefficient of ε^2 to zero; this serves as a check on the algebra.

The expressions (4.2.5) and (4.2.7) for u_2 and v_2 can be substituted into the sets (3.3.7), (3.2.6) to obtain u_3 and v_3. Then, after applying the boundary conditions, the final results can be written as

$$u_3 = \begin{cases} J_1 + \omega L_3 y^3 - \omega L_2 y^2 + \omega L_1 y + \bar{u}_{3+}(x,t) & y > H_1 \\ J_1 + \frac{\omega}{24}\frac{\partial^2}{\partial x^2}(\frac{1}{\rho})y^4 - \frac{\omega y^4}{2\rho^3} + \bar{u}_3(x,t) & H_1 > y > -H_1 \\ J_1 - \omega L_3 y^3 - \omega L_2 y^2 - \omega L_1 y + \bar{u}_{3-}(x,t) & y < -H_1 \end{cases} \qquad (4.2.12)$$

where $J_1 = 2\Omega_2 y - \frac{\Omega_1 y^2}{\rho} + \int^y \frac{\partial K}{\partial x} + \frac{Jy}{\rho} + \frac{\partial \bar{v}_2}{\partial x} y - \frac{\bar{u}_2 y}{\rho}$,

$L_1 = \frac{1}{6\rho} \frac{\partial^2 H_1^3}{\partial x^2} + \frac{\partial}{\partial x} (\frac{H_1^3}{6\rho})$, $L_3 = \frac{1}{\rho} \frac{\partial^2 H_1}{\partial x^2} + \frac{2}{3} \frac{\partial}{\partial x}(\frac{1}{\rho}) \frac{\partial H_1}{\partial x} + \frac{H_1}{6} \frac{\partial^2}{\partial x^2}(\frac{1}{\rho}) - \frac{H_1}{\rho^3}$

$L_2 = \frac{1}{\rho} \frac{\partial^2 H_1^2}{\partial x^2} + \frac{3}{4} \frac{\partial H_1^2}{\partial x} \frac{\partial}{\partial x}(\frac{1}{\rho}) + \frac{H_1^2}{4} \frac{\partial^2}{\partial x^2} (\frac{1}{\rho}) - \frac{H_1^2}{2\rho^3}$,

and $\bar{u}_{3\pm}(x,t)$ are given by

$$\bar{u}_{3\pm}(x,t) = \bar{u}_3 - \frac{\omega H_1^3}{6} \frac{\partial H_1}{\partial x} \frac{\partial}{\partial x} (\frac{1}{\rho}) - \frac{\omega H_1^4}{24} \frac{\partial^2}{\partial x^2} (\frac{1}{\rho}) , \qquad (4.2.13)$$

$\bar{u}_3$ being arbitrary. Thus $\bar{u}_{3+} = \bar{u}_{3-}$. v_3 is given by

$$v_3 = \begin{cases} K_1 + \omega M_3 y^3 - \omega M_2 y^2 + \omega M_1 y + \bar{v}_{3+}(x,t) & y > H_1 \\ K_1 + \frac{5\omega}{12\rho} \frac{\partial}{\partial x} (\frac{1}{\rho}) y^4 + \bar{v}_3(x,t) & H_1 > y > -H_1 \\ K_1 - \omega M_3 y^3 - \omega M_2 y^2 - \omega M_1 y + \bar{v}_{3-}(x,t) & y < -H_1 \end{cases} \qquad (4.2.14)$$

where

$K_1 = \frac{\partial \Omega_1}{\partial x} \frac{y^2}{2} + \frac{Ky}{\rho} - \int^y \frac{\partial J}{\partial x} + \frac{\bar{v}_2 y}{\rho} - \frac{\partial \bar{u}_2}{\partial x} y$

$M_1 = \frac{1}{6\rho} \frac{\partial}{\partial x} (\frac{H_1^3}{\rho}) - \frac{1}{6} \frac{\partial^3}{\partial x^3} H_1^3$, $M_2 = \frac{5}{2} \frac{H_1}{\rho^2} \frac{\partial H_1}{\partial x} + \frac{H_1^2}{\rho} \frac{\partial}{\partial x} (\frac{1}{\rho}) - \frac{1}{2} \frac{\partial^2}{\partial x^2}(H_1 \frac{\partial H_1}{\partial x})$

$M_3 = \frac{5}{6\rho^2} \frac{\partial H_1}{\partial x} + \frac{7}{6} \frac{H_1}{\rho} \frac{\partial}{\partial x} (\frac{1}{\rho}) - \frac{1}{6} \frac{\partial^3 H_1}{\partial x^3}$

The boundary conditions at $y = \pm H_1$ imply that

$$\bar{v}_{3+} = \bar{v}_{3-} = \bar{v}_3 + \omega H_1 [\frac{H_1^2}{12\rho}(H_1 \frac{\partial}{\partial x}(\frac{1}{\rho}) - \frac{10}{\rho} \frac{\partial H_1}{\partial x}) + \frac{H_1^2}{6} \frac{\partial^3 H_1}{\partial x^3} + \frac{3H_1}{2} \frac{\partial H_1}{\partial x} \frac{\partial^2 H_1}{\partial x^2} + (\frac{\partial H_1}{\partial x})^3] \qquad (4.2.15)$$

and that

$$H_3 + \frac{\partial}{\partial x}\left(\frac{H_1^3}{3\rho}(\Omega_0 + \frac{\bar{u}_0}{\rho}) - \frac{H_1^3}{6}\frac{\partial^2\bar{u}_0}{\partial x^2} + \bar{u}_2 H_1\right) = 0 \qquad (4.2.16)$$

$$\frac{\bar{v}_{3+}+\bar{v}_{3-}}{2} = \frac{H_1^2}{2}\frac{\partial}{\partial x}(\Omega_1 + \frac{\bar{u}_1}{\rho}) + 2H_1\frac{\partial H_1}{\partial x}(\Omega_1 + \frac{\bar{u}_1}{\rho}) + \frac{H_1^2}{\rho}\frac{\partial \bar{u}_1}{\partial x} - \omega H_1 \times$$

$$\times\left[\frac{5H_1^2}{6\rho^2}\frac{\partial H_1}{\partial x} + \frac{H_1^2}{3}\frac{\partial^3 H_1}{\partial x^3} + \frac{H_1^3}{3\rho}\frac{\partial}{\partial x}(\frac{1}{\rho}) + H_1\frac{\partial^2 H_1}{\partial x^2}\frac{\partial H_1}{\partial x}\right] \qquad (4.2.17)$$

Equation (4.2.16) again serves as a check on the algebra since it can be obtained by expanding the circulation density equation (see expression for U_c below).

Finally, the convection speed, defined by

$$U_c \equiv \frac{1}{2H_1}\int_{-H_1}^{H_1} u\,dy = \frac{1}{2H_1}\int_{-H_1}^{H_1}(u_0+\varepsilon u_1+\varepsilon^2 u_2+\varepsilon^3 u_3+\ldots)\,dy$$

can be calculated to $O(\varepsilon^3)$. Substituting for u_i $(i = 0,1,2,3)$ and integrating gives

$$U_c = \bar{u}_0 + \varepsilon[\bar{u}_1 - \frac{\omega H_1^2}{6\rho}] + \varepsilon^2[\bar{u}_2 + \frac{H_1^2}{3}(\frac{\Omega_0}{\rho} + \frac{\bar{u}_0}{\rho^2} - \tfrac{1}{2}\frac{\partial^2\bar{u}_0}{\partial x^2})] + \varepsilon^3[\bar{u}_3 + \frac{H_1^2}{3\rho}(\Omega_1 + \frac{\bar{u}_1}{\rho}) -$$

$$- \frac{H_1^2}{6}\frac{\partial^2\bar{u}_1}{\partial x^2} + \omega H_1^2(\frac{H_1^2}{120}\frac{\partial^2}{\partial x^2}(\frac{1}{\rho}) - \frac{H_1^2}{10\rho^3} - \frac{1}{2\rho}\frac{\partial}{\partial x}(H_1\frac{\partial H_1}{\partial x}) - \frac{H_1}{6}\frac{\partial}{\partial x}(\frac{1}{\rho})\frac{\partial H_1}{\partial x}]$$

$$+ O(\varepsilon^4) \qquad (4.2.18)$$

§3 The outer solution to $O(\varepsilon^3)$

From (3.4.4), in view of the vorticity distribution (4.2.1), the complex velocity at z, a point exterior to the layer, is given by (after a re-arrangement),

$$q(z,t) = -\frac{i}{2\pi}\int_0^{a(t)} \frac{ds'}{z-Z(s',t)} \int_{-H}^{H} \bar{\omega}_0 \left(1 - \frac{n'}{\rho(s',t)}\right)\left(1 - \frac{ie^{i\alpha'}n'}{z-Z(s',t')}\right)^{-1} dn' \tag{4.3.1}$$

where Z and α' are as in Ch. 3, §4.

The integrand in the inner integral can be expanded in terms of powers of n (see M (3.5)-(3.9)) and term-by-term integration carried out so that, since odd powers of n integrate to zero, we have

$$q(z,t) = -\frac{i}{2\pi}\int_0^{a(t)} \frac{2\bar{\omega}_0 H(s',t)ds'}{z-Z(s',t)} - \frac{i}{2\pi}\int_0^{a(t)} \frac{\frac{2}{3}\bar{\omega}_0 H^3(s',t)I_2(s',t)ds'}{z-Z(s',t)}$$

$$- \frac{i}{2\pi}\int_0^{a(t)} \frac{\frac{2}{5}\bar{\omega}_0 H^5(s',t)I_4(s',t)ds'}{z-Z(s',t)} + \ldots. \tag{4.3.2}$$

where

$$I_m(s,t) = \frac{i^m e^{im\alpha}}{(z-Z)^m} - \frac{i^{m-1}e^{(m-1)i\alpha}}{\rho(z-Z)^{m-1}} \tag{4.3.3}$$

Let z be given by

$$z = Z(s,t) + ine^{i\alpha} \tag{4.3.4}$$

As noted in Ch. 3, §4 the integrals on the right hand side of (4.3.2) remain bounded as $z \to Z(s,t)$, a point on the centre-line. Thus, uniformly in z, the outer solution, in terms of the inner variables, is

$$q(z,t) = -\frac{i}{2\pi}\int_0^{a(t)} \frac{\gamma dx'}{Z(x,t)+i\varepsilon ye^{i\alpha}-Z(x',t)} - \frac{i\varepsilon^2}{2\pi}\int_0^{a(t)} \frac{\frac{1}{3}\gamma H_1^2 I_2 dx'}{Z(x,t)+i\varepsilon ye^{i\alpha}-Z(x',t)}$$

$$+ O(\varepsilon^4) \tag{4.3.5}$$

where $H(s,t) = \varepsilon H_1(s,t)$ is written and the fact that the circulation density $\gamma(s,t)$ as defined in Ch. 3 is given by $\gamma(s,t) = 2\bar{\omega}_0 H$ is used.

In (4.3.5) the integral proportional to ε^3 is zero since the distribution of vorticity is symmetrical about the centre-line. In the case of a general distribution of vorticity this would be no longer so and the integral has to be considered in order to evaluate the third order approximation.

The inner limit of the outer solution is now sought. Let

$$Q_{\pm}^{(0)}(Z,t) = \lim_{y\to 0_{\pm}} \left(-\frac{i}{2\pi}\int_0^{a(t)} \frac{\gamma(x',t)dx'}{Z(x,t)+i\varepsilon y e^{i\alpha}-Z(x',t)}\right) \tag{4.3.6}$$

$$Q_{\pm}^{(2)}(Z,t) = \lim_{y\to 0_{\pm}} \left(-\frac{i}{2\pi}\int_0^{a(t)} \frac{\frac{1}{3}\gamma H_1{}^2 I_2 dx'}{Z(x,t)+i\varepsilon y e^{i\alpha}-Z(x',t)}\right) \tag{4.3.7}$$

Then from (M(4.5),(4.6)), $Q_{\pm}^{(0)}(Z,t)$ is given by

$$Q_{\pm}^{(0)}(Z,t) = -\frac{i}{2\pi}\int_0^{a(t)} \frac{\gamma(x',t)dx'}{Z(x,t)-Z(x',t)} \mp \tfrac{1}{2}\gamma(x,t)e^{-i\alpha} \tag{4.3.8}$$

where the slash denotes Cauchy principal value integral.

Now on substituting for I_2 in the integral in (4.3.7) and noting that $\frac{\partial Z}{\partial x} = e^{i\alpha}$, the term in ( ) becomes

$$\frac{i}{6\pi}\left\{\int_C \frac{\gamma H_1{}^2 e^{i\alpha'}dZ'}{(z-Z')^3} + \int_C \frac{i\gamma \frac{H_1{}^2}{\rho}dZ'}{(z-Z')^2}\right\} \tag{4.3.9}$$

where z is as in (4.3.4) and C is the centre-line. For z,Z real and z on the path of the integration, Mangler (1952) has defined principal values for integrals of the type appearing in (4.3.9). However, here it is convenient to proceed in the following manner.

Define

$$f(Z) = -\frac{i\gamma H_1^2 e^{i\alpha}}{6\pi}, \qquad g(Z) = \frac{-\gamma \frac{H_1^2}{\rho}}{6\pi} \tag{4.3.10}$$

$f(Z)$ and $g(Z)$ are analytic and

$$f'(Z) = e^{-i\alpha}\frac{\partial}{\partial x}\left(-\frac{i\gamma H_1^2}{6\pi}e^{i\alpha}\right) = -\frac{i}{24\pi\omega^2}\{3\gamma^2\frac{\partial\gamma}{\partial x} + \frac{i\gamma^3}{\rho}\}$$

$$f''(Z) = e^{-i\alpha}\frac{\partial}{\partial x}\left(e^{-i\alpha}\frac{\partial}{\partial x}\left(-\frac{i\gamma H_1^2 e^{i\alpha}}{6\pi}\right)\right) = -\frac{ie^{i\alpha}}{24\pi\omega^2}\{\frac{\partial^2}{\partial x^2}\gamma^3 + i\frac{\partial}{\partial x}(\frac{\gamma^3}{\rho})\}$$

where $\gamma = 2\omega H_1$ is used. Similarly,

$$g'(Z) = -\frac{1}{24\pi\omega^2}\frac{\partial}{\partial x}(\frac{\gamma^3}{\rho})$$

Note that since $\gamma(x,t)$ is assumed to vanish at the ends $x = 0$, $x = a(t)$ (Ch. 3, §1), f, g, f', f'' and g' also vanish there. Also g'' vanishes at the ends while f''' will vanish there provided $\frac{\partial\gamma}{\partial x}$ does; this will be assumed to be so. Then (4.3.9) can be written

$$\int_C (\frac{f(Z)}{(Z-z)^3} + \frac{g(Z)}{(Z-z)^2})dZ = \int_C (-\frac{d}{dZ}(\frac{\frac{1}{2}f(Z)}{(Z-z)^2} + \frac{g(Z)}{Z-z}) + \frac{\frac{1}{2}f'(Z)}{(Z-z)^2} + \frac{g'(Z)}{Z-z})dZ$$

$$= -[\frac{f(Z)}{2(Z-z)^2} + \frac{g(Z)}{Z-z}]_{\text{ends}} + \int_C (\frac{\frac{1}{2}f'(Z)}{(Z-z)^2} + \frac{g'(Z)}{Z-z})dZ$$

The term [ ] is, uniformly in z, equal to zero since f, $f'''(Z)$ and g, $g''(Z)$ vanish at the ends. Then

$$\int_C (\frac{\frac{1}{2}f'(Z)}{(Z-z)^2} + \frac{g'(Z)}{Z-z})dZ = \int_C \{-\frac{d}{dZ}(\frac{\frac{1}{2}f'(Z)}{(Z-z)}) + \frac{\frac{1}{2}f''(Z) + g'(Z)}{Z-z}\}\, dZ$$

$$= -[\frac{\frac{1}{2}f'(Z)}{Z-z}]_{\text{ends}} + \int_C \frac{\frac{1}{2}f''(Z) + g'(Z)}{Z-z}\, dZ$$

Again the term [ ] is, uniformly in z, equal to zero since f', f"(Z) vanish at the ends. Thus

$$Q_{\pm}^{(2)}(Z) = \lim_{\substack{z\to Z \\ \text{from} \pm \text{side} \\ \text{of C}}} \int_C \frac{\frac{1}{2}f''(Z) + g'(Z)}{Z-z}\, dZ \qquad (4.3.11)$$

From the Plemelj formulae (Mushkelishvili (1958), p.42), we have

$$Q_{\pm}^{(2)}(Z) = \oint_C \frac{\frac{1}{2}f''(Z')+ g'(Z')}{Z'-Z}\, dZ' \pm \pi i\{ \frac{f''(Z)}{2} + g'(Z)\} \qquad (4.3.12)$$

On substituting for f" and g', (4.3.12) becomes

$$Q_{\pm}^{(2)}(Z(x,t)) = \frac{i}{12\pi} \int_0^{a(t)} \frac{\frac{\partial^2}{\partial x^2}(\gamma(x')H_1(x')^2) - i\frac{\partial}{\partial x'}(\frac{\gamma(x')H_1^2(x')}{\rho(x')})}{Z(x,t) - Z(x',t)}\, dx'$$

$$\pm \frac{e^{-i\alpha}}{12}\{\frac{\partial^2}{\partial x^2}(\gamma H_1^2) - i\frac{\partial}{\partial x}(\frac{\gamma H_1^2}{\rho})\} \qquad (4.3.13)$$

Then the inner limit of the outer solution is given by

$$q(z,t) = Q_{\pm}^{(0)} + i\varepsilon y \frac{\partial Q_{\pm}^{(0)}}{\partial Z} + \varepsilon^2(Q_{\pm}^{(2)} - \frac{(ye^{i\alpha})^2}{2!}\frac{\partial^2 Q_{\pm}^{(0)}}{\partial Z^2})$$

$$+ i\varepsilon^3(ye^{i\alpha}\frac{\partial Q_{\pm}^{(2)}}{\partial Z} - \frac{(ye^{i\alpha})^3}{3!}\frac{\partial^3 Q_{\pm}^{(0)}}{\partial Z^3}) + O(\varepsilon^4) \qquad (4.3.14)$$

according as $z \to Z$ from $\pm$ side of C respectively.

In the next section (4.3.14) is matched with the outer limit of the inner solution.

§4 Matching

Introducing the expansion (3.5.3) for $\frac{\partial Z^*}{\partial t}$ into (3.5.2), the inner velocity, in complex notation, for points z exterior to the layer is given by

$$q^I(z,t) = \Pi_0^* + u_0 e^{-i\alpha} + \varepsilon\{\Pi_1^* + (u_1 - iv_1)e^{-i\alpha} - y\Omega_0 e^{-i\alpha}\}$$
$$+ \varepsilon^2\{\Pi_2^* + (u_2 - iv_2)e^{-i\alpha} - y\Omega_1 e^{-i\alpha}\} + \varepsilon^3\{\Pi_3^* + (u_3 - iv_3)e^{-i\alpha} - y\Omega_2 e^{-i\alpha}\}$$
$$+ O(\varepsilon^4) \qquad (4.4.1)$$

where u_i and v_i are evaluated at $y > H_1$ or $y < -H_1$ according as z is on $\pm$ side of C. Then (4.4.1) constitutes the outer limit of the inner solution and must coincide with (4.3.14) as $\varepsilon \to 0$ with y fixed.

The $O(1)$ and $O(\varepsilon)$ terms can be matched to obtain Π_0^*, Π_1^*. These are given by (M (4.7), (4.12)).

Matching of the $O(\varepsilon^2)$ terms which are independent of y requires that

$$\Pi_2^* + (\bar{u}_{2\pm} - i\bar{v}_{2\pm})e^{-i\alpha} = Q_\pm^{(2)} \qquad (4.4.2)$$

where $\bar{u}_{2\pm}$ and $\bar{v}_{2\pm}$ are given by (4.2.6) and (4.2.8) respectively. On adding the two equations (4.4.2) and substituting for $Q_\pm^{(2)}$ from (4.3.13),

$$\Pi_2^* + (\bar{u}_2 - i\bar{v}_2)e^{-i\alpha} = \frac{i}{12\pi}\int_0^{a(t)} \frac{(\frac{\partial^2}{\partial x'^2}(\gamma H_1^2) - i\frac{\partial}{\partial x'}(\frac{\gamma H_1^2}{\rho}))dx'}{Z(x,t) - Z(x',t)} \qquad (4.4.3)$$

On subtracting the two equations (4.4.2)

$$(\bar{u}_{2+} - \bar{u}_{2-}) - i(\bar{v}_{2+} - \bar{v}_{2-}) = 2(\frac{\partial^2}{\partial x^2}(\frac{\omega H_1^3}{6}) - i\frac{\partial}{\partial x}(\frac{\omega H_1^3}{6\rho})) \qquad (4.4.4)$$

in agreement with (4.2.6), (4.2.8). Matching of terms proportional to y and y^2 reveal no new information but is accomplished in Appendix A for consistency.

Similarly, matching of $O(\varepsilon^3)$ terms independent of y require that

$$\Pi_3^* + \left(\frac{\bar{u}_{3+} + \bar{u}_{3-}}{2} - i\,\frac{\bar{v}_{3+} + \bar{v}_{3-}}{2}\right)e^{-i\alpha} = 0 \tag{4.4.5}$$

and that

$$\begin{aligned} \bar{u}_{3+} &= \bar{u}_{3-} \\ \bar{v}_{3+} &= \bar{v}_{3-} \end{aligned} \tag{4.4.6}$$

Equations (4.4.6) are in agreement with (4.2.13) and (4.2.15). Hence, in view of expansion (3.5.3),

$$\frac{\partial Z^*}{\partial t} + \Big[\bar{u}_0 + \varepsilon\left(\frac{(\bar{u}_{1+}+\bar{u}_{1-})}{2} - i\,\frac{(\bar{v}_{1+}+\bar{v}_{1-})}{2}\right) + \varepsilon^2(\bar{u}_2 - i\bar{v}_2) + \varepsilon^3\left(\frac{\bar{u}_{3+}+\bar{u}_{3-}}{2} - i\,\frac{(\bar{v}_{3+}+\bar{v}_{3-})}{2}\right)\Big]e^{-i\alpha} = I + \varepsilon^2 N + O(\varepsilon^4) \tag{4.4.7}$$

where

$$I = -\frac{i}{2\pi}\int_0^{a(t)} \frac{\gamma(x,t)\,dx'}{Z(x,t) - Z(x',t)} \tag{4.4.8}$$

and

$$N = \frac{i}{48\pi\omega^2}\int_0^{a(t)} \frac{\left(\frac{\partial^2}{\partial x'^2}(\gamma^3) - i\,\frac{\partial}{\partial x'}\left(\frac{\gamma^3}{\rho}\right)\right)dx'}{Z(x,t) - Z(x',t)}$$

It is convenient to introduce the convection velocity U_c given by (4.2.18).

Thus, on substituting for the $O(\varepsilon)$ term in (4.4.7) from M (4.13), and using (4.2.6), (4.2.8), (4.2.13) and (4.2.17), (4.4.7) can be written,

$$\frac{\partial Z^*}{\partial t} + U_c e^{-i\alpha} = I + \varepsilon P_1 e^{-i\alpha} + \varepsilon^2(N + P_2 e^{-i\alpha}) + \varepsilon^3 P_3 e^{-i\alpha} + O(\varepsilon^4) \tag{4.4.9}$$

where

$$P_1 = -\frac{\gamma}{2\omega}\left(\frac{\gamma}{3\rho} + i\frac{\partial\gamma}{\partial x}\right)$$

$$P_2 = \frac{\gamma}{4\omega^2}\left[\frac{\gamma}{3}\left(\frac{1}{\rho}\left(\Omega_0 + \frac{\bar{u}_0}{\rho}\right) - \frac{1}{2}\frac{\partial^2\bar{u}_0}{\partial x^2}\right) + i\left(2\frac{\partial\gamma}{\partial x}\left(\Omega_0 + \frac{\bar{u}_0}{\rho}\right) + \frac{\gamma}{\rho}\frac{\partial\bar{u}_0}{\partial x} + \frac{\gamma}{2}\frac{\partial}{\partial x}\left(\Omega_0 + \frac{\bar{u}_0}{\rho}\right)\right)\right]$$

$$P_3 = \frac{\gamma}{8\omega^3}\left[\frac{2\omega\gamma}{3\rho}\left(\Omega_1 + \frac{\bar{u}_1}{\rho}\right) - \frac{\omega\gamma}{3}\frac{\partial^2\bar{u}_1}{\partial x^2} + \frac{\gamma}{4}\left(\frac{\gamma^2}{10}\frac{\partial^2}{\partial x^2}\left(\frac{1}{\rho}\right) - \frac{\gamma^2}{5\rho^3} - \frac{1}{\rho}\frac{\partial}{\partial x}\left(\gamma\frac{\partial\gamma}{\partial x}\right)\right)\right.$$

$$+ i\left\{\omega\gamma\frac{\partial}{\partial x}\left(\Omega_1 + \frac{\bar{u}_1}{\rho}\right) + 4\omega\frac{\partial\gamma}{\partial x}\left(\Omega_1 + \frac{\bar{u}_1}{\rho}\right) + \frac{2\omega\gamma}{\rho}\frac{\partial\bar{u}_1}{\partial x}\right.$$

$$\left.\left. - \frac{\gamma}{2}\left(\frac{5\gamma}{6\rho^2}\frac{\partial\gamma}{\partial x} + \frac{\gamma}{3}\frac{\partial^3\gamma}{\partial x^3} + \frac{\gamma^2}{3\rho}\frac{\partial}{\partial x}\left(\frac{1}{\rho}\right) + \frac{\partial^2\gamma}{\partial x^2}\frac{\partial\gamma}{\partial x}\right)\right\}\right] \qquad (4.4.10)$$

In (4.10) $H_1 = \gamma/2\omega$ has been used.

Now

$$\Omega = ie^{i\alpha}\frac{\partial^2 Z}{\partial x \partial t} \qquad (4.4.11)$$

so that

$$\Omega_0 = ie^{i\alpha}\frac{\partial}{\partial x}\Pi_0 = ie^{i\alpha}\frac{\partial}{\partial x}\left(I - \bar{u}_0 e^{-i\alpha}\right)$$

or

$$\Omega_0 + \frac{\bar{u}_0}{\rho} = ie^{i\alpha}\frac{\partial I}{\partial x} - i\frac{\partial\bar{u}_0}{\partial x} \qquad (4.4.12)$$

and

$$\Omega_1 = ie^{i\alpha}\frac{\partial}{\partial x}\Pi_1 = ie^{i\alpha}\frac{\partial}{\partial x}\left(-e^{-i\alpha}\left(\bar{u}_1 + \frac{\gamma^2}{8\omega\rho} + \frac{i\gamma}{2\omega}\frac{\partial\gamma}{\partial x}\right)\right)$$

or

$$\Omega_1 + \frac{\bar{u}_1}{\rho} = \frac{1}{2\omega}\frac{\partial}{\partial x}\left(\gamma\frac{\partial\gamma}{\partial x}\right) - \frac{\gamma^2}{8\omega\rho^2} - i\left(\frac{3\gamma}{4\omega\rho}\frac{\partial\gamma}{\partial x} + \frac{\gamma^2}{8\omega}\frac{\partial}{\partial x}\left(\frac{1}{\rho}\right) + \frac{\partial\bar{u}_1}{\partial x}\right) \qquad (4.4.13)$$

The expressions for Π_0 and Π_1 have been obtained from M((4.7), (4.12)). On separating the real and imaginary parts in (4.4.12), we have

$$\Omega_0 + \frac{\bar{u}_0}{\rho} = \mathrm{Re}(ie^{i\alpha} \frac{\partial I}{\partial x}) \tag{4.4.14}$$

and

$$\frac{\partial \bar{u}_0}{\partial x} = \mathrm{Re}(e^{i\alpha} \frac{\partial I}{\partial x}) \tag{4.4.15}$$

Similarly, on separating the real and imaginary parts in (4.4.13) gives

$$\Omega_1 + \frac{\bar{u}_1}{\rho} = \frac{1}{2\omega} (\frac{\partial}{\partial x} (\gamma \frac{\partial \gamma}{\partial x}) - \frac{\gamma^2}{4\rho^2}) \tag{4.4.16}$$

$$\frac{\partial \bar{u}_1}{\partial x} = -\frac{1}{4\omega} (\frac{3\gamma}{\rho} \frac{\partial \gamma}{\partial x} + \frac{\gamma^2}{2} \frac{\partial}{\partial x} (\frac{1}{\rho})) \tag{4.4.17}$$

Equations (4.4.15) and (4.4.17) could also have been obtained from the circulation density equation.

If the expressions given by equations (4.4.14)-(4.4.17) are substituted into (4.4.9), then on using (3.5.11)-(3.5.14), (3.5.16) and the notation (3.5.15) the circulation coordinate Γ can be introduced and (4.4.9) can be written

$$\frac{\partial z^*}{\partial t} (\Gamma,t) = \tilde{I} + \frac{\tilde{P}_1}{\bar{\omega}_0} + \frac{1}{\bar{\omega}_0^2} (\tilde{N} + \tilde{P}_2) + \frac{\tilde{P}_3}{\bar{\omega}_0^3} + O(\frac{1}{\bar{\omega}_0^4}) \tag{4.4.18}$$

where

$$\tilde{I} = -\frac{i}{2\pi} \int_0^{\Gamma_e} \frac{d\Gamma'}{z(\Gamma,t) - z(\Gamma',t)}$$

$$\tilde{N} = \frac{i}{48\pi} \int_0^{\Gamma_e} \frac{\frac{\partial^2 U^4}{\partial \Gamma_1^2} + \frac{\partial}{\partial \Gamma_1}\left(U^6 \frac{\partial z}{\partial \Gamma_1} \frac{\partial^2 z^*}{\partial \Gamma_1^2}\right) d\Gamma_1}{z(\Gamma,t) - z(\Gamma_1,t)}$$

$$\tilde{P}_1 = -\frac{i}{6} \frac{\partial}{\partial \Gamma}\left(U^4 \frac{\partial z^*}{\partial \Gamma}\right)$$

$$\tilde{P}_2 = -\frac{1}{24}\{2 \frac{\partial}{\partial \Gamma}(U^4 \frac{\partial \tilde{I}}{\partial \Gamma}) - (\frac{\partial z^*}{\partial \Gamma})^2 \frac{\partial}{\partial \Gamma}(U^6 \frac{\partial \tilde{I}^*}{\partial \Gamma}) - U^6[(\frac{\partial z^*}{\partial \Gamma} \frac{\partial^2 z}{\partial \Gamma^2} - \frac{\partial z}{\partial \Gamma} \frac{\partial^2 z^*}{\partial \Gamma^2})\frac{\partial I}{\partial \Gamma}$$

$$- \frac{\partial z^*}{\partial \Gamma} \frac{\partial^2 z^*}{\partial \Gamma^2} \frac{\partial I^*}{\partial \Gamma}]\}$$

$$\tilde{P}_3 = \frac{i}{24}[U^3 \frac{\partial}{\partial \Gamma}(U \frac{\partial z^*}{\partial \Gamma})\frac{\partial}{\partial \Gamma}(U^2 \frac{\partial U}{\partial \Gamma}) + \frac{2}{5} U^9 (\frac{\partial z}{\partial \Gamma})^2 (\frac{\partial}{\partial \Gamma}(U \frac{\partial z^*}{\partial \Gamma}))^3 + \frac{U^2}{4} \frac{\partial z^*}{\partial \Gamma} \frac{\partial}{\partial \Gamma}(U \frac{\partial}{\partial \Gamma}(U \frac{\partial}{\partial \Gamma} U^4))$$

$$+ \frac{U}{5} \frac{\partial z^*}{\partial \Gamma} \frac{\partial}{\partial \Gamma}(U^6 \frac{\partial}{\partial \Gamma}(\frac{\partial z}{\partial \Gamma} U^2 \frac{\partial}{\partial \Gamma}(U \frac{\partial z^*}{\partial \Gamma}))) + \frac{2}{3} U^2 \frac{\partial}{\partial \Gamma}(U \frac{\partial z^*}{\partial \Gamma})\frac{\partial}{\partial \Gamma}(U^6 \frac{\partial z}{\partial \Gamma} \frac{\partial}{\partial \Gamma}(U \frac{\partial z^*}{\partial \Gamma}))]$$

It may be noted that although the complexity of the modified equation has increased with the higher order matching, the evaluation of the higher order terms is straightforward once z and $\tilde{I}$ are known; $\tilde{N}$ may be evaluated by standard methods.

Some checks on the correctness of the higher order terms in (4.4.18) are available. Firstly, the growth rate of perturbations on a straight uniform vortex layer is given by Rayleigh (1896, p.392) and the corresponding value obtained on using the modified equation (4.4.18) must agree with this in the long wave limit. This is discussed in §5.

Secondly, it can be shown that (4.4.18) is satisfied by the limiting form of the solution for a uniform circular vortex layer of thickness h_0 in the limit h_0/ρ_0 small, where ρ_0 is the radius of the

centre line of the layer; the radial velocity at the centre line is zero while the azimuthal velocity is given by the velocity of convection of vorticity which can be evaluated directly from the kinematic vorticity equation.

Finally, (4.4.18) can be compared with the limiting form of Kirchoff's (1876) solution for a rotating uniform elliptical vortex in the limit of a small value of the minor axis, large value of the contained vorticity $\bar{\omega}$ and finite total circulation Γ_0. For put

$$z = -a \exp(i\mu t)\cos\theta, \tag{4.4.19}$$

$$\Gamma = (\Gamma_0/\pi)(\theta - \tfrac{1}{2}\sin 2\theta) \tag{4.4.20}$$

where $0 \leq \theta \leq \pi$, a is the semi-minor axis and μ is a constant, to be determined; μ is the rate of increase of eccentric angle of a fluid particle lying on a con-focal ellipse within the vortex. On noting that

$$\frac{\partial}{\partial\Gamma} = \frac{\partial\theta}{\partial\Gamma}\frac{\partial}{\partial\theta},$$

it can be shown that

$$\tilde{I} = \frac{i\Gamma_0 e^{-i\mu t}}{\pi a}\cos\theta \tag{4.4.21}$$

(so that with $\mu = \dfrac{\Gamma_0}{\pi a^2}$, (4.4.19)-(4.4.20) is an exact solution of Birkhoff's equation for a vortex sheet. See Moore (1976)), $U = 2\Gamma_0 \sin\theta/\pi a$ and that

$$\tilde{N} = \frac{i\Gamma_0^3 e^{-i\mu t}}{\pi^3 a^5}\cos\theta \tag{4.4.22}$$

Substituting these into (4.4.18) and equating the coefficient of $e^{-i\mu t}\cos\theta$ to zero gives

$$\mu = \frac{\Gamma_0}{\pi a^2}\left[1 - \frac{2\Gamma_0}{\pi a^2\omega} + \frac{3\Gamma_0^2}{\pi^2 a^4\omega^2} - \frac{4\Gamma_0^3}{\pi^3 a^3\omega^3} + O(\frac{1}{\omega^4})\right] \tag{4.4.23}$$

Since $b = \Gamma_0/\pi a\bar{\omega}$ is the semi-minor axis of the elliptical vortex, it can be verified that (4.4.23) is an expansion in b/a of

$$\mu = \frac{ab\bar{\omega}}{(a + b)^2}$$

which is the value given by Kirchoff for the rate of increase of eccentric angle of a fluid particle on a confocal ellipse within the vortex.

§5 Growth of long waves on a straight uniform vortex layer

A straight uniform vortex layer of thickness h_0 with velocities on the two sides of the layer given by $\pm V/2$ is, in the notation of §4, represented by $z = \Gamma V^{-1}$. Moore (M) used the modified equation (4.4.18) without the $O(1/\bar{\omega}^2)$ and $O(1/\bar{\omega}^3)$ terms to consider a sinusoidal disturbance of spatial wavenumber k to the straight layer. Thus, in the disturbed state $z(\Gamma,t)$ was taken to be

$$z(\Gamma,t) = \Gamma V^{-1} + a(t)e^{ik\Gamma/V} + b(t)e^{-ik\Gamma/V} \qquad (4.5.1)$$

where a(t) and b(t) are complex-valued. The growth rate obtained was found to agree with Rayleigh to $O(kh_0)$.

Repeating Moore's analysis with the $O(1/\bar{\omega}^2)$ and $O(1/\bar{\omega}^3)$ terms included in (4.4.18), it can be shown that

$$\frac{\partial a^*}{\partial t} = \frac{iVk}{2}\left[b - \frac{kh_0}{3}(2b + a^*) + \frac{k^2h_0^2}{12}(2b+a^*) - \frac{(kh_0)^3}{30}(3b+2a^*)\right] \qquad (4.5.2)$$

$$\frac{\partial b^*}{\partial t} = \frac{iVk}{2}\left[a - \frac{kh_0}{3}(2a + b^*) + \frac{k^2h_0^2}{12}(2a+b^*) - \frac{(kh_0)^3}{30}(3a+2b^*)\right] \qquad (4.5.3)$$

(cf. M((5.19)-(5.20))). These equations imply that the amplitudes grow like $e^{\sigma t}$ where

$$\sigma = \tfrac{1}{2}Vk\left[\left(1 - \frac{kh_0}{3} + \frac{(kh_0)^2}{12} - \frac{(kh_0)^3}{60}\right)\left(1 - kh_0 + \frac{(kh_0)^2}{4} - \frac{(kh_0)^3}{12}\right)\right]^{\frac{1}{2}} \qquad (4.5.4)$$

However, in view of the approximation leading to the governing equation (4.4.18), it is legitimate to retain only terms up to $O(k^3h_0^3)$. Thus

$$\sigma = \tfrac{1}{2}Vk\left[1 - \frac{2}{3}kh_0 + \frac{k^2h_0^2}{9} - \frac{28k^3h_0^3}{135} + O(k^4h_0^4)\right] \qquad (4.5.5)$$

which agrees with Rayleigh if terms of $O(k^4h^4)$ are neglected.

Although the theory is valid for $kh << 1$, it is of interest to consider σ for finite values of kh. In Fig. 4.1, σ^2, as given by (4.5.4), is plotted against kh_0 (curve (d)). The maximum growth rate is achieved when $kh_0 = 0.78$ and the growth is stopped when $kh_0 = 1.23$. The corresponding exact values obtained by Rayleigh are 0.80 and 1.28.

Also included in Fig. 4.1, for the purpose of comparison, are plots of σ^2 corresponding to (i) Rayleigh's exact result (curve (a)), (ii) case when $O(1/\bar{\omega}^3)$ term in the governing equation (4.4.18) has been omitted from the analysis (curve (c)) and (iii) case when both $O(1/\bar{\omega}^3)$ and $O(1/\bar{\omega}^2)$ terms have been omitted (curve (b)). For small values of kh_0 the agreement with (a) becomes better with higher degree of approximation. However, for large values of kh_0 the three curves (b), (c), (d), corresponding to the different levels of approximation, show that σ^2 is positive and increases with kh_0. Thus short waves are unstable. As pointed out by Moore, this means that spurious short wave disturbances which will be excited in any numerical attack on the integro-differential equation (4.4.18) would be amplified. Thus the hope that inclusion of higher order terms in (4.18) would resolve the numerical difficulty revealed by Moore's analysis for case (iii) above has not been realised.

APPENDIX A: Completion of higher order matching

For consistency in $O(\varepsilon^2)$ matching, terms proportional to y and y^2 in the $O(\varepsilon^2)$ terms in (4.3.14) and (4.4.1) must be matched although the matching reveals no new information.

Note that there are no terms of $O(\varepsilon^2)$ proportional to y in the outer solution (4.3.14). Thus the corresponding terms in (4.4.1) must equate to zero. Substituting for u_2 and v_2 into (4.4.1), the $O(\varepsilon^2)$ terms proportional to y are given by

$$e^{-i\alpha}\{2\Omega_1 + \frac{\bar{u}_{1\pm}}{\rho} + \frac{\partial \bar{v}_1}{\partial x} - \omega \frac{\partial}{\partial x}\left(H_1 \frac{\partial H_1}{\partial x}\right) - i\left[\frac{\bar{v}_1}{\rho} - \frac{\partial \bar{u}_1}{\partial x} - \frac{\omega H_1^2}{2}\frac{\partial}{\partial x}\left(\frac{1}{\rho}\right) - \frac{2\omega H_1}{\rho}\frac{\partial H_1}{\partial x}\right] - \Omega_1\} \tag{A4.1}$$

according as $y \gtrless 0$. However, since from (M(2.21))

$$\bar{u}_{1_+} = \bar{u}_{1_-} = \bar{u}_1 + \tfrac{1}{2}\frac{\omega H_1^2}{\rho} \tag{A4.2}$$

the coefficient of y on either side of the centre line is the same, as it must be. On writing $\gamma = 2\omega H_1$ in (4.4.13) gives

$$\Omega_1 = -\frac{\bar{u}_1}{\rho} + \omega\frac{\partial}{\partial x}\left(H_1\frac{\partial H_1}{\partial x}\right) - \frac{\omega H_1^2}{2\rho^2} - i\left(\frac{3\omega H_1}{\rho}\frac{\partial H_1}{\partial x} + \frac{\omega H_1^2}{2}\frac{\partial}{\partial x}\left(\frac{1}{\rho}\right) + \frac{\partial \bar{u}_1}{\partial x}\right) \tag{A4.3}$$

Substituting (A4.2) and (A4.3) into (A4.1) and noting that $\bar{v}_1 = -\omega H_1 \frac{\partial H_1}{\partial x}$, we find that the term in { } in (A4.1) vanishes as required.

For terms of $O(\varepsilon^2)$ proportional to y^2 to match, it is required that

$$e^{-i\alpha}\{\frac{\Omega_0}{\rho} \mp \frac{\omega H_1}{\rho^2} + \frac{\bar{u}_0}{\rho} - \tfrac{1}{2}\frac{\partial^2 \bar{u}_0}{\partial x^2} \pm \frac{\omega}{2}\frac{\partial^2 H_1}{\partial x^2} - i[-\tfrac{1}{2}\frac{\partial \Omega_0}{\partial x} - \frac{3}{2\rho}\left(\frac{\partial \bar{u}_0}{\partial x} \mp \omega\frac{\partial H_1}{\partial x}\right)$$

$$- \tfrac{1}{2}\frac{\partial}{\partial x}\left(\frac{1}{\rho}\right)(\mp\omega H_1 + \bar{u}_0)]\} = -\frac{e^{2i\alpha}}{2}\frac{\partial^2 Q_\pm(0)}{\partial Z^2} \tag{A4.4}$$

according as $y \gtrless 0$.

Since $Q_+^{(0)}$ and $Q_-^{(0)}$ are analytic, its derivatives can be evaluated in any direction. Thus

$$\frac{\partial Q_\pm^{(0)}}{\partial Z} = e^{-i\alpha}\frac{\partial Q_\pm^{(0)}}{\partial x}, \quad \frac{\partial^2 Q_\pm^{(0)}}{\partial Z^2} = e^{-2i\alpha}\left(\frac{\partial^2 Q_\pm^{(0)}}{\partial x^2} - \frac{i}{\rho}\frac{\partial Q_\pm^{(0)}}{\partial x}\right) \qquad (A4.5)$$

From M(A8), M(4.4),

$$\frac{\partial Q_\pm^{(0)}}{\partial x} = -ie^{-i\alpha}\{\Omega_0 + \frac{\bar{u}_0}{\rho} + i\frac{\partial \bar{u}_0}{\partial x} - i\omega\frac{\partial H_1}{\partial x} - \frac{\omega H_1}{\rho}\} + O(\varepsilon) \qquad (A4.6)$$

so that

$$\frac{\partial^2 Q_\pm^{(0)}}{\partial x^2} = -e^{-i\alpha}\{\frac{\Omega_0}{\rho} + \frac{\bar{u}_0}{\rho^2} - \frac{\omega H_1}{\rho^2} + \frac{\partial^2}{\partial x^2}(\omega H_1 - \bar{u}_0) - i[\frac{1}{\rho}\frac{\partial}{\partial x}(\omega H_1 - \bar{u}_0) - \frac{\partial}{\partial x}(\Omega_0 + \frac{\bar{u}_0}{\rho} - \frac{\omega H_1}{\rho})]\} + O(\varepsilon) \qquad (A4.7)$$

On substituting (A4.6) and (A4.7) into (A4.5) we find that (A4.4) is satisfied.

Similarly, it can be shown that terms of $O(\varepsilon^3)$ proportional to y, y^2 and y^3 in (4.3.14) match with the corresponding terms in (4.4.1).

PART II: MOTION OF VORTEX FILAMENTS IN THREE DIMENSIONS

For God' s Sake

Let us sit upon the ground and tell sad stories
Of vortex filaments.
How some have been ill-posed, some singular,
Some poisoned by their self-induction, some core size killed,
some haunted by the mathematics they have involved.

All murderous.

For within the swirling motion that rounds the mortal circulation
Of a vortex
Keeps futility his court,
And there the non-linearity sits
Scoffing at his state and grinning at his theories
Allowing him a breath, a little scene to linearize, compute
and fill with approximations
And then at last he comes and with a little inconsistency bores through
the costly hopes and

Farewell .....

Shakespeare

Richard II. Act 3 Scene 2

(as told by Saffman and Yeun)

CHAPTER 5: THE EQUATION OF MOTION OF A THIN VORTEX FILAMENT

§1 Introduction

In this and subsequent chapters consideration will be given to the motion of thin vortex filaments. A vortex filament is considered to be a tube of small cross-section whose surface is composed of vortex lines and which is surrounded by irrotational fluid. The cross-section of the core will be assumed to be circular to leading order, the radius of the core c being small compared to the local radius of curvature, ρ. Thus it is required that $c/\rho \ll 1$. Deformation of the circular cross-section as the flow evolves will be ignored throughout. This is justified because the self-induced strain-field to which the vortex is subjected is weak (see Moore & Saffman (1971)). The motion of the filament is then determined by tracking the axis of the filament.

In flows in which a thin vortex filament is present, the velocity field at points distant from the filament does not depend on the core structure, and the induced flow at these points can be calculated using the Biot-Savart line integral (5.1.1). However, in order to do this, the instantaneous position of the vortex filament must be known.

The equation for the motion of a thin vortex filament of arbitrary shape and internal structure has been obtained intuitively by Crow (1970) and rigorously justified by Moore & Saffman (1972). Since this equation is basic to the considerations of subsequent chapters, it is briefly discussed below.

The fluid is regarded as inviscid, incompressible and of uniform density. The equation of motion of the filament derived by Crow is a statement of Helmholtz's law that in a non-viscous fluid vortex lines move with the fluid. Thus the motion of the filament is determined

once the velocity at the vortex is established.

In the absence of axial flow in the vortex filament, which is the case in the considerations of subsequent chapters, Moore & Saffman show that the error in Crow's equation is $O(c^2/\rho^2)$.

Let $\underline{x}$ be the position vector in a fixed coordinate system and let a vortex filament of strength Γ be specified by its centre-line which has the parametric equation $\underline{x} = \underline{X}(\xi,t)$. Here ξ is a Lagrangian parameter such that ξ = constant represents always the same fluid particle and t is the time variable. Let $\hat{\underline{t}}(\xi,t)$ denote the unit tangent vector and $s = s(\xi,t)$ the distance along the filament. The velocity at $\underline{X}$ is that induced by the vorticity in the filament itself and by any external means such as another vortex present in the flow field.

Now, at a point $\underline{x}$ exterior to the vortex filament, the velocity $\underline{u}(\underline{x})$ induced by the vortex is given by the Biot-Savart law as

$$\underline{u}(\underline{x}) = \frac{\Gamma}{4\pi} \int_{\text{filament}} \frac{\hat{\underline{t}}(\xi,t) \wedge (\underline{x} - \underline{X}(\xi,t))ds}{|\underline{x} - \underline{X}(\xi,t)|^3} \qquad (5.1.1)$$

The integral (5.1.1) cannot be used to obtain the velocity at $\underline{x} = \underline{X}(\xi_0,t)$, a point on the filament itself because in deriving (5.1.1) it is assumed that $\underline{x} - \underline{y}$, where $\underline{y}$ denotes the position of a point in the vortex core, does not vary across the vortex cross-section and this is no longer true in the vicinity of $\underline{X}(\xi_0,t)$ as $\underline{x} \to \underline{X}(\xi_0,t)$. Further, the integrand has a singularity at $\underline{x} = \underline{X}(\xi_0,t)$ so that $\underline{u}(\underline{X}(\xi_0))$ may be infinite. The difficulty is overcome by a suitable cut-off in the integral so as to make the integral finite and to allow for the internal structure of the filament in the vicinity of $\underline{X}(\xi_0,t)$.

Two forms of the cut-off are described in §2 and in §3, the equation of motion of the filament is written down.

§2 The cut-off method

Crow (1970) defined the velocity given by (5.1.1) in the limit $\underline{x} \to \underline{X}(\xi_0,t)$ as

$$\underline{u}(\underline{X}(\xi_0)) = \frac{\Gamma}{4\pi} \int_{[d]} \frac{\hat{\underline{t}}(\xi) \Lambda (\underline{X}(\xi_0) - \underline{X}(\xi))ds(\xi)}{|\underline{X}(\xi_0) - \underline{X}(\xi)|^3} \tag{5.2.1}$$

where the explicit time dependence has been suppressed for convenience and where [d] means that an interval $(s(\xi_0)-d,\ s(\xi_0) + d)$ is removed from the range of the integration. The integral is then finite and the velocity is given in terms of d. The length d is chosen so that

$$d = \delta_c c(\xi_0,t) \tag{5.2.2}$$

where $c(\xi_0,t)$ is the core radius at ξ_0 and δ_c is a constant. δ_c is determined by evaluating the cut-off integral for the particular case of a circular vortex ring and comparing the velocity with the known exact result given by Saffman (1970). The crucial assumption is that the value of d depends only on the local structure of the vortex, and not on the geometric configuration of the filament so that the same value of d for a circular ring can be used for a filament of arbitrary shape so long as their local structures (i.e., the core size and the swirl and axial velocity distribution) are the same.

Thus, using Saffman's results,

$$\log 2\delta_c = \tfrac{1}{2} - \frac{4\pi^2}{\Gamma^2} \int_0^c rv^2 dr \tag{5.2.3}$$

where v is the swirl velocity in the core and there is no axial flow in the filament.

Crow's cut-off method is inconvenient to use for numerical work because it would be difficult to remove an interval from the range of the line integral if the interval is not terminated by grid points of a

finite difference scheme. An alternate form of cut-off, which is more suitable for numerical work, is suggested by Moore (1972); the cut-off was first used by Rosenhead (1930). The integration is carried out over the entire range but the denominator of the integrand in (5.1.1) is replaced by $|(\underline{X}(\xi_0) - \underline{X}(\xi))^2 + \mu^2|^{3/2}$ where the quantity μ is given by

$$\mu = 2\delta_R c(\xi_0, t) \tag{5.2.4}$$

where δ_R is a constant. As with Crow's cut-off length, δ_R can be chosen by evaluating the new integral for the case of a circular vortex ring and comparing it with the known results. This gives

$$\delta_R = \delta_c e^{-1} \tag{5.2.5}$$

where δ_c is as in (5.2.3). For a uniform vortex with no axial flow, i.e. with $v = \frac{\Gamma r}{2\pi c}$

$$\delta_c = \tfrac{1}{2} e^{\frac{1}{4}} \tag{5.2.6}$$

and

$$\delta_R = \tfrac{1}{2} e^{-\frac{3}{4}} \tag{5.2.7}$$

§3 Equation of motion

Since the fluid is non-viscous, it follows from Helmholtz's law that the vortex lines move with the fluid. Thus, assuming the cross-section of the vortex filament remains circular, the equation of motion of the centre-line can be written,

$$\frac{\partial \underline{X}(\xi_0,t)}{\partial t} = \frac{\Gamma}{4\pi} \oint \frac{\underline{ds}' \wedge (\underline{X}-\underline{X}')}{|\underline{X}-\underline{X}'|^3} + \underline{V}_E(\underline{X}(\xi_0),t) \qquad (5.3.1)$$

where $\oint$ implies that one of the cut-off methods described in §2 is used to make the integral finite and $\underline{V}_E(\underline{X}(\xi_0),t)$ is the contribution to the velocity at $\underline{X}(\xi_0)$ from external sources which produce an irrotational field at $\underline{X}(\xi_0)$.

The right hand side of (5.3.1) is given in terms of d or μ depending on the method of cut-off used. Thus, in view of (5.2.2) or (5.2.4), the radius of the core $c(\xi_0,t)$ has to be determined before $\partial\underline{X}/\partial t$ can be evaluated.

In order to consider the response of a vortex filament to a disturbance whose amplitude is small, the core radius may be taken to be constant and given by its initial value; the error is of the second order in amplitude. However, for finite amplitude disturbances, the variation of the core size cannot be neglected.

It can be shown that the disturbances which cause the area of the cross-section to change propagate along the filament with a much faster speed than the disturbances which cause the curvature of the filament to change. Moore & Saffman argue that the variation in cross-sectional area along the filament are smoothed out in a time which is short compared to the time it takes for the position of the filament to shift by a significant amount. Thus, on the time scale of the filament motion,

the core can be regarded as being uniform along the filament, so that

$$c = c(t) \tag{5.3.2}$$

Moore & Saffman show that the error is $O(\frac{c^2(0)}{\rho^2})$, where $\rho(\xi_0,t)$ is the radius of curvature. The dependence on t follows from the conservation of volume (in the absence of diffusion)†. Hence

$$Lc^2 = \text{constant} \tag{5.3.3}$$

where L(t) is the total length of the filament; L(t) is given by

$$L(t) = \int_{\text{filament}} ds \tag{5.3.4}$$

Likewise the swirl velocity v = v(r,t), where r is the radial distance from the centre-line of the filament is independent of position along the filament so that, in view of conservation of circulation,

$$v = \frac{\Gamma}{2\pi r} f(\frac{r}{c}) \qquad f(1) = 1 \tag{5.3.5}$$

where f is determined from the initial structure of the vortex. Thus in (5.2.3),

$$\frac{4\pi^2}{\Gamma^2} \int_0^c rv^2 dr = \int_0^1 \eta f^2(\eta) d\eta \tag{5.3.6}$$

so that this is constant throughout the motion as required.

Hence, once the initial structure and configuration of the vortex is known, its motion can be followed using (5.3.1), evaluating the cut-off length at each time step.

---

†Leonard (1974) has considered models where the cut-off length is chosen so that the volume of local filament segment is conserved and also where the influence of viscous diffusion of vorticity is incorporated in the cut-off length.

In Chapter 6, (5.3.1) is used to study the evolution of an elliptic vortex ring while in Chapter 7 it is used to study the evolution of an infinitely long straight vortex in the presence of an approaching rigid sphere.

CHAPTER 6: THE EVOLUTION OF AN ELLIPTIC VORTEX RING

§1 Introduction

There is at present considerable interest in identifying the mechanism responsible for destroying the trailing vortex system of an aircraft. The trailing vortices, made visible by the condensation of moisture in their cores, are observed to undergo a slow instability: wavy disturbances grow on both trailing vortices and reach an amplitude such that the vortices touch at the nearer points and break up into a sequence of distinct vortex rings. The form of the rings is such that its projection onto the plane of maximum projected area is roughly elliptic in shape. Once the rings have formed, the vortex trail soon ceases to be visible.

The growth of waves on trailing vortices was studied analytically by Crow (1970) who showed that small perturbations of the vortices in the form of plane waves of sufficiently long wavelength are unstable. Later Moore (1972) followed the growth of symmetrical waves on trailing vortices numerically and showed that waves grow to such an amplitude that they touch at the nearer points. Thus an explanation of the observed looping process is to hand.

The mechanism by which the vortices break up to form vortex rings is not understood. Nor is it clear that the rapid loss of visibility of the rings implies their disintegration; care must be taken in interpreting observations which depend on the retention of smoke particles or water droplets in the vortex cores. It is possible that the non-circular form of the vortex rings which are formed is significant to the observations. Thus it is of interest to know what happens to an initially non-circular vortex ring.

In this chapter an initial value problem is studied. Given a plane elliptic vortex ring, it is proposed to follow its subsequent motion and deformation numerically. It will be shown below that a non-circular ring must necessarily deform.

The choice of a vortex ring of elliptic shape is also relevant to the study of a wake of a bird in forward flight. Photographs from Kokshaysky's (1979) experiments clearly show deforming vortex rings in the wake. The motion of the wings is such that in one complete beat the bird leaves behind it a vortex ring of roughly elliptic shape in a plane inclined at an angle to the direction of flight. Rayner (1979) has modelled such a wake by a chain of elliptic vortex rings to estimate power consumption and mean lift coefficients. He ignores the deformation of the rings in his calculations.

Previous numerical study of the motion of an elliptic vortex ring is due to Arms and Hama (1965), who used local induction approximation in their calculation of the motion. This assumes that the motion of a thin vortex filament is governed by the approximate equations

$$\frac{\partial \underline{X}(s,t)}{\partial t^*} = \frac{\underline{b}(s,t)}{\rho(s,t)}, \qquad t^* = \frac{\Gamma}{4\pi} \ln\left(\frac{1}{\varepsilon}\right) t \qquad (6.1.1)$$

where $\underline{b}$ and ρ are respectively the local binormal and radius of curvature at $\underline{X}$, a point on the filament, and s is the arc distance along the filament. ε is taken to be an unspecified constant although a proper treatment of the Biot-Savart integral shows that $\varepsilon = c/\rho$, where c is the core radius. Thus the approximation neglects the dependence of ε on ρ and on any variations of the core size during the motion as well as the contribution to velocity from distant parts of the vortex. The neglect of this contribution means that the approximation loses Crow instability. Thus the approximation is not satisfactory if this important feature of the evolution of a vortex filament is not to be excluded from consideration.

The cut-off theory described in Chapter 5 provides a more accurate method of approach and is used in this chapter to follow the motion of the vortex ring.

It may be noted from (6.1.1) that the velocity at a point on the vortex is approximately inversely proportional to the local curvature. Since the curvature varies along the length of an elliptic vortex ring, the velocity will vary accordingly so that the ring will deform from its elliptic shape as it moves.

In §2, small perturbations of elliptic mode to a circular vortex ring are discussed while in §3 the numerical procedure used to integrate the equation of motion (5.3.1) for an elliptic vortex ring is described. In §4 numerical results are presented for rings of different eccentricity and core size. The initial size of the core used for each ellipse is that predicted by considering the impulsive motion, in a perfect fluid, of a flat elliptic disk which is then dissolved away. This method of fixing the core size is due to G.I. Taylor (1953) and is described in Appendix A. In §5 a quantitative experiment is described for observing the motion of an initially elliptic vortex ring and the results are compared with those of the numerical calculations in §6. Estimates of the vortex parameters are obtained in Appendix B using a simple model (Saffman (1978)) of the flow.

In §7 the relevance of the results to the vortex trail of an aircraft is discussed.

§2 Linear theory

The stability of a thin circular vortex ring to small sinusoidal perturbations was considered by Widnall and Sullivan (1973). In a coordinate system moving with the velocity of an unperturbed circular vortex ring $\underline{V}$, the perturbed ring was taken to be

$$\underline{X} = (R + re^{im\theta})\,\underline{e}_r + ze^{im\theta}\underline{e}_z \qquad (6.2.1)$$

where $\underline{e}_r$ and $\underline{e}_z$ are unit vectors in the radial and axial directions, θ is the azimuthal angle, R is the radius of the unperturbed ring and $|r|, |z| \ll R$. The wavenumber m is an integer.

On substituting (6.2.1) into the equation of motion ((5.3.1) with $\underline{V}_E$ set to $\underline{0}$) and linearizing in z and r, it was shown that for moderate values of m (for which it is valid to use (5.3.1)), for each m the ring oscillates with angular frequency $\pm\alpha_m$ (given in their paper).

In the case m = 2, the two solutions corresponding to $\pm\alpha_2$ can be superposed to satisfy the condition that initially the perturbed vortex ring has a plane elliptic form. This gives

$$r(t) = r_0 \cos(\alpha_2 t), \quad z(t) = z_0 \sin(\alpha_2 t) \qquad (6.2.2)$$

where r_0 and z_0 are real constants.

Using the value of α_2 as given by Widnall and Sullivan, it follows that the period of oscillation $2\pi/\alpha_2$, which depends on R and the internal structure of the vortex (i.e. core radius and vorticity distribution), is given by

$$\tau(R,c,A) = \frac{8\pi^2R^2}{\Gamma}\left[\left\{4\left(\ln\frac{c}{R} - A\right) + .22\right\}\left\{3\left(\ln\frac{c}{R} - A\right) + 2.23\right\}\right]^{-\frac{1}{2}} \qquad (6.2.3)$$

where c is the core radius and

$$A = \frac{4\pi^2}{\Gamma^2}\int_0^c rv^2\,dr \qquad (6.2.4)$$

Here v is the swirl velocity in the core and there is no axial flow in the filament. Note that in linearized stability theory the length of the vortex filament remains constant so that c must also be a constant.

The self-induced mean velocity of the ring is that of the unperturbed circular ring,

$$\underline{V}(R,c,A) = \frac{\underline{e}_z \Gamma}{4\pi R} \left(\ln \frac{8R}{c} + A - \tfrac{1}{2}\right) \qquad (6.2.5)$$

§3 Numerical solution of the equation of motion

In this section the procedure for numerical integration of (5.3.1) for the case of an elliptic vortex ring with no external velocity field is described. Following Moore (1972), the method of cut-off for the Biot-Savart integral is chosen to be that due to Rosenhead; this was described in the latter part of Ch. 5, §2.

Thus in (5.3.1), with $\underline{V}_E = \underline{0}$, the denominator in the integral is replaced by $\{|\underline{X}(\xi_0) - \underline{X}(\xi)|^2 + \mu^2\}^{3/2}$, where μ is given by (5.2.4), and the integration is carried out over the entire range of the integral.

The Lagrangian parameter ξ is chosen so that in a fixed Cartesian coordinate system Oxyz, the vortex ring is initially given by

$$\underline{X}(\xi,0) = (a\cos(\xi),\ b\sin(\xi),\ 0) \qquad -\pi \leq \xi \leq \pi \tag{6.3.1}$$

where a and b are respectively the semi-major and semi-minor axes of the ellipse. At subsequent times ξ = constant always represents the same fluid particle.

For time $t > 0$, it is assumed that the vortex ring retains its symmetry about $x = 0$ and $y = 0$ so that with $\underline{X} = (x,y,z)$,

$$\left.\begin{aligned} x(-\pi+\xi,t) &= x(\pi-\xi,t) = -x(\xi,t) = -x(-\xi,t) \\ y(-\pi+\xi,t) &= -y(\pi-\xi,t) = -y(\xi,t) = y(-\xi,t) \\ z(-\pi+\xi,t) &= z(\pi-\xi,t) = z(\xi,t) = z(-\xi,t) \end{aligned}\right\} \quad 0 \leq \xi \leq \pi/2 \tag{6.3.2}$$

Hence it is only necessary to follow, say, the portion $0 \leq \xi \leq \pi/2$ of the ring to obtain the shape of the whole ring.

The evolution of the vortex ring can now be determined by simply integrating (5.3.1) forward in time and calculating the length of the filament at each time step to obtain the value of $\mu(t)$. However, the integrand in the cut-off integral, although it is finite everywhere,

is large in the neighbourhood of ξ_0. For near ξ_0 (suppressing the explicit time-dependence for convenience),

$$\frac{\partial \underline{X}}{\partial \xi} \wedge \frac{\underline{X}(\xi_0) - \underline{X}(\xi)}{\{|\underline{X}(\xi_0) - \underline{X}(\xi)|^2 + \mu^2\}^{3/2}} \sim \left(\frac{\partial \underline{X}}{\partial \xi}\right)_0 \wedge \left(\frac{\partial^2 \underline{X}}{\partial \xi^2}\right)_0 P(\xi) \qquad (6.3.3)$$

where 0 implies that the quantities are evaluated at ξ_0 and

$$P(\xi) = \frac{\frac{1}{2}(\xi-\xi_0)^2}{\{(\xi-\xi_0)^2\left(\frac{\partial \underline{X}}{\partial \xi}\right)_0^2 + \mu^2\}^{3/2}} .$$

This would cause a loss of accuracy in evaluating the integral. To overcome this difficulty, the equation of motion is written as

$$\frac{\partial \underline{X}}{\partial t}(\xi_0,t) = \frac{\Gamma}{4\pi} \int_{-\pi}^{\pi} \left(\frac{\partial \underline{X}}{\partial \xi} \wedge \frac{\underline{X}(\xi_0,t) - \underline{X}(\xi,t)}{\{|\underline{X}(\xi_0,t)-\underline{X}(\xi,t)|^2+\mu^2\}^{3/2}} - \left(\frac{\partial \underline{X}}{\partial \xi}\right)_0 \wedge \left(\frac{\partial^2 \underline{X}}{\partial \xi^2}\right)_0 P(\xi,t)\right) d\xi$$

$$+ \frac{\Gamma}{4\pi} \left(\frac{\partial \underline{X}}{\partial \xi}\right)_0 \wedge \left(\frac{\partial^2 \underline{X}}{\partial \xi^2}\right)_0 \int_{-\pi}^{\pi} P(\xi,t)d\xi \qquad (6.3.4)$$

The integrand in the first integral is O(1) everywhere while the second integral can be evaluated analytically.

From (5.2.4) and (5.3.3),

$$\mu(t) = 2\delta_R c_0 \left\{ \frac{1}{L_0} \int_{-\pi}^{\pi} \left|\frac{\partial \underline{X}}{\partial \xi}\right| d\xi \right\}^{-1/2} \qquad (6.3.5)$$

where L_0 and c_0 are the respective initial values of the length and core radius of the vortex ring. For an ellipse,

$$L_0 = 4aE(e) \qquad (6.3.6)$$

where e is eccentricity of the ellipse, $e^2 = (a^2-b^2)/a^2$, and E(e) is the complete elliptic integral of the second kind.

In (6.3.5), using (5.2.5) and (6.2.4), δ_R is given by

$$\log 2\delta_R = -\tfrac{1}{2} - A \qquad (6.3.7)$$

Once the values of A and c_0 are given, equations (6.3.4), (6.3.5) and (6.3.1) completely specify the initial value problem and the evolution of the vortex ring can be determined numerically. The interval $(-\pi,\pi)$ was divided into 4(N-1) portions by 4N-3 equally spaced grid points. The spatial derivatives were calculated using four-point centred differences and Simpson's Rule was used to carry out spatial integration. Because of its stability, the fourth-order Runge-Kutta formula was used to carry out the integration forward in time.

The calculations were carried out for four different axes ratios of the initial elliptic ring and the results are described in the next section.

§4 Numerical results

The equation of motion is made dimensionless by choosing the semi-major axis a as the unit of length and $4\pi a^2/\Gamma$ as the unit of time. Thus the dimensionless time t_1 is given by

$$t_1 = \frac{\Gamma}{4\pi a^2} t \qquad (6.4.1)$$

Before calculations can be performed, the value of A in (6.3.7) and the initial value of the core radius c_0 are needed. These depend on the process of generation of the vortex ring. One method of generation in an ideal fluid is to give an impulse to a flat disk of elliptic shape and then to dissolve it away. By equating the energy and impulse of the disk to that of the resulting vortex ring, in the manner of G.I. Taylor (1953), the core size and the circulation of the vortex ring can be evaluated. The details are pursued in Appendix A. The initial distribution of potential at the edge of the disc (A6.2) suggests that in the core of the resulting vortex ring the appropriate distribution of velocity to take is

$$v = \frac{\Gamma}{2\pi(cr)^{1/2}} \qquad w = 0 \qquad (6.4.2)$$

where v and w are respectively the azimuthal and axial velocities relative to the centre of the core and r is the radial distance from it. This implies that in (5.3.5) $f = (\frac{r}{c})^{\frac{1}{2}}$ so that

$$A = 1 \qquad (6.4.3)$$

The initial core radius is given by (A6.11). For the cases considered here the values are tabulated below (Table 6.1); the case $\frac{b}{a} = 1$ is also included.

The radius of curvature ρ of an ellipse varies from a value b^2/a at the major axis to a value a^2/b at the minor axis. The maximum and minimum values of c_0/ρ are also shown in Table 6.1. These values

b/a	c_0/a	$c_0/\rho_{max} = c_0 a/b^2$	$c_0/\rho_{min} = c_0 b/a^2$
0.2	0.109	2.73	0.022
0.4	0.207	1.29	0.083
0.6	0.287	0.797	0.172
0.8	0.347	0.542	0.278
1.0	0.393	0.393	0.393

Table 6.1. Predicted core-size of vortex ring produced by the process described in Appendix A.

are not small as required by the cut-off theory. However, in the absence of axial flow, the error in the cut-off approximation is of the same order in c_0/ρ as in Saffman's (1970) formula for the velocity of a circular vortex ring. By comparing with numerical calculations of the full equations of motion, Fraenkel (1970) and Norbury (1973) have shown that Saffman's formula is fairly good for values of c_0/ρ which are not small compared with unity. Thus, although no rigorous proof is available, it is reasonable to expect that the cut-off theory will hold equally good for such values of c_0/ρ. Preliminary experiments with smoke rings tend to support this view.

In any case the results are not sensitive to the precise value of c_0/ρ since the velocity obtained from the cut-off theory depends only logarithmically on the cut-off length and hence the radius of the core. Thus as far as the motion of the centre-line of the vortex ring is concerned, the results obtained here are applicable, within a small error, to a vortex ring of the same configuration but smaller core size.

Only those inferences which depend directly on the core size will differ.

Table 6.2 shows the values of N and time step Δt_1 used in each of the cases considered. Trial and error showed that these gave adequate accuracy. Smaller time steps were needed with increasing eccentricity of the initial ellipse because of the rapid changes associated with the large curvature at the major axis.

b/a	N	Δt_1
0.2	41	0.0001
0.4	41	0.001
0.6	41	0.001
0.8	21	0.002

Table 6.2. Number of points per quadrant and time step used.

In view of the results of §2, it is anticipated that in the case of small eccentricity the vortex ring will oscillate with a period given by (6.2.3). As a check on the computer program, this was verified. In order to measure the oscillations, an amplitude B is defined and monitored together with the variance of the points on the ring from a plane parallel to the plane of the original ellipse and moving with the velocity of the centroid of the ring. If the vortex ring has an impulse I, its centroid is given by (Saffman (1970))

$$\underline{\bar{x}}(t) = \frac{\Gamma}{2} \oint \frac{(\underline{X} \wedge \hat{\underline{t}}.\underline{I})}{I^2} \underline{X} \, ds \qquad (6.4.4)$$

so that for a ring which is symmetric about x = 0 and y = 0 in Cartesian coordinates fixed in the plane of the original ellipse,

$$\bar{\underline{x}}(t) = (0,\ 0,\ \frac{1}{2\pi ab}\oint (\ x\frac{dy}{ds} - y\frac{dx}{ds})z\ ds) \tag{6.4.5}$$

since $I = \Gamma\pi ab$ is conserved (this was checked by evaluating I at various times during the calculations). Then amplitude B is defined as

$$B = \frac{A_1 - B_1}{A_1 + B_1} \tag{6.4.6}$$

where

$$A_1(t) = \max|\underline{X}(\xi,t) - \bar{\underline{x}}(t)|\ ,$$

$$B_1(t) = \min|\underline{X}(\xi,t) - \bar{\underline{x}}(t)|$$

The variance Σ is defined as

$$\Sigma = \frac{1}{2\pi ab}\oint (x\frac{dy}{ds} - y\frac{dx}{ds})(z-\bar{z})^2 ds \tag{6.4.7}$$

where $\bar{z}(t) = \bar{\underline{x}} \cdot \underline{k}$.

The values of $\Sigma(t_1)$ and $B(t_1)$ have been plotted against time in Fig. 6.1(a,b). Initially, when the vortex ring is flat and elliptic in shape, Σ is zero and $B = \frac{a-b}{a+b}$. Subsequently, Σ and B oscillate in time. For $t_1 > 0$, Σ first achieves a minimum at a time defined as $t_1 = \frac{1}{2}\tau_A$. Except in the case of b/a = 0.8 the value of the minimum is different from zero; the difference is small but not negligible. Thus at $t_1 = \frac{1}{2}\tau_A$, the vortex ring is flat in the case b/a = 0.8 and nearly so in the other cases considered. The numerical calculations were stopped just after $t_1 = \frac{1}{2}\tau_A$.

For the b/a = 0.8 case the shape of the centre-line of the vortex ring at various instants of the evolution is shown in Fig. 6.2. At $t_1 = \frac{1}{2}\tau_A$, as expected from the value of $\Sigma(\frac{1}{2}\tau_A)$, the vortex ring is flat.

It is also elliptic in shape with the orientation of its axes reversed. Thus in this case the vortex ring oscillates periodically since it can be rotated through an angle of 90^{o} to obtain the initial configuration. The time $\frac{1}{2}\tau_A$ is in good agreement with the half-period of oscillation of an equivalent perturbed circular vortex ring of radius R = 0.9a, given by $\frac{1}{2}(\Gamma/4\pi a^2\tau(0.9a, 0.347, 1))$, where τ is as in (6.2.3).

In the other more eccentric cases considered, the vortex ring assumes complicated forms during the evolution.

For the b/a = 0.6 and 0.4 cases, the different stages of the evolution are shown in Fig. 6.3 and Fig. 6.4 respectively. At $t_1 = \frac{1}{2}\tau_A$, as expected from $\Sigma(\frac{1}{2}\tau_A)$, the vortex ring is not exactly flat. Nor is the shape of the vortex ring elliptic, although the orientation of the axes is reversed as in b/a = 0.8 case. After $t_1 = \frac{1}{2}\tau_A$, the vortex ring starts deforming in such a way that the axes tend to attain their initial orientation. Thus, although the vortex ring oscillates, the oscillations are not periodic in these cases. Thus a flat elliptic vortex ring is not, in general, a periodic solution of the vortex ring configurations. τ_A will be referred to as the "apparent period" of oscillation of the elliptic vortex ring.

The different stages of evolution of the vortex ring in the case b/a = 0.2 are shown in Fig. 6.5. In this case, at $t_1 = 0.1355$ ($<\frac{1}{2}\tau_A$), the points on y = 0 are 0.214a distance apart, which implies that the cores are touching. Since the calculations are based on the assumption that the separation of such points on the vortex ring is large compared with the core radius, the results at this stage may be viewed with scepticism. However, by performing a numerical calculation with vortices in two-dimensions, in which the core was allowed for, Moore (1972) was able to show that the Biot-Savart formula gives roughly the correct velocity even when the cores are touching. Thus, as Moore points

out, it is expected that, while the cores will be distorted so that the cut-off length will change, the approximations on which the present calculations are based will be reasonably adequate even when the cores are close to each other.

The relevance of the calculations to the real situation at the instant of touching is difficult to assess. However, experiments, due to Fohl & Turner (1975), with colliding vortex rings suggest that since the vortex cores, where they touch, have vorticity of opposite sign, viscous diffusion would annihilate the vorticity locally. Although the actual process is complicated, the net result would be that the vortex lines would connect on either side of the region of contact to form two smaller rings.

It is not meaningful to continue with the numerical integration beyond the approximate instant of touching. However, in order to obtain an estimate of the nearest distance of approach of the core centres, it was decided to carry the integration forward in time as far as possible using the same number of points and time step. Numerical instability sets in near $y = 0$ at $t_1 = 0.15$ when the two centre-line points on $y = 0$ are $0.014a$ distance apart. The instability is presumably due to this separation distance being small compared with the grid spacings and could be remedied by using smaller grid spacings and smaller time step. However, this was not attempted in view of the dubious implication of the results at this stage. The shape of the centre-line of the ring at $t_1 = 0.149$ is shown in Fig. 6.6.

At $t_1 = \frac{1}{2}\tau_A$ $(= 0.147)$, the separation of the two centre-line points on $y = 0$ is $0.05a$. The overall length is greater by 2% over its initial value so that the core size is not significantly different from its initial value. Thus, within logarithmically small error, it appears that an elliptic vortex ring of axes ratio 0.2 and core radius c_1 such

$c_1 > 0.025a$ would break up into two smaller rings before the apparent half-period stage is reached.

The values of $\tau_N = \frac{a\tau_A}{b}$ for the cases considered are shown in Table 6.3. The reason for tabulating τ_N instead of τ_A is that τ_N is independent of the impulse of the vortex ring. τ_N is in good agreement with

$$\tau_L = \frac{\Gamma}{4\pi ab}\,\tau\left(\frac{a+b}{2},\ c_0,\ 1\right) \tag{6.4.8}$$

where τ is given by (6.2.3) and c_0 is tabulated in Table 6.2. For comparison, the values of τ_L are also shown in Table 6.3.

It may be of interest to note that the velocity $\bar{U}$ of the centroid of the ring, defined by

$$\bar{U} = \frac{d\bar{z}}{dt} \tag{6.4.9}$$

where $\bar{z}$ is given by (6.4.7), oscillates in time about a mean value $\bar{\bar{U}}$ with an apparent period approximately equal to $\frac{1}{2}\tau_A$. A plot of $\bar{U}$ against time is shown in Fig. 6.1(c). $\bar{\bar{U}}$ is in good agreement with the velocity of an equivalent circular vortex ring,

$$V_L = \left(\frac{\Gamma}{4\pi a}\right)^{-1} V\left(\frac{a+b}{2},\ c_0,\ 1\right) \tag{6.4.10}$$

where V is given by (6.2.5). For comparison, the values of $\bar{\bar{U}}$ and V_L for the cases considered are shown in Table 6.3.

b/a	$\tau_N = \frac{a\tau_A}{b}$	τ_L	$\bar{\bar{U}}$	V_L
0.8	1.213	1.212	3.935	3.925
0.6	1.220	1.217	4.522	4.506
0.4	1.290	1.244	5.564	5.425
0.2	1.47	1.432	7.383	7.142

Table 6.3 Apparent period of oscillation τ_N and mean velocity $\bar{\bar{U}}$ compared with τ_L and V_L respectively.

§5 Experimental measurements

The elliptic vortex rings were produced by puffing air through sharp-edged elliptic orifices of the same eccentricities as those used in the numerical calculations. Each orifice, of semi-major axis a_0, was cut in a thin plate of 14 cm diameter which was mounted on one end of a 70 cm long perspex tube of the same diameter. The other end of the tube was smoothly connected to a 8.3 cm diameter brass cylinder which contained the piston (Fig. 6.7). The piston was driven, through a gear box, by a high torque stepping motor which was operated by a logic control circuit. With this arrangement it was possible to provide high initial and terminal accelerations with a uniform velocity over most of the piston stroke. The acceleration and deceleration times, the top piston speed and the length of the stroke could be easily adjusted. In order to provide draught-free conditions, the vortex rings were produced in a 40×40×70 cm perspex box. The arrangement made it possible to obtain reproducible vortex rings.

The experiment consisted of hot-wire anemometer measurements to determine the circulation and core size and flow visualization studies to determine the mean translational velocity $\bar{U}_E$, the equivalent ring radius R_0 and the oscillatory features of the vortex rings.

Glycerine smoke was used to provide flow visualization. The motion of the vortex rings was recorded on a 16 mm ciné film at 32 f/s and 64 f/s. The film was analysed to determine the characteristics of the motion of the ring. Starting from the moment of generation, the maximum y-displacement (see Fig. 6.7), y_m, of the vortex ring was recorded and Fourier-analysed. y_m for the cases 0.6 and 0.8 are shown in Fig. 6.8; the figure also shows the average values of y_m over five different runs. The ends of an oscillation cycle were defined to be the times when y_m was a minimum and the time interval between the ends

of an oscillation was defined as the oscillation time $\tilde{\tau}_E$, to be compared with the corresponding apparent period τ_A of §4.

A survey of the velocity field in a plane parallel to the plane of the orifice and at a fixed distance from it was made by recording hot-wire anemometer signals at various positions in the plane. At each position, several different recordings were made; for each recording, a vortex ring was produced, checking that the piston velocity had the same value each time. For a circular vortex ring, a few hot-wire traces are needed (Sallet and Widmayer (1974)) to obtain a qualitative description of the flow field. However, in the present case the vortex ring is deforming as it moves and traces at several positions are needed. The order of the difficulty of the analysis increases when more eccentric cases are considered. The measurements were repeated at a further distance from the orifice.

From the available traces, the ones corresponding to the axis of the ring and the centre of the core were identified. For the $b/a = 0.8$ and $b/a = 0.4$ cases, these are shown in Fig. 6.9. The core-position trace was used to determine the core size of the ring. From the axis-position trace, the velocity component u along the z-axis can be determined (by symmetry the other components are zero). This enables (see e.g. Didden 1977) the circulation Γ to be determined: within a closed curve C containing the vortex core, Γ is found by integrating the velocity along the z-axis and closing the curve C outside the z-axis at infinity where u and v (y-velocity component, say) are zero. Thus

$$\Gamma = \oint_C (u\,dz + v\,dy) = \int_0^\infty u(z,y=0)\,dz = \int_0^\infty u\bar{U}_E(t)\,dt \qquad (5.5.1)$$

where the transformation $dz = \bar{U}_E dt$ has been used. From the ciné film, $\bar{U}_E$ is determined by analysing the end view of the evolution as the average of the z-velocity of the projection on the y-z plane of those

points on the vortex ring which lie in its planes (fixed) of symmetry. The velocity at each of these points on the vortex ring is obtained by noting its instantaneous z-displacement and numerically differentiating it with respect to time. The oscillatory behaviour of $\bar{U}_E$, anticipated by the numerical calculations, was noticeable only in the more eccentric cases and appeared in the form of fluctuations approximately about $\bar{\bar{U}}$ (defined in §4).

To obtain estimates of the vortex parameters, it is not satisfactory to model the flow by a uniform flow past an equivalent disk and use the method described in Appendix A; see e.g. Sallet (1975). Instead, the estimates are obtained using a model of the flow, given by Saffman (1978), in which it is assumed that when the flow is first set into motion, the vortex sheet at the orifice behaves locally like a two-dimensional vortex sheet formed at the edge of a semi-infinite plate. Then applying the similarity law for the roll up of the vortex sheet and using the estimates given by Pullin (1978) for the constants associated with the law, it is possible to obtain estimates of the circulation Γ, the length of the axes, and the core size of the ensuing elliptic vortex ring. The details are given in Appendix B and the estimates for the circulation Γ, the semi-major axis a, the equivalent radius R and the core size c_E for the cases considered are given in Table 6.4. Here L and W refer to the displacement and velocity respectively of an equivalent slug of fluid in the perspex cylinder (see Fig. 6.7). The flux of fluid through a cross-section of the slug is equated to the flux through the orifice. The fluid velocity in the perspex cylinder was checked and found to be approximately uniform over the time of the stroke. For comparison, the corresponding measured values are given in Table 6.5 where $Re(= \Gamma/\nu)$ is the vortex Reynolds number and $\tilde{V} = \frac{4\pi\bar{\bar{U}}R}{\Gamma}$.

§6 Comparison of numerical and experimental results

Plate 6.1 shows the contrast between a vortex ring produced from a circular orifice and that produced from an elliptic orifice of axes ratio 0.4.

For axes ratios b/a = 0.8, 0.6 and 0.4, the vortex ring was observed to oscillate in the manner anticipated by the numerical calculations. In fact, qualitative comparisons between some of the stills of the vortex ring from the ciné film and the computed configurations in Figs 6.2-6.4 showed striking resemblance. Plate 6.2 shows the plan view of the evolution of the vortex ring for the case b/a = 0.4. As may be noticed from the plate, at the end of the first half cycle the vortex ring assumes the shape shown in Fig. 6.4 for time T_7. This shape was observed at each subsequent end of cycle for three cycles indicating that this configuration may be a possible periodic solution of the vortex ring. The contortions seen in the photographs in the set of frames on the far right in Plate 6.2 are a defect of the photography and do not indicate a short-wave instability of the ring; the vortex ring has progressed beyond the depth of focus of the camera. However, a short-wave instability of the type described by Widnall and Tsai (1977) for a circular vortex ring was eventually observed for the b/a = 0.4 case; Plate 6.3 shows eight waves growing on the elliptic vortex ring. The pictures were taken at approximately 1s after generation time. From Saffman's (1978) formula (2.18), with $\epsilon = 0.62$ and $R = 2.95$ (see Table 6.5) and using his equation (3.6), the expected number of waves N on an equivalent circular vortex ring is $N = 8$ approximately. The agreement is remarkably good considering that the observed vortex ring is not circular.

It was found that in each case considered, the oscillation time $\tilde{\tau}_E$ had a greater value for each subsequent cycle. This increase in $\tilde{\tau}_E$ with

time is believed to be related to the accompanying increase in the equivalent radius of the ring observed at the end of each oscillation cycle. For the purpose of comparison with numerical computations

$$\tau_E = \frac{a\tilde{\tau}_E}{b} \tag{6.6.1}$$

is defined. The values of $\frac{1}{2}\tau_E$ for the first half cycle is compared with the corresponding numerical values of $\frac{1}{2}\tau_N$ in Fig. 6.10. It is found desirable to plot $\tau_E/\tau_L(\frac{a+b}{2}, c_E, 1)$ and $\tau_N/\tau_L(\frac{a+b}{2}, c_0, 1)$ instead of τ_E and τ_N in view of the differences in core size between that used in the computations and the corresponding observed value. The results are in fair agreement in the cases b/a = 0.8 and 0.6. For the case b/a = 0.4, the value of τ_E/τ_L is much greater than τ_N/τ_L. However, the error margin in the value of τ_E/τ_L is large. This is due to the difficulty in ascertaining the value of Γ as a result of the high fluctuations in $\bar{U}_E$ observed in this case.

In the case b/a = 0.2, the vortex ring was observed to break up into two smaller rings as anticipated in §4, provided the Reynolds number of the flow was high enough (Γ/ν > 1300 approximately). Plate 6.4 shows the end view of the break-up process. The shape of the vortex ring prior to the break-up may be compared with the configuration shown in Fig. 6.5(c). After break-up, the two ensuing vortex rings are observed to oscillate and travel in directions inclined at equal angles to the z-axis; the size of the angles is such that the vortex rings move almost parallel to each other. At the Reynolds number of the experiment, the rings were not observed to rejoin. In Plate 6.5 individual photographs of the plan view of the vortex ring at different stages of the break-up process are shown. The time of the break-up of the vortex ring is shown in Fig. 6.10; the time of the break-up anticipated in §4 is also shown in the figure.

§7 Discussion

By means of numerical calculations using the cut-off approximation, it has been shown that a flat elliptic vortex ring of axes ratio, 0.8, 0.6 and 0.4, oscillates in time, the oscillations being periodic only in the first of these cases. At the end of a half oscillation cycle, the deviations of the shape of the vortex ring from an ellipse with the orientation of its axes reversed becomes more pronounced as more eccentric cases are considered. In the case of a ring of axes ratio 0.2, it is anticipated in §4 that the vortex ring would break up through the touching of the cores of distinct portions of the vortex ring. This suggests that there is a critical axes ratio, $(b/a)_{cr}$, $0.4 > (b/a)_{cr} \geq 0.2$, above which an elliptic vortex ring oscillates and below which it breaks up.

The results from experiments conducted at moderate Reynolds number ($\Gamma/\nu \sim 2000$) are in fair agreement with the results of the numerical computations. The vortex ring oscillates in the cases of axes ratios 0.8, 0.6 and 0.4 in a manner strikingly similar to that anticipated by the numerical calculations. In the case of the vortex ring of axes ratio 0.2, the vortex ring breaks up into two smaller rings; however, the break up only occurs when the Reynolds number is high enough ($\Gamma/\nu > 1300$ approximately).

The vortex trail of an aircraft breaks up into vortex rings as can be seen from the photograph (Fig. 1) in Crow's (1970) paper. The photograph shows that in the plane of maximum area (the horizontal plane) the vortex rings, when they form, have roughly elliptic shape .

Using, as approximations, the data from Crow's paper ($\Gamma = 268$ m^2/s, so that $\Gamma/\nu = 1.8 \times 10^7$, core radius $c_0 = 2.7$ m for a B-47 aircraft of span 35 m and moving at 220 m/s), and assuming that each ring when formed has an elliptic shape with axes ratio 0.2, is flat and lies in a

horizontal plane, the results of §§4-6 suggest that each ring would break up into two smaller rings at 107 s after the initial ring formation; here the influence of other vortex rings in the trail is neglected. Since a vortex ring in an aircraft trail, when formed, is not flat and since the axes ratio appears from the photograph in Crow's paper to be closer to 0.15 than 0.2 (also the size of the core is comparatively much smaller than that used in the calculations and observed in the experiments) it is expected that the actual break up of the vortex ring would occur at an earlier time.

Not enough information is available in the photograph. However, on comparison with Fig. 6.5, it appears that the break-up may occur 30-40 s after the initial ring formation.

axes ratio $b_0/a_0 = b/a$	semi-major axes of orifice a_0 cm	L cm	W cm/s	a cm	R=a+b/2 cm	c_E/a	Γ cm^2/s
0.8	3.1	0.7	11.7	3.38	2.95	0.33	390
0.6	4	1.4	11.5	4.44	3.55	0.31	332
0.4	4	1.2	9.1	4.61	3.22	0.32	370
0.2	4	0.4	4	4.72	2.83	0.23	196

Table 6.4 Estimates of vortex parameters predicted by method given in Appendix B.

$b_0/a_0 = b/a$	a cm	$R=\frac{a+b}{2}$ cm	c_E/a	$\tilde{V}$ cm/s	Γ cm^2/s	Re = Γ/ν
0.8	3.17	2.85	0.31 ± .07	3.0	407	2714
0.6	4.37	3.5	0.25 ± .05	2.8	437	2914
0.4	4.28	2.95	0.29 ± .05	2.7	471	3140
0.2	-	-	0.26 ± .05	3.0	211	1473

Table 6.5 Measured values of vortex parameters.

APPENDIX A: Initial core size used in the numerical calculations

A process of generation of a vortex ring in a perfect fluid by an impulsive motion and subsequent annihilation of a flat elliptic disk is considered here (c.f. G.I. Taylor (1953)).

Suppose in Cartesian coordinate system the edge of the disk is given by

$$\frac{x^2}{c^2} + \frac{y^2}{d^2} = 1 \qquad (c > d) \tag{A6.1}$$

Then if the disk is moved impulsively from rest at speed U normal to its plane, the velocity potential at the disk is given by

$$\phi = \mp \frac{Ud}{E(e)} \left(1 - \frac{x^2}{c^2} - \frac{y^2}{d^2}\right)^{1/2} \tag{A6.2}$$

where

$$e = \frac{(c^2-d^2)}{c^2} \quad \text{and} \quad E(e) = \int_0^{\pi/2} \sqrt{1 - e^2 \sin^2\theta}\, d\theta$$

are respectively the eccentricity of the ellipse and elliptic integral of the second kind. The kinetic energy of the flow is given by

$$\begin{aligned} T_D &= -\tfrac{1}{2} \int\int_{\text{disk}} \phi \frac{\partial \phi}{\partial n} dS \\ &= \frac{2\pi c d^2 U^2}{3E(e)} \end{aligned} \tag{A6.3}$$

and the impulse is given by

$$\begin{aligned} I_D &= \frac{dT_D}{dU} \\ &= \frac{4\pi c d^2 U}{3E(e)} \end{aligned} \tag{A6.4}$$

If now the disk is dissolved away, a finite vortex sheet is left behind, the vortex lines being ellipses of the same axes ratio as the disk. Writing $x = cr_e \cos\theta$, $y = dr_e \sin\theta$ $(0 \leq r_e \leq 1;\ -\pi \leq \theta \leq \pi)$, the circulation in the portion $(r_e, 1)$ for any fixed θ is, from (A6.2),

$$\frac{2Ud}{E(e)}(1 - r_e^2)^{\frac{1}{2}} \tag{A6.5}$$

This configuration cannot persist because the self-induced velocity is infinite at $r_e = 1$. The vortex elements respond in such a way that the stronger vortex lines near $r_e = 1$ tend to roll up the weaker parts near $r_e = 0$ round them. Thus the vorticity tends to concentrate in an elliptic ring of major axis a and minor axis b, say, and of circulation Γ given by

$$\Gamma = \frac{2Ud}{E(e)} \tag{A6.6}$$

The impulse I and kinetic energy T of a vortex filament are given by Moore & Saffman (1972) to be

$$\underline{I} = \frac{\Gamma}{2}\oint \underline{X} \wedge \hat{\underline{t}}\, ds$$

$$T = \oint \{\frac{\Gamma^2}{4\pi}[\ln\frac{8\rho}{c_0} - 2 + A + \frac{\hat{\underline{t}}.\underline{X}}{\rho}\frac{\partial\rho}{\partial s}] - \Gamma(\underline{X} \wedge (\underline{V}_E+\underline{V}_I).\hat{\underline{t}})\}ds$$

where $\rho(s)$ is the radius of curvature at $\underline{X}$, a point on the ring and $\underline{V}_E+\underline{V}_I$ is approximately given by the right hand side of (5.3.1) less the velocity of a circular vortex ring of radius ρ and lying along the osculating circle as $\underline{X}$. For an elliptic vortex ring, therefore,

$$\underline{I} = \underline{I}_R = \Gamma\pi b\underline{k} \tag{A6.7}$$

and $$T = T_R = \frac{\Gamma^2 a}{\pi}[(\ln(\frac{8(ab)^{\frac{1}{2}}}{c_0}) - 1 + A)E(e) - (1 - \tfrac{1}{2}e^2)K(e)] \tag{A6.8}$$

where K(e) is the elliptic intergral of the first kind.

Following G.I. Taylor (1953), it may be assumed that

$$T_D = T_R, \qquad \underline{I}_D = \underline{I}_R \tag{A6.9}$$

so that using (A6.6), we have

$$ab = \frac{2}{3} cd \tag{A6.10}$$

and core radius c_0 is

$$c_0 = 8(ab)^{\frac{1}{2}} \exp\left[-\frac{\pi^2}{2\sqrt{6}} - 1 + A - (1 - \tfrac{1}{2}e^2)\frac{K(e)}{E(e)}\right] \tag{A6.11}$$

Hence the cut-off length

$$\mu(t) = c_0\left(\frac{L(t)}{L(0)}\right)^{-\frac{1}{2}} e^{-\frac{1}{2}-A}$$

$$= 8(ab)^{\frac{1}{2}}\left(\frac{L(t)}{L(0)}\right)^{-\frac{1}{2}} \exp\left[-\frac{\pi^2}{2\sqrt{6}} - \frac{3}{2} - (1 - \tfrac{1}{2}e^2)\frac{K(e)}{E(e)}\right] \tag{A6.12}$$

Thus with this process of generation the cut-off length does not depend on the choice of A. This implies that any information obtained from the governing equation (6.3.4) using the above cut-off length will be independent of the choice of swirl and axial velocities in the core. In particular the period τ of small oscillations of a circular vortex ring of radius $R = \frac{a+b}{2}$ is independent of A.

APPENDIX B: Estimate of vortex parameters using Saffman's (1978) method

Estimates of the circulation Γ, the core radius c_E and the size of the elliptic vortex ring generated can be obtained in the manner suggested by Saffman (1978) for circular vortex rings. Here it is assumed that when the flow has just been set into motion, and the vortex sheet is of small extent and close to the edge, it behaves like a two-dimensional vortex sheet formed at the edge of a semi-infinite flat plate lying along $z = 0$, $n > 0$ (see fig. 6.11). Initially the velocity potential is given by

$$\phi = -\alpha r^{\frac{1}{2}} \cos \tfrac{1}{2}\chi \qquad \text{(B6.1)}$$

where $r = (n^2+z^2)^{\frac{1}{2}}$ and α is determined by matching to the flow far from the edge. For flow through an elliptic orifice of semi-major axis a_0 and semi-minor axis b_0 in an infinite plane, the normal velocity V_z at the orifice is given by Lamb (1932, p.151). Near a point (x_0,y_0) on the edge of the ellipse, this is approximately

$$\frac{\sqrt{2}\,A|n|^{-\frac{1}{2}}}{(a_0^2 b_0)^{\frac{1}{2}}(1 - e^2\cos^2\theta_0)^{\frac{1}{4}}}$$

where $4\pi A$ is the flux through the hole. By comparing this with $\frac{1}{r}\frac{\partial \phi}{\partial \chi}\Big|_{\substack{\chi=\pi \\ r=|n|}}$, an estimate of α can be obtained. However, α varies along the edge of the orifice which is undesirable. Thus an average value is taken,

$$\alpha = 2\left(\frac{\int_0^{\pi/2} V_z^2 \left|\frac{ds}{d\theta}\right| d\theta}{\int_0^{\pi/2} \left|\frac{ds}{d\theta}\right| d\theta}\right)^{\frac{1}{2}} = \frac{2\sqrt{\pi}\,A}{(a_0^2 b_0)^{\frac{1}{2}} E(e)^{\frac{1}{2}}} \qquad \text{(B6.2)}$$

Then for small times, the vortex sheet which appears at the edge depends on α and t only. Its centre (N_1,Z_1), circulation $\Gamma(r_1)$ about a small circle centred on the vertex of the spiral and total circulation Γ shed from the edge is given by

$$N_1 = c_1(\alpha t)^{2/3}, \quad Z_1 = c_2(\alpha t)^{2/3}, \quad \Gamma(r_1) = c_3\alpha r_1^{\frac{1}{2}},$$

$$\Gamma = c_4\alpha^{4/3}t^{1/3} \tag{B6.3}$$

where c_1, c_2, c_3 and c_4 are constants (estimates can be obtained from Pullin's (1978) calculations as $c_1 = 0.08$, $c_2 = 0.34$, $c_3 = 4.08$, $c_4 = 2.40$).

If the piston stops moving at time $t = W/L$ where W is the velocity of the piston and L is the displacement, the rolled up vortex sheet breaks away from the edge of the orifice. The semi-axes, a and b, core radius c_E and circulation Γ of the ensuing vortex ring are then given by

$$a = a_0 + c_1(\frac{\alpha L}{W})^{2/3}, \quad b_1 = b_0 + c_1(\frac{\alpha L}{W})^{2/3}, \quad c_E = \frac{c_4^2}{c_3^2}(\frac{\alpha L}{W})^{2/3},$$

$$\Gamma = c_4\alpha^{4/3}(\frac{L}{W})^{1/3} \tag{B6.4}$$

Since $a/b \neq a_0/b_0$, the vortex ring will have a different eccentricity from that of the orifice. However, for small values of L this change will be small. Also, the interaction of the ring with the stopping image vortex would lead to a decrease in a and b below that given in (B6.4) (Sheffield 1977). Hence, for the range of eccentricities used here, this discrepancy is ignored and a and b are taken to be

$$a = a_0(1 + \frac{c_1(a_0+b_0)}{2a_0b_0}(\frac{\alpha L}{W})^{2/3}), \qquad b = b_0(1 + \frac{c_1(a_0+b_0)}{2a_0b_0}(\frac{\alpha L}{W})^{2/3}) \tag{B6.5}$$

From (B6.1) the swirl velocity in the core is $\sim r^{-\frac{1}{2}}$.

CHAPTER 7: INTERACTION BETWEEN A VORTEX FILAMENT AND AN APPROACHING RIGID SPHERE

§1 Introduction

In consideration of vortex filaments in inviscid flow, it is often of interest to determine how these interact with each other or with surfaces present in the flow field. The trailing vortices of an aircraft and motion of two co-axial vortex rings are examples of interacting vortex filaments. The objective of this chapter is to determine the interaction between a vortex filament and a moving bluff body.

The particular situation considered is that when a rigid sphere, which can be regarded as a typical bluff body, approaches an infinitely long straight vortex filament from infinity at a uniform speed. The evolution of the vortex in such a situation, from its straight configuration, is studied. The fluid is regarded as being inviscid and incompressible and of uniform density.

The motion of the vortex is symmetrical about a plane which passes through the centre of the sphere and whose normal is parallel to the axis of the undisturbed straight vortex. Thus the situation is equivalent to the case of a vortex filament moving in a uniform stream over a rigid plane with a hemi-spherical hump in its path.

The problem is treated in two stages. When the sphere is at a large distance away from the vortex, the interaction between the sphere and the vortex is weak so that the evolution can be determined from linear theory. Thus in §§2,3(b) the equation of motion of the filament (5.3.1) is linearized and solved to obtain the expression for the instantaneous shape of the vortex; the velocity contribution $\underline{V}_E$ in (5.3.1) is obtained approximately using spherical harmonic analysis.

The shape of the vortex given by linear theory is evaluated at a time t_s when the sphere, approaching at a uniform speed U, is at a prescribed distance away from the position of the undisturbed vortex. This is used as the starting configuration of the vortex for the full non-linear marching problem (5.3.1) which is integrated numerically for subsequent times. In §4, the numerical procedure used in the calculation is described while in §5 the image system of a vortex element in a sphere, due to Lighthill (1956), is described and a full expression for $\underline{V}_E$ is obtained for use in the numerical calculations.

The vortex is chosen to have a uniform distribution in its core. In (5.3.1), Crow's (1970) method of cut-off is used for the linear analysis and that of Rosenhead (Moore (1972)) for the numerical calculations.

The numerical results are presented in §6. The neglect of viscous diffusion and the wake of the sphere means that the results are of only approximate validity in real fluid flows. Indeed a qualitative experiment with a bath-tub vortex shows that although the vortex commences to move as anticipated in §6, when the sphere is close to the vortex, the wake appears to interact strongly with the vortex causing it to break up.

In §3(a) the interaction between a point source and a vortex is discussed and for a hollow vortex the results are compared with those obtained from classical analysis and given in Appendix A; the case of an interaction between a source and a vortex in compressible flow was studied by Ffowcs Williams & O'Shea (1971). The two results are compared in Table 7.1 and provide a check on the cut-off theory in the case of infinitesimal disturbances to a vortex.

§2 Linearized equation of motion

The equation of motion of a vortex filament, discussed in Chapter 5, is linearized in this section in order to consider the evolution of an infinitely long straight vortex filament when subjected to infinitesimal disturbances due to a non-uniform external velocity field.

Let rectangular axes Oxyz be chosen so that in the undisturbed state, Oz lies along the axis of the vortex filament. If the vortex has strength Γ and if at time t its axis occupies the curve given parametrically by $\underline{X}(\xi,t)$, then its motion is governed by equation (5.3.1),

$$\frac{\partial \underline{X}}{\partial t}(\xi_0,t) = \frac{\Gamma}{4\pi} \oint_{-\infty}^{\infty} \frac{\partial \underline{X}}{\partial \xi}(\xi,t) \wedge \frac{(\underline{X}(\xi_0,t) - \underline{X}(\xi,t))d\xi}{|\underline{X}(\xi_0,t) - \underline{X}(\xi,t)|^3} + \underline{V}_E(\xi_0,t) \qquad (7.2.1)$$

where $\underline{V}_E(\xi_0,t)$ is the contribution to the velocity at ξ_0 from external sources which produce an irrotational velocity field. The notation $\oint$ implies that a suitable cut-off is used to make the line integral finite at $\xi = \xi_0$. For the linear analysis, the method of cut-off employed here is that due to Crow (1970) and described in Chapter 5, §2. This requires that a portion $(\xi_0-\varepsilon, \xi_0 + \varepsilon)$ be removed from the range of integration, ε being chosen so that $|s(\xi_0+\varepsilon, t) - s(\xi_0-\varepsilon,t)| = 2\delta_c c$ where $s(\xi,t)$ denotes distance along the filament, c is the core-radius and δ_c is a constant. Note that since $\frac{\partial \underline{X}}{\partial s} = \hat{\underline{t}}$, a unit tangent vector to the vortex, it follows that $\frac{\partial s}{\partial \xi} = \left|\frac{\partial \underline{X}}{\partial \xi}\right|$ so that the cut-off length may be written

$$2\delta_c c = \int_{\xi_0-\varepsilon}^{\xi_0+\varepsilon} \left|\frac{\partial \underline{X}}{\partial \xi}\right| d\xi \qquad (7.2.2)$$

From (5.2.3), the constant δ_c is given by

$$\log 2\delta_c = \tfrac{1}{2} - \frac{4\pi^2}{\Gamma^2} \int_0^c r v^2 dr \qquad (7.2.3)$$

where v is the swirl velocity in the core and there is no axial flow in the filament. For a uniform vortex $v = \Gamma r/2\pi c^2$ so that

$$\log 2\delta_c = 1/4 \tag{7.2.4}$$

and for a hollow vortex

$$\log 2\delta_c = 1/2 \tag{7.2.5}$$

As explained in Chapter 5, the core cross-section is uniform along the filament, the core radius c being just that function of time only which conserves the volume of the filament. Thus $c = c(t)$.

However, as pointed out in Chapter 5, for infinitesimal disturbances to the vortex, the effect of the variation of c with time on the governing equation is of second order in the perturbation quantity and is neglected. Thus, for linear analysis, $c = c_0$ where c_0 is the initial value of the core radius.

Equation (7.2.1) is to be linearized and solved subject to the initial condition applied at time $t = t_0$

$$\underline{X}(\xi,t_0) = \ell\xi\underline{k} \qquad -\infty < \xi < \infty \tag{7.2.6}$$

where ℓ is the length scale of the particular problem considered.

For an infinitesimal disturbance to the vortex, the parametric equation of the perturbed vortex is taken as

$$\underline{X}(\xi,t) = \ell(\xi\underline{k} + \alpha\underline{x}'(\xi,t) + O(\alpha^2)) \tag{7.2.7}$$

where $\alpha << 1$. α measures the amplitude of the response of the vortex. The external velocity field $\underline{V}_E$ must also be expanded in terms of α. Thus

$$\underline{V}_E(\xi,t) = \alpha\underline{V}'_E(\xi,t) + O(\alpha^2) \tag{7.2.8}$$

Substituting (7.2.7) and (7.2.8) into (7.2.1) and retaining terms to order α only gives

$$\frac{\partial \underline{x}'}{\partial t}(\xi_0,t) = \frac{\Gamma}{4\pi\ell^2}\,\underline{k}\,\Lambda \int_{-\infty}^{\infty}_{[\delta_c]} \frac{\underline{x}'(\xi_0,t)-\underline{x}'(\xi,t)-(\xi_0-\xi)\frac{\partial \underline{x}'}{\partial \xi}(\xi,t)}{|\xi_0-\xi|^3}\,d\xi + \frac{\underline{V}_E'(\xi_0,t)}{\ell} \tag{7.2.9}$$

In view of (7.2.5) and the constancy of the core radius

$$\delta_c c_0 = \ell\varepsilon(1+O(\alpha)) \tag{7.2.10}$$

To solve (7.2.9) for a given $\underline{V}_E'$, the Fourier transform of the equation with respect to ξ_0 is taken. Thus, writing

$$\hat{\underline{x}}(k,t) = \int_{-\infty}^{\infty} \underline{x}'(\xi_0,t)e^{ik\xi_0}d\xi_0,\quad \hat{\underline{V}}_E(k,t) = \int_{-\infty}^{\infty} \underline{V}_E(\xi_0,t)e^{ik\xi_0}d\xi_0 \tag{7.2.11}$$

the transform equation, after a change in variable of the cut-off integral, becomes

$$\frac{\partial \hat{\underline{x}}}{\partial t}(k,t) = \frac{\Gamma}{4\pi\ell^2}\,\underline{k}\,\Lambda \int_{-\infty}^{\infty} e^{ik\xi_0}d\xi_0 \int_{[\delta_c]}^{\infty} \frac{\underline{x}'(\xi_0,t)-\underline{x}'(\xi_0+\chi,t)+\chi\frac{\partial}{\partial\chi}\underline{x}'(\xi_0+\chi,t)}{|\chi|^3}\,d\chi + \hat{\underline{V}}_E(k,t)$$

where now the cut-off in the inner integral is implied at $\chi = 0$. Thus, since the range of this integral is now independent of ξ_0, the order of the integration can simply be changed to give (suppressing the time dependence),

$$\int_{-\infty}^{\infty} e^{ik\xi_0}d\xi_0 \int_{[\delta_c]}^{\infty} \frac{\underline{x}'(\xi_0)-\underline{x}'(\xi_0+\chi)+\chi\frac{\partial}{\partial\chi}\underline{x}'(\xi_0+\chi)}{|\chi|^3}\,d\chi$$

$$= \hat{\underline{x}}(k)\int_{-\infty}^{\infty}_{[\delta_c]} \frac{(1-e^{ik\chi}-ik\chi e^{ik\chi})}{|\chi|^3}\,d\chi = k^2\hat{\underline{x}}(k)\int_{\frac{k\delta_c c_0}{\ell}}^{\infty} \frac{1-\cos x - x\sin x}{x^3}dx$$

in view of (7.2.10). The integral on the right-hand side can be written in terms of cosine integral ($C_i(\eta)$) to give

$$\frac{\partial \hat{\underline{x}}}{\partial t}(k,t) = -\frac{\Gamma}{2\pi\ell^2} k^2 \omega\left(\frac{k\delta_c c_0}{\ell}\right)\underline{k} \wedge \hat{\underline{x}}(k,t) + \frac{\hat{\underline{V}}_E}{\ell}(k,t) \qquad (7.2.12)$$

where

$$\omega(\eta) = \tfrac{1}{2}[(\cos\eta - 1)/\eta^2 + \sin\eta/\eta - C_i(\eta)]$$

In §3, (7.2.12) is used to consider the response of an infinitely long straight vortex to (a) a point source switched on at t = 0 at a distance f from the vortex and (b) a sphere approaching the vortex from infinity.

§3 Vortex interaction: Linear theory

(a) A point source in the external field.

Suppose a point source of strength $Q(t)$ is switched on at time $t = 0$ at $\underline{x}_1 = (-f,0,0)$ where f is its distance from the undisturbed position of the vortex. In the absence of the vortex the velocity potential of the flow at a field point $\underline{x}$ is given by

$$\phi_E(\underline{x}) = -\frac{H(t)Q(t)}{|\underline{x} - \underline{x}_1|} \tag{7.3.1}$$

so that the external irrotational velocity field $\underline{U}_E(\underline{x})$ is given by $\underline{U}_E = \nabla\phi_E$.

The length scale of the problem is f. Thus in (7.2.7) we choose

$$\ell = f \tag{7.3.2}$$

The contribution to velocity at $\underline{X}(\xi,t)$ due to the source is given by $\underline{V}_E = \underline{U}_E(\underline{X}(\xi,t))$. Thus in view of (7.3.2),

$$\underline{V}_E(\xi_0,t) = \frac{H(t)Q(t)}{f^2}\left[\frac{\xi_0\underline{k}-\underline{i}}{|\xi_0\underline{k}-\underline{i}|^3} + \alpha\left(\frac{\underline{x}'}{|\xi_0\underline{k}-\underline{i}|} - \frac{3(\xi_0\underline{k}-\underline{i})(\underline{x}'\cdot(\xi_0\underline{k}-\underline{i}))}{|\xi_0\underline{k}-\underline{i}|^5}\right) + O(\alpha^2)\right] \tag{7.3.3}$$

Thus if the response of the vortex is considered on a time scale $O(\frac{f^2}{\Gamma})$ and Q_0 is a typical magnitude of $Q(t)$, it follows from (7.2.8) and (7.2.9) that the appropriate choice of α is

$$\alpha = \frac{Q_0}{\Gamma f} \tag{7.3.4}$$

and this is required to be small in the linear analysis. Thus in view of (7.2.9)

$$\underline{V}_E'(\xi_0,t) = \frac{H(t)\Gamma Q(t)}{Q_0 f^2}\left[\frac{\xi_0\underline{k} - \underline{i}}{|\xi_0\underline{k}-\underline{i}|^3}\right] \tag{7.3.5}$$

Thus substituting this into (7.2.9) and writing $\underline{x}' = (x',y',z')$, it follows from the initial condition $\underline{x}'(\xi,0) = \underline{0}$ that

$$z'(\xi_0,t) = \frac{\Gamma\xi_0}{Q_0 f^2(1+\xi_0^2)^{3/2}}\int_0^t Q(t)dt \tag{7.3.6}$$

(7.3.6) implies that the approximation obtained here will hold so long as $\int_0^t Q(t)dt = O(\frac{Q_0 f^2}{\Gamma})$.

To determine x' and y' the Fourier transform of $\underline{V}_E'$ is taken with respect to ξ_0 and substituted into (7.2.12). Thus writing $\hat{x}(k,t) = \hat{\underline{x}}.\underline{i}$ and $\hat{y}(k,t) = \hat{\underline{x}}.\underline{j}$ we have

$$\frac{\partial\hat{x}}{\partial t} = \frac{\Gamma}{2\pi f^2}k^2\omega(k\delta_c\, c_0/f)\hat{y} + \frac{2H(t)\Gamma Q(t)}{f^2 Q_0}|k|K_1(|k|)$$

$$\frac{\partial\hat{y}}{\partial t} = -\frac{\Gamma}{2\pi f^2}k^2\omega(k\delta_c\, c_0/f)\hat{x} \tag{7.3.7}$$

Hence,

$$x'(\xi_0,t) = \frac{2\Gamma}{\pi f^2}\int_0^t \frac{Q}{Q_0}(t-\tau)\int_0^\infty kK_1(k)\cos[\frac{\Gamma}{2\pi f^2}k^2\omega(k\delta_c\, c_0/f)\tau]\cos k\xi_0 dk\, d\tau$$

$$y'(\xi_0,t) = -\frac{2\Gamma}{\pi f^2}\int_0^t \frac{Q}{Q_0}(t-\tau)\int_0^\infty kK_1(k)\sin[\frac{\Gamma}{2\pi f^2}k^2\omega(k\delta_c\, c_0/f)\tau]\cos k\xi_0\, dk\, d\tau \tag{7.3.8}$$

In Appendix A, for comparison, results corresponding to (7.3.8) are obtained using a classical method for the case of a hollow vortex.

For a hollow vortex δ_c is given by (7.2.5) and in Table 7.1 y'(ξ,t) as given by (7.3.8) for this case is compared with the corresponding

result $y_c(z,t) = \frac{\bar{y}}{\alpha f}(z,t)$ (see A7.1), where $z = f(\xi+\alpha z'(\xi,t))$, for a range of values of the parameter c_0/f. For definiteness, $Q(t) = Q_0$, $\xi = 0$ and $t = 2\pi f^2/\Gamma$ are chosen; note that $z'(0,t) = 0$. There is a good agreement between the results for values of $c_0/f \leq 0.1$.

c_0/f	$\left\lvert\frac{y' - y_c}{y_c}\right\rvert$
.001	2.3×10^{-7}
.01	3.5×10^{-5}
.1	9.8×10^{-4}
.2	5.2×10^{-2}
.3	.22
.5	.77

Table 7.1

(b) An approaching sphere in the external field

We now consider the response of the infinitely long straight vortex to an approaching rigid sphere which is brought at a uniform speed from infinity to the vortex.

When the sphere is sufficiently far away from the vortex, the response is weak and can be approximately determined from the linearized equation (7.2.9) with the appropriate choice of $\underline{V}_E'$. The solution to the equation is obtained here and is used later to determine the approximate shape of the vortex at a time when the sphere is at a prescribed distance from the position of the undisturbed vortex. This shape is then used as the initial configuration of the vortex for the fully non-linear marching problem (7.2.1) and the subsequent evolution of the vortex is determined numerically.

For convenience, the origin of time is chosen so that at $t = 0$ the centre of the approaching sphere is at the position of the undisturbed vortex. Thus $t = -\infty$ corresponds to the time when the sphere is at infinity and the vortex is straight. If the undisturbed position of the vortex is given by (7.2.6), where now

$$\ell = a \tag{7.3.9}$$

and $t_0 = -\infty$, and if the sphere has a uniform speed U, then at time t the centre of the sphere is at (see Fig. 7.1)

$$\underline{X}_0(t) = (-f, 0, 0) \tag{7.3.10}$$

where

$$f = -Ut, \qquad -\infty < t < \infty$$

The external velocity field is due to the image vorticity in the sphere and due to the motion of the sphere. In the absence of the vortex, the velocity at a field point $\underline{x}$ can be described by the potential

$$\phi_E(\underline{x}) = \phi_I + \phi_M \tag{7.3.11}$$

where ϕ_I and ϕ_M are respectively the contributions due to the image vorticity and the motion of the sphere.

To evaluate ϕ_I when the vortex is given by its perturbed position (7.2.7), we write

$$\phi_I = \phi_{0I}(1 + \alpha\phi_{1I} + O(\alpha^2)) \tag{7.3.12}$$

where ϕ_{0I} is the velocity potential due to image of the undisturbed vortex in the sphere and the $O(\alpha\phi_{0I})$ terms allow for the perturbation from the straight vortex.

ϕ_{0I} can be determined by a spherical harmonic analysis as follows. In a coordinate frame $\tilde{O}\tilde{x}\tilde{y}\tilde{z}$, fixed with respect to the centre of the sphere, the undisturbed position of the vortex is given by $\underline{Y} = \overline{\underline{Y}}$ where

$$\overline{\underline{Y}} = \underline{X}(\xi,-\infty) - \underline{X}_0(t) = (f, 0, a\xi) \qquad -\infty < \xi < \infty \tag{7.3.13}$$

In the absence of the sphere, the velocity field at a field point $\underline{Y} = (\tilde{x},\tilde{y},\tilde{z})$ is due to the straight vortex and the velocity potential is given by

$$\phi_0 = \frac{\Gamma}{2\pi} \tan^{-1} \frac{\tilde{y}}{\tilde{x} - f}$$

$$= \frac{\Gamma}{2\pi} \tan^{-1} \left(\frac{r \sin\theta \sin\psi}{r \sin\theta \cos\psi - f}\right) \tag{7.3.14}$$

in terms of spherical polars (r,θ,ψ), $r^2 = \tilde{x}^2 + \tilde{y}^2 + \tilde{z}^2$. We seek the disturbance potential ϕ_{0I} when a rigid sphere is introduced. ϕ_{0I} is to satisfy the boundary condition

$$\frac{\partial}{\partial r} (\phi_0 + \phi_{0I})\Big|_{r=a} = 0 \tag{7.3.15}$$

For $r/f < 1$, ϕ_O can be expanded in terms of spherical solid harmonics (Lamb, Ch. V, 1932) as

$$\phi_O = -\frac{\Gamma}{2\pi}\{\frac{r \sin\theta}{f} P_1^1(\cos\theta) + \frac{r^2 \sin 2\psi}{6f^2} P_2^2(\cos\theta) + \frac{r^3 \sin 3\psi}{45} P_3^3(\cos\theta)+\ldots\} \tag{7.3.16}$$

where $P_n^s(\mu)$ are the modified Legendre polynomials. Corresponding to each harmonic term on the right hand side of (7.3.16), there exists a complementary harmonic function obtained by dividing the term by r^{2n+1} where n is the degree of the given harmonic. ϕ_{OI} is the appropriate linear combination of these complementary functions. Thus in view of (7.3.15),

$$\phi_{OI} = -\frac{\Gamma}{2\pi}\{\frac{a^3}{2r^2 f}\sin\psi\, P_1^1(\cos\theta) + \frac{a^5}{9r^3 f^2}\sin 2\psi\, P_2^2(\cos\theta) + \frac{a^7 \sin 3\psi}{60 r^4 f^3} \times$$

$$\times\, P_3^3(\cos\theta) + \ldots\}$$

or in terms of $\tilde{x}$, $\tilde{y}$, $\tilde{z}$

$$\phi_{OI} = -\frac{\Gamma a^3}{2\pi f r^3}\{\frac{\tilde{y}}{2} + \frac{2a^2\tilde{x}\tilde{y}}{3fr^2} + \frac{a^7(3\tilde{x}^2-\tilde{y}^2)}{4f^2 r^4}\tilde{y} + \ldots\ldots\} \tag{7.3.17}$$

(Alternatively, from the sphere theorem (Weiss (1944))

$$\phi_{OI} = -\frac{\Gamma r f \tilde{y}}{2\pi a}\int_0^{a^2} \frac{udu}{(\tilde{ux}-r^2 f)^2+\tilde{y}^2 u^2})$$

$\phi_M(\underline{Y})$ in (7.3.10) is given by

$$\phi_M(\underline{Y}) = -\tfrac{1}{2} a^3 \frac{\underline{U}.\underline{Y}}{r^3} \tag{7.3.18}$$

Thus the external velocity field $\underline{U}_E(\underline{Y})$ is given by

$\underline{U}_E(\underline{Y}) = \nabla(\phi_M + \phi_{OI}(1 + O(\alpha)))$.

In view of (7.2.7), the parametric equation of the perturbed vortex in $\tilde{O}\tilde{x}\tilde{y}\tilde{z}$ frame is

$$\underline{Y}(\xi,t) = \overline{\underline{Y}} + \alpha a \underline{x}'(\xi,t) + O(a\alpha^2) \tag{7.3.19}$$

where $\overline{\underline{Y}}$ is given by (7.3.13). Then $\underline{V}_E(\xi,t) \equiv \underline{U}_E(\underline{Y}(\xi,t))$ is given by

$$\underline{V}_E(\xi,t) = -\frac{\Gamma a^3}{4\pi|\overline{\underline{Y}}|^3 f}\{\underline{j}(1 + \frac{4a^2}{3|\overline{\underline{Y}}|^2} + \frac{3a^4}{2|\overline{\underline{Y}}|^4} + \ldots.) + O(\alpha)\} -$$

$$-\frac{a^3}{2|\overline{\underline{Y}}|^3}\{\underline{U} - \frac{3(\underline{U}.\overline{\underline{Y}})\overline{\underline{Y}}}{|\overline{\underline{Y}}|^2} + O(\alpha)\} \tag{7.3.20}$$

Thus if the response of the vortex is considered on a time scale of $O(\frac{a^2}{\Gamma})$ and $U = O(\frac{\Gamma}{a})$, then it follows from (7.2.8) and (7.2.9) that $\alpha = O(\frac{a^3}{f^3})$ (since $|\overline{\underline{Y}}| = O(f)$), and this is required to be small in the linear analysis. Thus, since $f = f(t)$, the linear analysis will be valid provided $t \leq T < 0$, where T is such that

$$\alpha = \frac{a^3}{f_T^3} << 1 \tag{7.3.21}$$

where $f_T = |f(T)|$. Thus

$$\underline{V}_E'(\xi_0,t) = -\frac{\Gamma f_T^3}{4\pi f|\overline{\underline{Y}}|^3}(1 + \frac{4a^2}{3|\overline{\underline{Y}}|^2})\underline{j} - \frac{f_T^3}{2|\overline{\underline{Y}}|^3}(\underline{U} - \frac{3(\underline{U}.\overline{\underline{Y}})\overline{\underline{Y}}}{|\overline{\underline{Y}}|^2}) \tag{7.3.22}$$

The contribution from the two terms in (7.3.22) is comparable if $f = O(\Gamma/U)$.

Substituting (7.3.22) into (7.2.9) and writing $\underline{x}' = (x',y',z')$ and using $\underline{x}'(\xi,-\infty) = \underline{0}$ gives

$$\alpha z'(\xi_0,t) = \frac{a^3 \xi_0}{2(U^2t^2 + a^2\xi_0^2)^{3/2}} \qquad -\infty < t \leq T \tag{7.3.23}$$

To determine $x'(\xi_0,t)$ and $y'(\xi_0,t)$, the Fourier transform of $\underline{V}'_E$ is taken with respect to ξ_0 and substituted into (7.2.10). This gives

$$\frac{\partial \hat{x}}{\partial t} = \frac{\Gamma k^2 \omega}{2\pi a^2}(k\delta_c\, c_0/a)\hat{y} + A_1(k,t)$$

$$\frac{\partial \hat{y}}{\partial t} = -\frac{\Gamma k^2 \omega}{2\pi a^2}(k\delta_c\, c_0/a)\hat{x} + A_2(k,t) \qquad t \leq T < 0 \qquad (7.3.24)$$

where

$$\alpha A_1(k,t) = -\frac{U}{a}\left\{\frac{ka}{f} K_1\left(\frac{kf}{a}\right) - k^2 K_2\left(\frac{kf}{a}\right)\right\}$$

$$\alpha A_2(k,t) = -\frac{\Gamma}{2\pi a f}\left\{\frac{ka}{f} K_1\left(\frac{kf}{a}\right) + \frac{4a^2k^2}{9f^2} K_2\left(\frac{kf}{a}\right)\right\} \qquad k > 0 \qquad (7.3.25)$$

Here $K_m(\eta)$ is the m^{th} order Bessel's function of the second kind.

To solve (7.3.24), the definition of $A_1(k,t)$ and $A_2(k,t)$ is arbitrarily extended to the range $t > T$ and the Fourier-transform of (7.3.24) with respect to t is taken. Defining half-range Fourier-transforms as

$$\begin{bmatrix} x_+^T \\ y_+^T \\ A_{1+}^T \\ A_{2+}^T \end{bmatrix} = \int_0^\infty \begin{bmatrix} \hat{x} \\ \hat{y} \\ A_1 \\ A_2 \end{bmatrix} e^{ist}\, dt, \quad \begin{bmatrix} x_-^T \\ y_-^T \\ A_{1-}^T \\ A_{2-}^T \end{bmatrix} = \int_{-\infty}^0 \begin{bmatrix} \hat{x} \\ \hat{y} \\ A_1 \\ A_2 \end{bmatrix} e^{ist} dt \qquad (7.3.26)$$

Equations for (x_+^T, y_+^T) and (x_-^T, y_-^T), obtained on transforming (7.3.19) appropriately, are solved and inverted as

$$\begin{bmatrix}\hat{x}\\ \hat{y}\end{bmatrix} = \frac{1}{2\pi}\int_{-\infty+ib}^{\infty+ib}\begin{bmatrix}x_+^T\\ y_+^T\end{bmatrix}e^{-ist}d\xi + \int_{-\infty-ic}^{\infty-ic}\begin{bmatrix}x_-^T\\ y_-^T\end{bmatrix}e^{-ist}d\xi \qquad (7.3.27)$$

where the paths of integration are closed in the appropriate half of the s-plane (b,c > 0) for inversion. Finally, $\hat{x}$ and $\hat{y}$ are inverted with respect to k to give

$$\begin{bmatrix}\alpha x'(\xi_0,t)\\ \alpha y'(\xi_0,t)\end{bmatrix} = \frac{1}{\pi}\int_0^\infty\int_0^\infty\left\{\alpha A_1(k,t+t_1)\begin{bmatrix}\cos\hat{\theta}\\ -\sin\hat{\theta}\end{bmatrix} - \alpha A_2(k,t+t_1)\begin{bmatrix}\sin\hat{\theta}\\ \cos\hat{\theta}\end{bmatrix}\right\}\cos k\xi_0\,dt_1\,dk \quad t < T \qquad (7.3.28)$$

where $\hat{\theta} = \frac{\Gamma}{2\pi a^2}k^2\omega\left(\frac{k\delta_c c_0}{a}\right)t_1$ and αA_1 and αA_2 are given by (7.3.25).

§4. Approaching sphere in the proximity of the vortex

In this section, a procedure is described for following the evolution of the vortex filament in the presence of the approaching sphere from its configuration at a time t_s ($\leq T < 0$), given by (7.2.7), (7.3.23) and (7.3.28), for times subsequent to t_s.

The evolution is followed by a step-wise numerical integration of the integro-differential equation (7.2.1), the contribution $\underline{V}_E(\xi_0,t)$ due to the evolving image system and due to the motion of the sphere being evaluated at each time step. The image system is discussed in §5 where an expression for $\underline{V}_E$ is obtained.

As explained in Chapter 5, the cut-off method employed in the linear analysis in §§2,3 is inconvenient to use for numerical work. Instead, (as in Chapter 6) following Moore (1972), Rosenhead's method of cut-off is used here; the method was described in the latter part of Chapter 5 §2. Thus in (7.2.1) the denominator of the integrand in the self-induced velocity line integral is replaced by $\{|\underline{X}(\xi_0,t) - \underline{X}(\xi,t)|^2+\mu^2\}^{3/2}$, where μ is proportional to the core-radius c and the integration is carried out over the entire range of the integration. Thus $\mu = 2\delta_R c$ where δ_R is given by (5.2.5). For a uniform vortex with no axial flow, this gives

$$\log 2\delta_R = -3/4 \tag{7.4.1}$$

The Lagrangian parameter ξ is chosen as in §3 so that in a fixed Cartesian coordinate system Oxyz the vortex filament in its undisturbed state is given by (7.2.6) as

$$\underline{X}(\xi,-\infty) = (0,0,a\xi) \qquad -\infty < \xi < \infty \tag{7.4.2}$$

since $t_0 = -\infty$ and $\ell = a$.

At subsequent times ξ = constant always represents the same fluid particle.

In view of (7.3.28), it is expected that the motion of the vortex filament will be symmetrical about z = 0 plane so that, writing $\underline{X}(\xi,t) = (x,y,z)$,

$$\left.\begin{aligned} x(-\xi,t) &= x(\xi,t) \\ y(-\xi,t) &= y(\xi,t) \\ z(-\xi,t) &= -z(\xi,t) \end{aligned}\right\} \quad 0 \leq \xi < \infty \tag{7.4.3}$$

Hence it is only necessary to follow the portion $0 \leq \xi < \infty$ of the filament, say, and use (7.4.3) to determine the shape of the remaining portion of the filament.

Thus, given an expression for $\underline{V}_E(\xi,t)$, the motion of the vortex can be determined by simply integrating (7.2.1) forward in time and calculating the length of the filament at each time step to obtain the value of $\mu(t)$. However, a method for dealing with the infinite range of the integration must be described.

It is expected that in the time of interest, the position of those portions of the vortex which are further than a distance of a few radii of the sphere away from z = 0 plane will not be significantly different from that given by (7.3.23) and (7.3.28). Thus, in view of the decay of $\underline{x}'$ with $\xi \to \pm\infty$, the range of the numerical integration is truncated from $(-\infty,\infty)$ to $[-A,A]$ and the portions of the vortex corresponding to $(-\infty,-A)$ and (A,∞) are assumed to be straight and fixed in their undisturbed position. The contribution from these straight portions to the velocity at the points on the portion corresponding to $[-A,A]$ is evaluated analytically.

This method of dividing up the range of integration means that small kinks will develop at $\xi = \pm A$ and these will affect the velocity at

points near $\xi = \pm A$. Thus A must be chosen so that these points are well outside the range of interest. However, the disturbance due to the kinks will propagate down the length of the vortex and the calculations must be stopped once this starts affecting the velocity at points in the range of interest. In the calculations described below, when the calculations were stopped, the disturbance due to the kinks had progressed only a short distance down the vortex and the difficulty did not arise.

Thus the self-induced velocity integral in (7.2.1) is written as

$$\int_{-\infty}^{\infty} \frac{\partial \underline{X}(\xi,t)}{\partial \xi} \Lambda \frac{(\underline{X}(\xi_0,t)-\underline{X}(\xi,t))d\xi}{\{|\underline{X}(\xi_0,t)-\underline{X}(\xi,t)|^2+\mu^2\}^{3/2}} =$$

$$= \int_{-A}^{A} \frac{\partial \underline{X}}{\partial \xi}(\xi,t) \Lambda \frac{(\underline{X}(\xi_0,t)-\underline{X}(\xi,t))d\xi}{(|\underline{X}(\xi_0,t)-\underline{X}(\xi,t)|^2+\mu^2)^{3/2}} + \underline{I}_s \qquad (7.4.4)$$

where

$$\underline{I}_s(\xi,t) = \left(\int_{-\infty}^{-A} + \int_{A}^{\infty} \right) \frac{\underline{k} \Lambda (\underline{X}(\xi_0,t)-a\xi\underline{k})}{\{|\underline{X}(\xi_0,t)-a\xi\underline{k}|^2+\mu^2\}^{3/2}} \, d\xi$$

$$= \frac{\underline{k} \Lambda \underline{X}(\xi_0,t)}{|\underline{X}(\xi_0,t)|^2+\mu^2} \left(2 - \frac{aA - z(\xi_0,t)}{(|\underline{X}(\xi_0,t)-aA\underline{k}|^2+\mu^2)^{1/2}} \right.$$

$$\left. - \frac{aA + z(\xi_0,t)}{(|\underline{X}(\xi_0,t)+aA\underline{k}|^2+\mu^2)^{1/2}} \right) \qquad (7.4.5)$$

Although the integrand in the cut-off integral is finite everywhere, it is large in the neighbourhood of $\xi = \xi_0$ and this would cause loss of accuracy in evaluating the integral. Thus, as in Chapter 6, it is necessary to subtract off a suitable function from the integrand and write the equation of motion (7.2.1) as

$$\frac{\partial \underline{X}}{\partial t}(\xi_0,t) = \frac{\Gamma}{4\pi}\int_{-A}^{A}\{\frac{\partial \underline{X}}{\partial \xi}\wedge\frac{(\underline{X}(\xi_0,t)-\underline{X}(\xi,t))}{(|\underline{X}(\xi_0,t)-\underline{X}(\xi,t)|^2+\mu^2)^{3/2}}$$

$$-(\frac{\partial \underline{X}}{\partial \xi})_0\wedge(\frac{\partial^2 \underline{X}}{\partial \xi^2})_0 P(\xi,t)\}d\xi$$

$$+\frac{\Gamma}{4\pi}(\frac{\partial \underline{X}}{\partial \xi})_0\wedge(\frac{\partial^2 \underline{X}}{\partial \xi^2})_0\int_{-A}^{A}P(\xi,t)d\xi+\underline{I}_s(\xi_0,t)+\underline{V}_E(\xi_0,t) \qquad (7.4.6)$$

where

$$P(\xi,t) = \frac{\frac{1}{2}(\xi-\xi_0)^2}{((\xi-\xi_0)^2(\frac{\partial \underline{X}}{\partial \xi})_0^2+\mu^2)^{3/2}} \qquad (7.4.7)$$

and $\underline{I}_s(\xi,t)$ is given by (7.4.5). The integrand in the first integral in (7.4.6) is O(1) everywhere while the second integral is elementary.

For the full non-linear problem, the variations in core size cannot be ignored so that in view of the uniformity of the vortex cross-section and conservation of volume,

$$\mu(t) = 2\delta_R c_0\{\frac{1}{2aA}\int_{-A}^{A}\left|\frac{\partial \underline{X}}{\partial \xi}\right| d\xi\}^{-1/2} \qquad (7.4.8)$$

where c_0 is the uniform radius of the vortex filament in the undisturbed state and where the volume of the portion of the vortex corresponding to [-A,A] is required to remain constant.

Since the displacement of the vortex from its undisturbed state decreases away from z = 0 plane (cf. (7.3.23)), the distribution of the Lagrangian points on the vortex can be chosen in such a way that the size of the spatial grid increases away from ξ = 0 point. The choice made here is

$$\xi = \mathrm{sgn}(V)V^2 \qquad -\infty < V < \infty \qquad (7.4.9)$$

However, any suitable choice of function can be used. The range $[-\sqrt{A}, \sqrt{A}]$ of V was divided into three parts, $[-\sqrt{A}, -A_1]$, $[-A_1, A_1]$ and $[A_1, \sqrt{A}]$. The range $[-A_1, A_1]$ was divided into $2N_1$ portions by $2N_1+1$ equally spaced grid points. In the outer ranges, $[-\sqrt{A}, -A_1]$ and $[A_1, \sqrt{A}]$, the grid spacing was chosen to be twice that in $[-A_1, A_1]$, A being chosen so that there are $2N_2$ portions of equal length in each of the outer ranges; hence a total of $2(N_1+N_2) + 1$ points per half range $[0, \sqrt{A}]$ was used. The spatial derivatives were calculated using four-point differences at all points; the particular choice of grid spacing allowed the use of the centred formulae at points near $V = \pm A_1$. Simpson's rule was used to evaluate the integrals. The integration forward in time was effected by the fourth-order Runge-Kutta formula, used because of its stability.

In §5 an expression for $\underline{V}_E$ is obtained and the results of the calculations are described in §6.

§5 External velocity field

The image system of a vortex element in a sphere has been given by Lighthill (1956). This is briefly described here and an expression for the velocity field due to the image system of an infinitely long vortex is obtained.

Suppose that, with the centre of a sphere of radius a at the origin, a vortex element of length ds and circulation Γ is situated at $\underline{Y}_1$ (see fig. 7.1). The strength of the element $\underline{J}$ is defined as

$$\underline{J} = \Gamma \frac{\partial \underline{Y}_1}{\partial s} \, ds \qquad (7.5.1)$$

Then, writing $|\underline{Y}_1| = r_1$, the image system of the vortex element is given by

(i) a vortex element of strength $\frac{2a}{r_1}\left(\frac{(\underline{J}.\underline{Y}_1)\underline{Y}_1}{r_1^2} - \tfrac{1}{2}\underline{J}\right)$ at the inverse point $\underline{Y}_I = \left(\frac{a}{r_1}\right)^2 \underline{Y}_1$ and

(ii) a line vortex of circulation $-(\underline{J}.\underline{Y}_1)/ar_1$ stretching from the inverse point to the centre of the sphere.

The image system satisfies the boundary condition at the surface of the sphere and the requirement that the vorticity field inside the sphere be solenoidal. The latter condition is necessary if the corresponding Biot-Savart velocity field is to be irrotational.

For an infinitely long straight vortex filament, (i) and (ii) imply that the image system consists of a vortex ring given by $|\underline{Y} - \underline{Y}_{I/2}|^2 = \frac{|\underline{Y}_I|^2}{4}$ and a vortex sheet extending over the interior of that circle (cf. Weiss (1944)).

In view of (i) and (ii) the velocity at a field point $\underline{Y}$ due to the image system of a vortex element at $\underline{Y}_1$ is given by

$$\underline{\delta u} = \frac{a}{4\pi r_1}\left[\frac{(2(\underline{J}.\hat{\underline{Y}}_1)\hat{\underline{Y}}_1-\underline{J})\Lambda(\underline{Y}-\frac{a^2\hat{\underline{Y}}_1}{r_1})}{|\underline{Y}-a^2/r_1\,\hat{\underline{Y}}_1|^3}\right]-\frac{(\underline{J}.\hat{\underline{Y}}_1)}{4\pi a}\int_0^{a^2/r_1}\frac{\hat{\underline{Y}}_1\Lambda(\underline{Y}-\lambda\hat{\underline{Y}}_1)}{|\underline{Y}-\lambda\hat{\underline{Y}}_1|^3}\,d\lambda \tag{7.5.2}$$

where $\hat{\underline{Y}}_1 = \underline{Y}_1/r_1$. Thus in view of (7.5.1),

$$\underline{\delta u} = \underline{W}\,ds \tag{7.5.3}$$

where

$$\underline{W} = \frac{\Gamma a}{4\pi r_1}\left[\left\{\frac{(2(\frac{\partial \underline{Y}_1}{\partial s}.\hat{\underline{Y}}_1)\hat{\underline{Y}}_1-\frac{\partial \underline{Y}_1}{\partial s})\Lambda(\underline{Y}-\frac{a^2\hat{\underline{Y}}_1}{r_1})}{|\underline{Y}-(\frac{a^2}{r_1})\hat{\underline{Y}}_1|^3}\right\}\right.$$

$$\left.-\frac{(\frac{\partial \underline{Y}_1}{\partial s}.\underline{Y}_1)}{a^2}\hat{\underline{Y}}_1\Lambda\underline{Y}\int_0^{a^2/r_1}\frac{d\lambda}{|\underline{Y}-\lambda\hat{\underline{Y}}_1|^3}\right] \tag{7.5.4}$$

Note that the integral in the expression is elementary.

Equation (7.5.3) is used here to obtain an expression for the instantaneous velocity due to the image system of the evolving infinitely long vortex filament of §4 so that $\underline{Y}_1$ is given parametrically by

$$\underline{Y}_1 = \underline{X}(\xi,t)-\underline{X}_0(t) \qquad \begin{matrix}-\infty<\xi<\infty\\ -\infty<t<\infty\end{matrix} \tag{7.5.5}$$

where $\underline{X}_0(t)$ is given by (7.3.9). The vortex is regarded as being closed by a semi-circle of infinite radius (this is consistent with the spherical harmonic analysis of §3 since in obtaining the velocity potential ϕ_0 (7.3.9) of an infinitely long straight vortex, the same assumption is made). The velocity field is then given by $\oint\underline{W}ds$ where the integral is taken round the closed loop. However, if $\underline{W}$ is expanded in powers of a/r_1 ($a/r_1 < 1$) as

$$\underline{W} = \frac{\Gamma a}{4\pi r^3}\{\underline{Y} \wedge \frac{\partial \hat{\underline{Y}}_1}{\partial s} + \frac{a^2}{r_1^2}[\frac{\partial \underline{Y}_1}{\partial s} \wedge \hat{\underline{Y}}_1 + \frac{(\underline{Y}.\hat{\underline{Y}}_1)}{r^2}(\frac{9}{2}(\frac{\partial \underline{Y}_1}{\partial s}.\hat{\underline{Y}}_1)(\hat{\underline{Y}}_1 \wedge \underline{Y}) - 3(\frac{\partial \underline{Y}_1}{\partial s} \wedge \underline{Y}))] + O(\frac{a^4}{r_1^4})\} \qquad (7.5.6)$$

and integrated term by term, the first term integrates to zero so that

$$\oint \underline{W}\, ds = \oint (\underline{W} - \frac{\Gamma a}{4\pi r^3} \underline{Y} \wedge \frac{\partial \hat{\underline{Y}}_1}{\partial s})\, ds \qquad (7.5.7)$$

The integrand in the integral on the right hand side is of $O(1/R^2)$ on the semi-circular path of integration, where R is the radius of the semi-circle, so that in the limit $R \to \infty$, integration along this path gives null contribution. Thus

$$\oint \underline{W}\, ds = \int_{-\infty<\xi<\infty} (\underline{W} - \frac{\Gamma a}{4\pi r^3} \underline{Y} \wedge \frac{\partial}{\partial s} \hat{\underline{Y}}_1) ds \qquad (7.5.8)$$

if the vortex is given by the parametric equation (7.5.5).

The instantaneous position of any point on the portion of the vortex filament corresponding to $-A \leq \xi \leq A$ is governed by the evolution equation (7.4.6). The portions corresponding to $-\infty < \xi < -A$ and $A < \xi < \infty$ are straight (see §4) and for points on these portions $\underline{Y}_1$ is given by

$$\underline{Y}_1(\xi,t) = (-Ut,\ 0,\ a\xi) \qquad \begin{matrix} \xi \in (-\infty, -A), (A,\infty) \\ t \in (-\infty,\infty) \end{matrix} \qquad (7.5.9)$$

so that $\underline{ds} = (0,\ 0,\ a)ds$.

An expression for the velocity due to the straight portions can be obtained from (7.5.3). After an integration by parts of the integral with respect to λ and a change of variable $\lambda = \frac{a^2}{r_1}\lambda_1$, the order of the integration can be changed and the integration with respect to ξ

performed. Thus (7.5.7) becomes

$$\oint \underline{W}\, ds = \int_{-A<\xi<A} (\underline{W} - \frac{\Gamma a}{4\pi r^3}\, \underline{Y} \wedge \frac{\partial}{\partial s}\, \hat{\underline{Y}}_1) ds + \underline{M}_s(\underline{Y}) \qquad (7.5.10)$$

where

$$\underline{M}_s(\underline{Y}) = \frac{\Gamma a}{4\pi r^3}\{\underline{Y} \wedge [(f^2 A_{10}(1) + 2 - \frac{2aA}{(f^2+a^2A^2)^{\frac{1}{2}}})\underline{k} - fA_{11}(1)\underline{i}] + a^2 fA_{10}(1)\underline{j}$$

$$+ \frac{3a^2}{r^2}\, \underline{Y} \wedge \int_0^1 [(\underline{Y}.\underline{k})(A_{22}(\lambda)f\underline{i} + A_{23}(\lambda)\underline{k}) + (\underline{Y}.P(\lambda))(A_{21}(\lambda)f\underline{i} + A_{22}(\lambda)\underline{k})]\, d\lambda\} \qquad (7.5.11)$$

Here

$$\underline{P}(\eta) = f\underline{i} - \frac{a^2\eta}{r}\, \hat{\underline{Y}}$$

and $A_{nm}(\eta)$ are given in Appendix B.

Putting A = 0 in (7.5.11), we obtain the velocity due to the image sytem of an infinitely long straight vortex. The result is in agreement with that given by Weiss (1944) for this case; Weiss obtained the result using his sphere theorem. Note that the sphere theorem is inconvenient to use in the present non-linear problem since it requires evaluating the velocity potential of the evolving vortex at each time step.

As a further check, putting A = 0 in (7.5.11) and expanding $\underline{M}_s$ in powers of a^2/r^2 gives a result in agreement with the spherical harmonic analysis of §3.

Finally, in view of the motion of the sphere, the external velocity $\underline{U}_E(\underline{Y})$ at a field point $\underline{Y}$ in the absence of the vortex filament is given by

$$\underline{U}_E(\underline{Y}) = \oint \underline{W}\, ds + \nabla\phi_M \qquad (7.5.12)$$

where ϕ_M is given by (7.3.17).

Hence, with $\underline{Y}_1$ given by (7.5.5) and writing

$$\underline{Y}_0 = \underline{X}(\xi_0,t) - \underline{X}_0(t) \qquad -\infty < t < \infty \tag{7.5.13}$$

and using (7.5.10), (7.5.4) and $ds = ad\xi$, we have $\underline{V}_E(\xi_0,t)$ ($\equiv \underline{U}_E(\underline{Y}_0)$) is given by

$$\underline{V}_E(\xi_0,t) = \frac{\Gamma a}{4\pi}\int_{-A}^{A}\Big[\frac{((2\frac{\partial \underline{Y}_1}{\partial\xi}.\hat{\underline{Y}}_1)\hat{\underline{Y}}_1 - \frac{\partial \underline{Y}_1}{\partial\xi})\wedge \underline{R}_0}{|\underline{Y}_1||\underline{R}_0|^3} - \frac{\hat{\underline{Y}}_0}{|\underline{Y}_0|^2}\wedge\frac{\partial}{\partial\xi}\hat{\underline{Y}}_1 - \frac{\underline{F}}{|\underline{Y}_1|}\Big]\,d\xi$$

$$+ \underline{M}_s(\underline{Y}_0) - \frac{\underline{U}a^3}{2|\underline{Y}_0|^3} + \frac{3a^3(\underline{U}.\underline{Y}_0)\underline{Y}_0}{|\underline{Y}_0|^5} \tag{7.5.14}$$

where

$$\underline{R}_0 = \underline{Y}_0 - \frac{a^2\hat{\underline{Y}}_1}{|\underline{Y}_1|} \quad ,$$

$$\underline{F} = (\frac{\partial \underline{Y}_1}{\partial s}\cdot\hat{\underline{Y}}_1)\hat{\underline{Y}}_1\wedge\underline{Y}\int_0^1\frac{d\lambda}{|\underline{Y}-\frac{\lambda a^2}{r_1}\hat{\underline{Y}}_1|^3}$$

and $\underline{M}_s$ is given by (7.5.11).

§6 Numerical results

To present the results, a, the radius of the sphere, is chosen as the unit of length and a non-dimensional time defined by

$$t_1 = \frac{\Gamma}{4\pi a^2}(t - t_s) \tag{7.6.1}$$

is used. Here the time origin is shifted to t_s ($\leq T < 0$), the "switch-over" time when the shape of the vortex is evaluated from the linear analysis of §3 and the evolution of the vortex from this configuration followed numerically for subsequent times. In view of the considerations of §3, the relative importance of the various terms in $\underline{V}_E$ as given by (7.5.14) depends on a parameter B which is defined as

$$B = \frac{\Gamma}{4\pi a U} \tag{7.6.2}$$

The initial core radius was chosen as

$$c_0/a = 0.125 \tag{7.6.3}$$

This allowed the evolution of the vortex to be followed using a reasonable number of grid points. The core size is not small as required by the cut-off theory since it is expected that when the sphere is close to the vortex, the portion of the vortex which is of interest will have a radius of curvature ρ of O(a). However, as explained in Chapter 6, in view of the agreement between Saffman's (1970) formula for the velocity of a circular vortex ring and the corresponding numerical results of Fraenkel (1970) and Norbury (1973) for values of c_0/ρ which are not small compared to unity, and because the error in the cut-off approximation to this velocity is of the same order as in Saffman's formula, it is reasonable to expect, although no rigorous proof is available, that the cut-off approximation will hold equally good for such values of c_0/ρ.

In any case the results are not very sensitive to the value of c_0/ρ; this is because the velocity obtained by the cut-off approximation depends only logarithmically on the cut-off length and hence on the core size.

The vorticity distribution in the vortex was taken to be uniform so that δ_R is given by (7.4.1).

It is clear from the results (7.3.28) of the linear analysis that at any given time the $\xi = 0$ point will be most displaced from its undisturbed position. The y-displacement of the $\xi = 0$ point was calculated from (7.3.28) for various values of the ratio a/f where f is as in (7.3.9). The double integral in (7.3.28) was evaluated by splitting the infinite range of the integral into various parts depending on the frequency of oscillation of the integrand. Over the parts where the integrand was highly oscillatory, one of the integrals was approximated using standard methods. Simpson's rule was used to evaluate the integrals. The results for three values of B, namely B = 10, 5 and 2.5, are shown in Fig. 7.2 where $|y/f|$ is plotted against a/f.

It was decided to follow the evolution of the vortex, subsequent to time t_s, numerically for the cases B = 10 and B = 5. The choice of t_s is made in the following way. For the two cases considered, the times $\tilde{t}_s$ when $|y/f|$ is 2½%, 5% etc. is determined from Fig. 7.2. At each time, the shape of the vortex is evaluated from (7.2.7), (7.3.23) and (7.3.28). Using this as starting configuration of the vortex, equation (7.4.6) is integrated numerically over a trial period and the values of y/f obtained from the calculations are compared with the results of linear analysis. t_s is then chosen to be the maximum value of $\tilde{t}_s$ for which there is reasonable agreement between the two results over the trial period.

For both B = 10 and B = 5 cases, it was found possible to choose t_s so that y/f was 9% at t_s. However, for convenience, t_s was chosen so that for both cases a/f = 0.5. This implies

$$t_s = -\frac{2a}{U} \tag{7.6.4}$$

From Fig. 7.2, $|y/f|$ is 9% at this time for B = 10 case and 7% for B = 5. Thus linear theory is adequate until the sphere is fairly close to the vortex.

Table 7.2 shows the values of N_1, N_2, A, A_1 and time step Δt_1 used in the calculations. Trial and error showed that these gave adequate accuracy.

B	N_1	N_2	A	A_1	Δt_1
5	10	11	16.384	.6325	.008
10	10	11	16.384	.6325	.016

Table 7.2

At time $t_1 = t_1^*$, shown in Table 7.3, the centre of the core at $\xi = 0$ point was a distance d^* (see Table 7.3) away from the centre of the sphere. This implies that the core of the vortex is touching the sphere. The situation is similar to that of two vortex filaments with their cores touching. The results at this stage may be viewed with scepticism since the calculations are based on the assumption that the separation between the vortex and its image is large. However, by means of a numerical calculation with vortices in two-dimensions, in which the core was allowed for, Moore (1972) was able to show that the Biot-Savart formula gives roughly the correct velocity even when the

cores are touching. In the present case, the vortex at $\xi = 0$ may be regarded as being in contact with a tangent plane and the local situation represented two-dimensionally*. Moore's study then suggests that although the cores will be distorted so that the cut-off length will change, the approximations on which the present calculations are based will be reasonably adequate even when the vortex core is close to the sphere.

In order to determine the maximum negative y-displacement, y_M, it was decided to continue with the numerical integration up to the time $t_1 = t_M$ when this was achieved. $|y_M|$ was maximum when the x-coordinate of $\xi = 0$ point coincided with the x-coordinate of the centre of the sphere. The values of y_M and t_M are shown in Table 7.3.

B	t_1^*	d^*	t_M	y_M	$\bar{t}_1$
5	2.568	1.119	2.672	-1.057	2.608
10	3.600	1.123	3.710	-1.057	3.696

Table 7.3

The position of the portion of the vortex near $z = 0$ plane, due to its proximity to the sphere, changes rapidly while points on the vortex a distance further than a from the $z = 0$ plane are displaced by a small amount. At $t_1 = \bar{t}_1$ (see Table 7.3) numerical instability set in in the neighbourhood of $z = 0$ plane, presumably because of the rapid changes there and because the distance between the grid points is not small

*An improvement on this would be to consider numerically the motion of a two-dimensional vortex of finite core round a cylinder. However, this has not been attempted.

compared with the separation between the vortex centre and the image. To cure this, the calculations were stopped at $t_1 = \bar{t}_1 - 2\Delta t_1$ and restarted with more points so that the grid spacing was reduced by half and the time step was taken to be $\frac{1}{4}\Delta t_1$. This removed the instability.

In Fig. 7.2 various values of $|y/f|$ for times subsequent to t_s are shown for the two cases considered and compared with the corresponding results of linear analysis. The results from the numerical calculations are shown up to the time when $|y/f|$ achieves a maximum value. For subsequent times the value of $|y/f|$ drops. The reason is apparent from Fig. 7.3 which shows the track of $\xi = 0$ point in the x-y plane for the case B = 10. As the vortex 'clears' the sphere at time $t_1 = t_M$ the vortex appears to follow a roughly circular path round the sphere so that the magnitude of the y-displacement falls. To follow the motion of the vortex for subsequent times, more grid points and smaller time steps are necessary. However, in view of the dubious significance of the results at this stage, this was not done.

In Fig. 7.4 three views of the side elevations at different stages of the evolution are shown for the B = 10 case while Fig. 7.5 shows the corresponding end elevations. The figures clearly show the rapid change in shape of the vortex near z = 0 plane subsequent to time $t_1 = t_1^*$. The plan view is shown in Fig. 7.6.

In both B = 5 and B = 10 cases, the overall increase in length of the portion of the vortex considered increased by less than 1.5%. The vortex stretched most in the neighbourhood of $\xi = 0$ point where, in the B = 10 case, the distance between two points, initially a distance δz apart, increased to $1.3\delta z$ at $t_1 = t_1^*$ and to $5\delta z$ at $t_1 = t_M$. The corresponding values in B = 5 case were similar. Away from $\xi = 0$ points, certain portions of the vortex underwent contraction.

At $t_1 = t_M$ the kinks at $\xi = \pm A$ due to the truncation of the vortex had progressed by a distance less than a down the length of the vortex and did not affect the velocity at points on the vortex a distance less than 5a from z = 0 plane.

A qualitative experiment was conducted in a cylindrical tank of water in which a 'bathtub vortex' was set up at the centre. From the edge of the tank, a sphere was moved towards the vortex at a speed corresponding to B = 10. Dye was used for flow visualization.

The vorticity distribution in the bathtub vortex is not uniform. However, it is expected that this will make only a quantitative difference to the motion of the vortex.

As anticipated here the vortex does not move appreciably until the sphere is quite close to the vortex when it commences to move in the sense indicated in Fig. 7.5. However, the cross stream induced by the vortex over the sphere produces a side wake in the region into which the vortex is starting to move. The wake appears to interact strongly with the vortex filament which soon breaks up.

Thus the present calculations are of approximate validity in real fluids since viscous diffusion and the wake of the sphere have been excluded in the calculations.

APPENDIX A: Source-vortex interaction using classical methods

The interaction between a hollow vortex and a point source in compressible fluid has been studied by Ffowcs Williams & O'Shea (1970). By taking the appropriate limit, the corresponding results for incompressible flow can be obtained from their results. However, the boundary condition used by them at the vortex surface (the material derivative of the pressure is required to vanish) does not facilitate the determination of the position of the vortex surface. The incompressible flow problem is therefore stated here and the solution is written down.

The velocity potential due to the undisturbed vortex is $\bar{\phi} = \kappa\theta \quad (r > c_0 > 0)$ in plane polar coordinates. The flow supports a cavity in $r < c_0$ where the pressure $p = 0$. At $t = 0$, a point source is switched on at $\underline{X}_0 = (f,\pi,0)$ and the velocity potential (7.3.1) is imposed on the mean flow. It is required that the pressure be continuous across the disturbed surface,

$$r = c = c_0 + c'(z,\theta,t) \tag{A1.1}$$

and that the normal velocity of the disturbed surface be equal to the normal fluid velocity at the surface. A solution is sought where the perturbation potential vanishes at infinity.

Thus for $r \geq c$ the perturbation velocity potential ϕ satisfies

$$\phi_{rr} + \frac{1}{r}\phi_r + \frac{\phi_{\theta\theta}}{r^2} + \theta_{zz} = 0 \tag{A1.2}$$

and the linearized boundary conditions which are applied at $r = c_0$ are given by

$$\left(\frac{\partial\phi}{\partial t}\right)_{r=c_0} + \frac{\kappa}{a_0^2}\left(\frac{\partial\phi}{\partial\theta}\right)_{r=c_0} - \frac{\kappa^2}{a_0^3}c' = 0$$

$$\frac{\partial c'}{\partial t} + \frac{\kappa}{a_0^2}\frac{\partial c'}{\partial\theta} = \left(\frac{\partial\phi}{\partial r}\right)_{r=c_0} \qquad \text{(A1.3)}$$

Then, in terms of the natural functions of the vortex, c' is given by

$$c'(r,\theta,z,t) = -\frac{2}{\pi c_0}\int_0^t Q(t-\tau)\int_0^\infty \cos kz \sum_{m=-\infty}^{\infty} \frac{(-1)^m e^{im\theta} K_{|m|}(kf)}{K_{|m|}(kc_0)} \times$$

$$\times\, e^{-\frac{im\kappa}{a_0^2}\tau} \cos\left[\frac{\Gamma}{2\pi c_0^2}\beta_{|m|}\tau\right] dk\, d\tau. \qquad \text{(A1.4)}$$

where

$$\beta_{|m|}^2 = -\frac{kc_0 K'_{|m|}(kc_0)}{K_{|m|}(kc_0)} > 0.$$

Similarly, ϕ can be written down.

For a fixed value of z, in the coordinate frame of §3, the vortex surface is given by the curve $x = c\cos\theta$, $y = c\sin\theta$ so that the centre of the curve is at

$$\bar{x}(z,t) = \frac{\int_0^{2\pi} c\cos\theta.cd\theta}{\int_0^{2\pi} cd\theta}, \qquad \bar{y}(z,t) = \frac{\int_0^{2\pi} c\sin\theta.cd\theta}{\int_0^{2\pi} cd\theta}. \qquad \text{(A1.5)}$$

With $c^2 = c_0^2 + 2c_0c'$, substitution for c' gives

$$\bar{x} = \frac{2}{\pi}\int_0^t Q(t-\tau)\int_0^\infty \frac{K_1(kf)}{c_0K_1(kc_0)}\left[\cos\left(\frac{\Gamma}{2\pi c_0^2}(1-\beta_1)\tau\right) + \cos\left(\frac{\Gamma}{2\pi c_0^2}(1+\beta_1)\tau\right)\right]\cos kz\, dkd\tau$$

$$\bar{y} = \frac{2}{\pi}\int_0^t Q(t-\tau)\int_0^\infty \frac{K_1(kf)}{c_0K_1(kc_0)}\left[\sin\left(\frac{\Gamma}{2\pi c_0^2}(1-\beta_1)\tau\right) + \sin\left(\frac{\Gamma}{2\pi c_0^2}(1+\beta_1)\tau\right)\right]\cos kz\, dkd\tau$$

(A1.6)

From the integrand in A(1.6) it appears that, unlike the results of §3 (cf. 7.3.7), for each wavenumber k, the contribution to the integrand is from two modes of vibration: a co-rotational mode of frequency $(\frac{\Gamma}{2\pi c_0^2})(1 + \beta_1)$ and a contra-rotational mode of frequency $(\frac{\Gamma}{2\pi c_0^2})(1-\beta_1)$. This is a feature of the hollow vortex and was noted by Kelvin (1880). For $kc_0 \ll 1$, expanding β_1 in kc_0 gives

$$(\frac{\Gamma}{2\pi c_0^2})(1 - \beta_1) = \frac{\Gamma}{2\pi c_0^2} \{- \tfrac{1}{2}k^2 c_0^{\,2}(\log \frac{1}{kc_0} + .1159) + O(k^4 c_0^{\,4})\}$$

and (A1.7)

$$(\frac{\Gamma}{2\pi c_0^2})(1 + \beta_1) = \frac{\Gamma}{2\pi c_0^2} \{2 + \tfrac{1}{2}k^2 c_0^2(\log \frac{1}{kc_0} + .1159) + O(k^4 c_0^{\,4})\}$$

Thus the co-rotational mode is much faster than the contra-rotational mode so that if the initial normal velocity of the displaced vortex is small, the amplitude of the co-rotational mode will be very small compared with that of contra-rotational mode. For $kc_0 \ll 1$, the contra-rotational mode frequency can be identified with the frequency of vibration given by the cut-off method. The error is $O(k^4 c_0^{\,4})$.

APPENDIX B: The coefficients $A_{n,m}$ in §5

In the expression for the velocity contribution $\underline{M}_s(\underline{Y})$ in equation (7.5.11), $A_{n,m}(\eta)$ are given by

$$A_{n,m}(\eta) = \sum_{k=0}^{m} \frac{m!(2n-k-1)!}{2n!(m-k)!} \left[\frac{(aA)^{m-k}}{(aA\pm|\underline{P}(\eta)|)^{2n-k}} - \frac{(-aA)^{m-k}}{(-aA\pm|\underline{P}(\eta)|)^{2n-k}} \right] \quad \begin{matrix} n=1,2,\ldots \\ m=0,1,2,\ldots \end{matrix}$$

if $\underline{k}.\underline{P}(\eta) = \pm|\underline{P}|$ where $\underline{P}(\eta)$ is as in (7.5.11). If $|\underline{k}.\underline{P}(\eta)| \neq |\underline{P}|$, i.e. $|\underline{k} \wedge \underline{P}| \neq 0$,

$$A_{2,m}(\eta) = \frac{1}{(4-m)}\{ \left[\frac{a^2A^2}{|aA\underline{k}+\underline{P}(\eta)|^3} - \frac{a^2A^2}{|-aA\underline{k}+\underline{P}(\eta)|^3} \right] + (2m-5)\underline{k}.\underline{P}(\eta)A_{2,m-1}$$

$$+ (m-1)|\underline{P}|^2 A_{2,(m-2)}\} \qquad m = 1,2,3$$

$$A_{2,0}(\eta) = \frac{1}{3|\underline{k}\wedge\underline{P}(\eta)|^2} \left[\frac{aA + \underline{k}.\underline{P}}{|aA\underline{k}+\underline{P}(\eta)|^3} + \frac{aA - \underline{k}.\underline{P}}{|-aA\underline{k}+\underline{P}(\eta)|^3} + 2A_{1,0} \right]$$

$$A_{1,1}(\eta) = \frac{1}{|\underline{k}\wedge\underline{P}(\eta)|^2} \left[\frac{|P(\eta)|^2+aA\underline{k}.\underline{P}(\eta)}{|aA\underline{k} + \underline{P}(\eta)|} - \frac{|\underline{P}|^2 - aA\underline{k}.\underline{P}}{|-aA\underline{k}+\underline{P}(\eta)|} \right]$$

$$A_{1,0}(\eta) = \frac{1}{|\underline{k}\wedge\underline{P}(\eta)|^2} \left[\frac{aA+\underline{k}.\underline{P}(\eta)}{|aA\underline{k}+\underline{P}(\eta)|} + \frac{aA-\underline{k}.\underline{P}(\eta)}{|-aA\underline{k}+\underline{P}(\eta)|} \right]$$

FIGURES AND PLATES

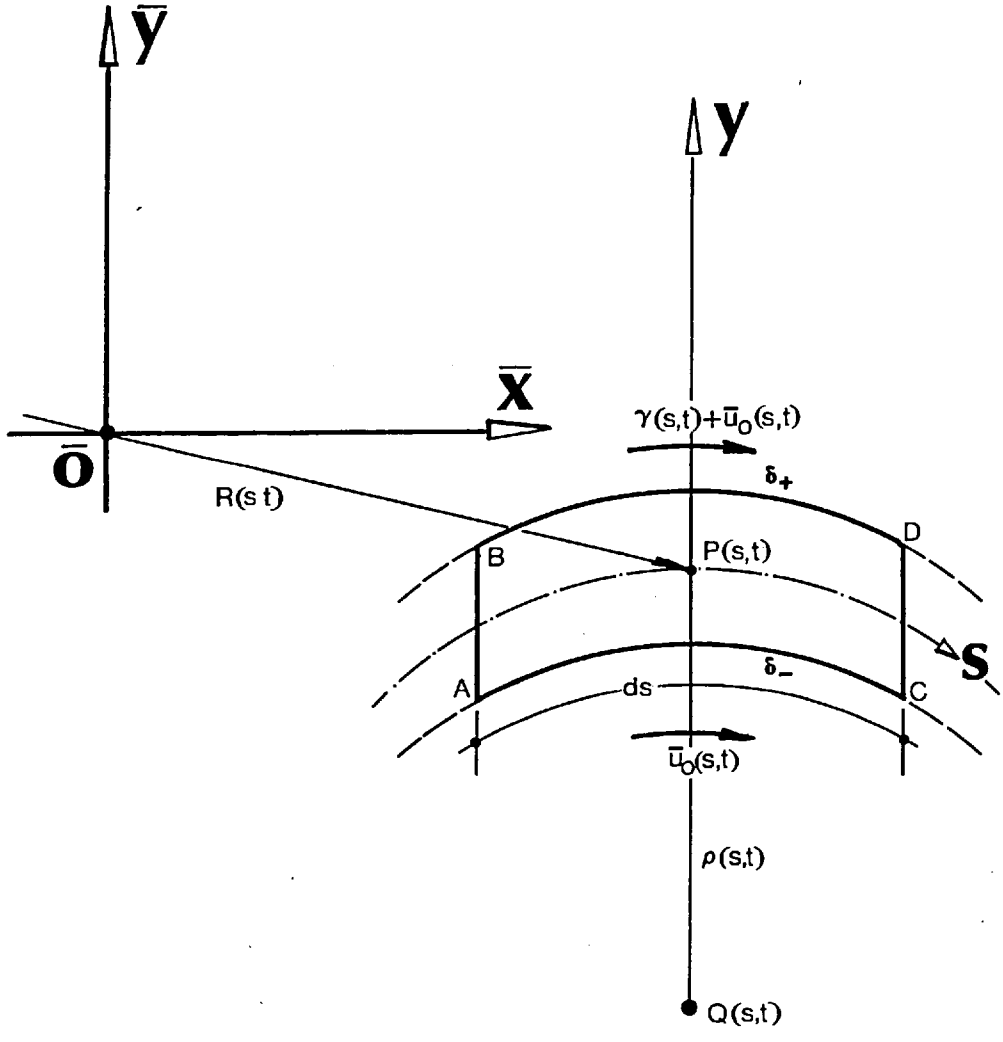

Fig. 3.1 An element of a vortex layer with centroid P(s) and radius of curvature ρ(s).

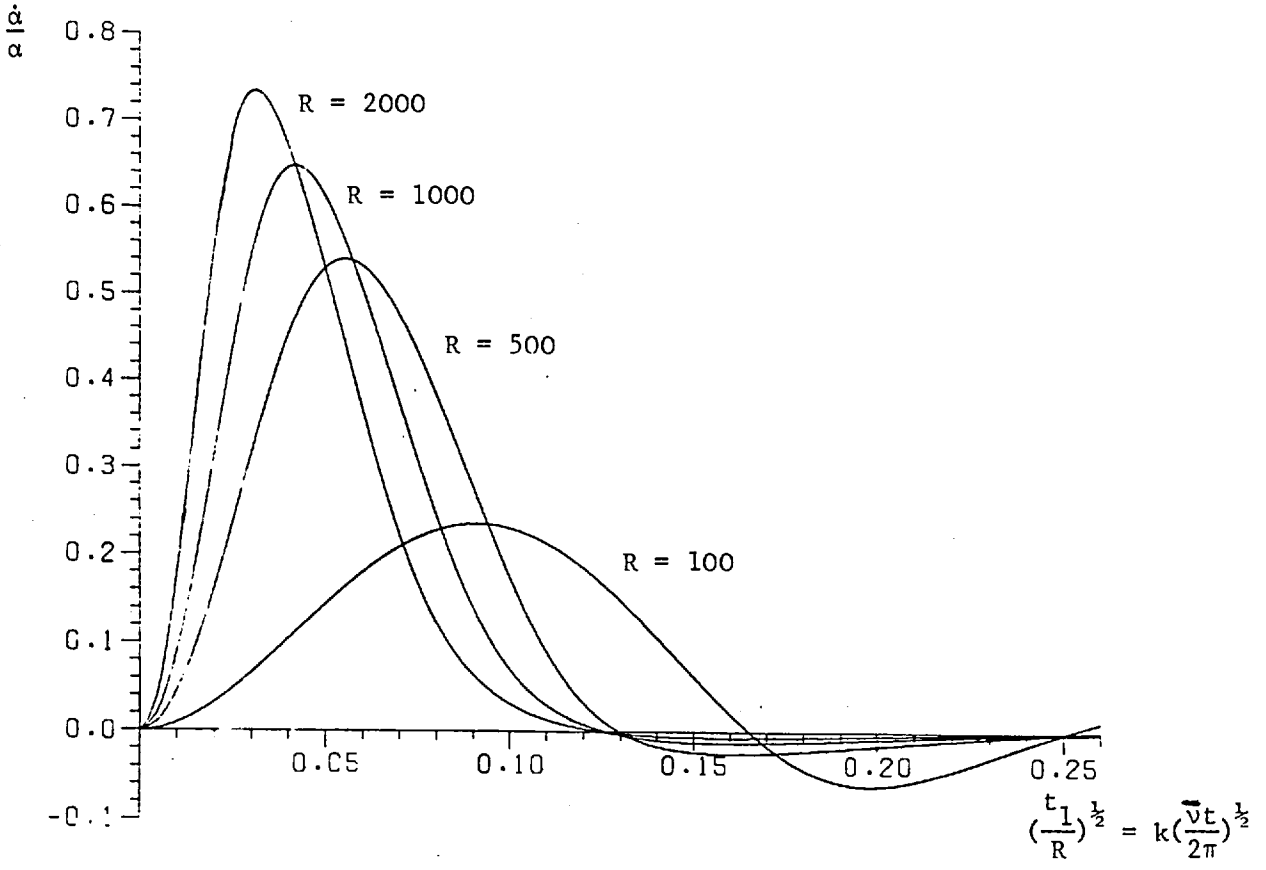

Figure 3.2 Growth of waves on a Rayleigh layer.
Amplification rate plotted against $(t_1/R)^{\frac{1}{2}}$.

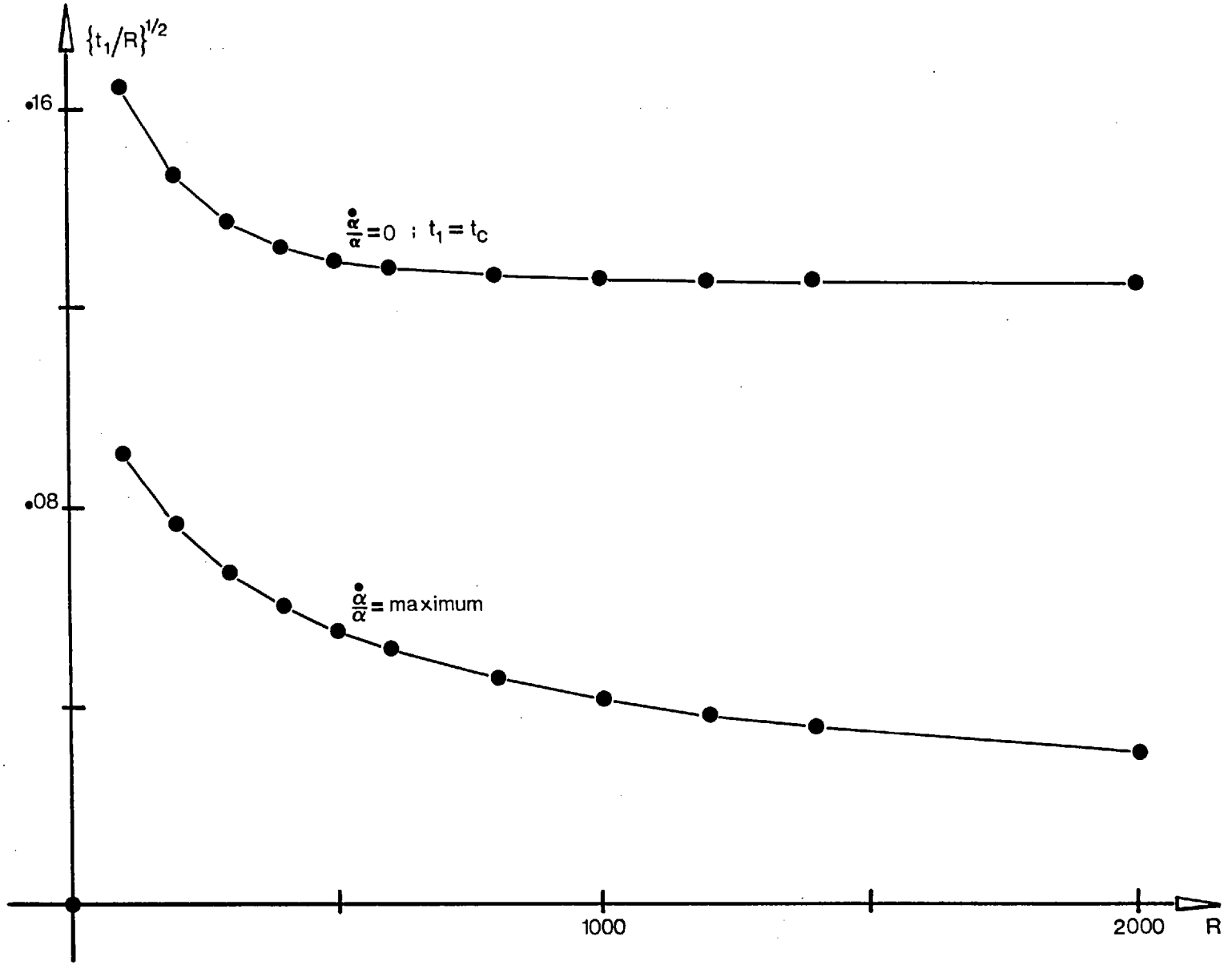

Figure 3.3 Dependence of $(t_1/R)^{\frac{1}{2}}_{max}$ and $(t_1/R)^{\frac{1}{2}}_{c}$ on R.

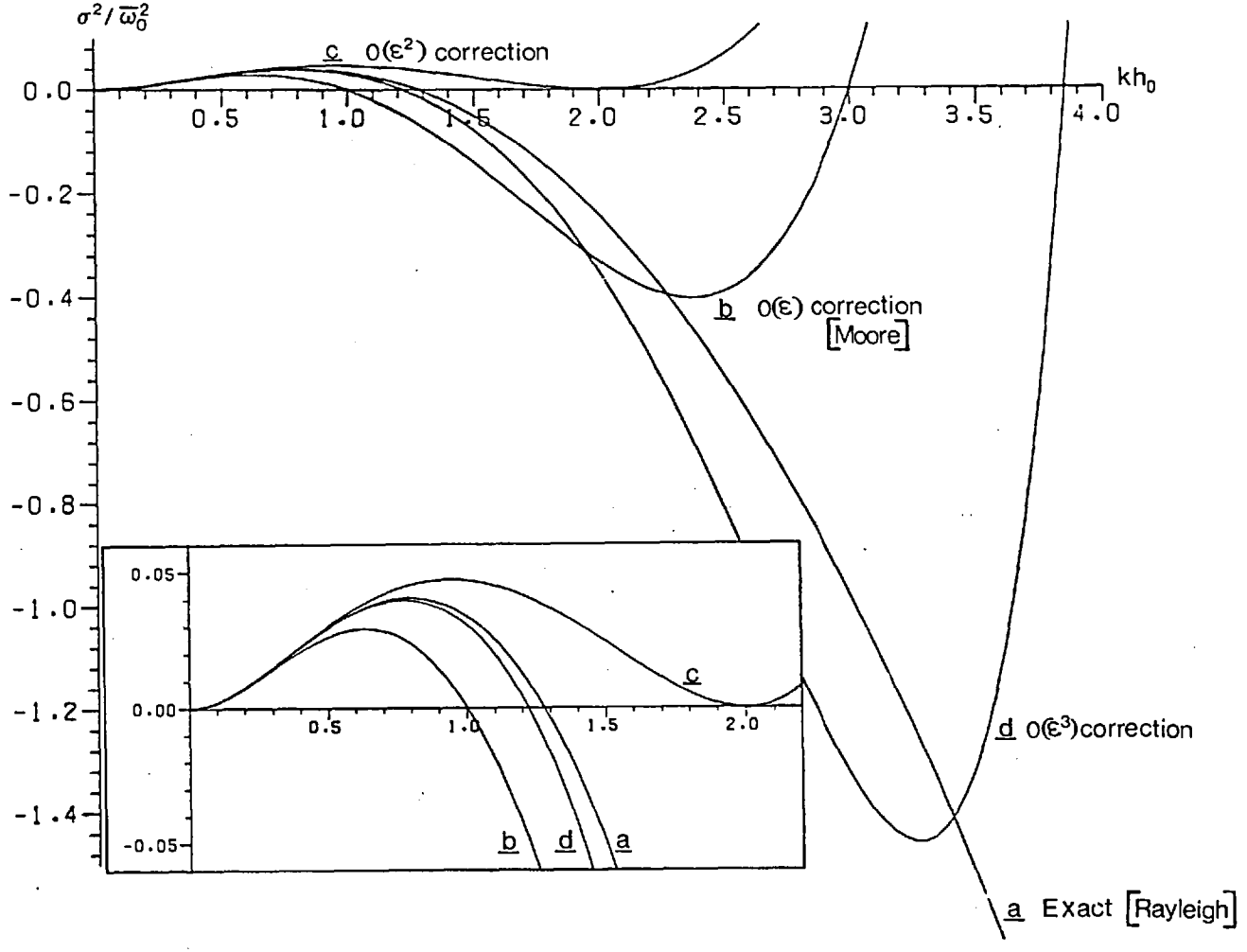

Figure 4.1 Growth of waves on a straight uniform vortex layer. Growth rates derived from using the governing equation with terms of (b) $O(\varepsilon)$, (c) $O(\varepsilon^2)$, (d) $O(\varepsilon^3)$ included in the analysis are compared with Rayleigh's exact result (a). The inset shows details of the plot for kh_0 small.

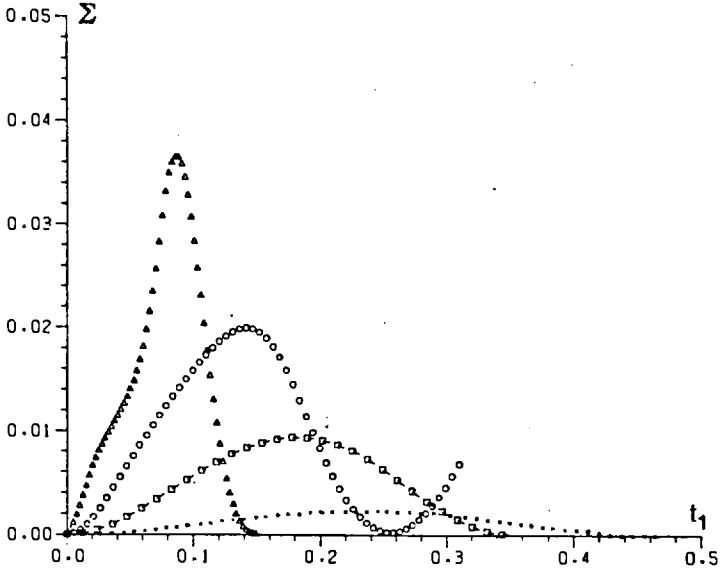

a

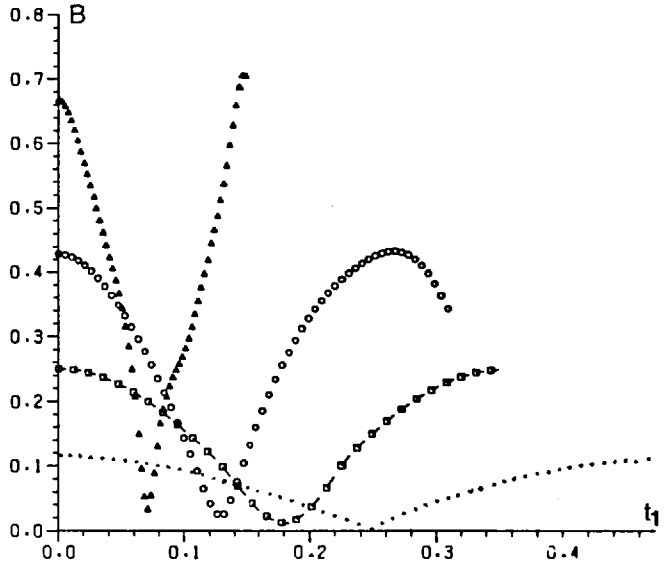

b

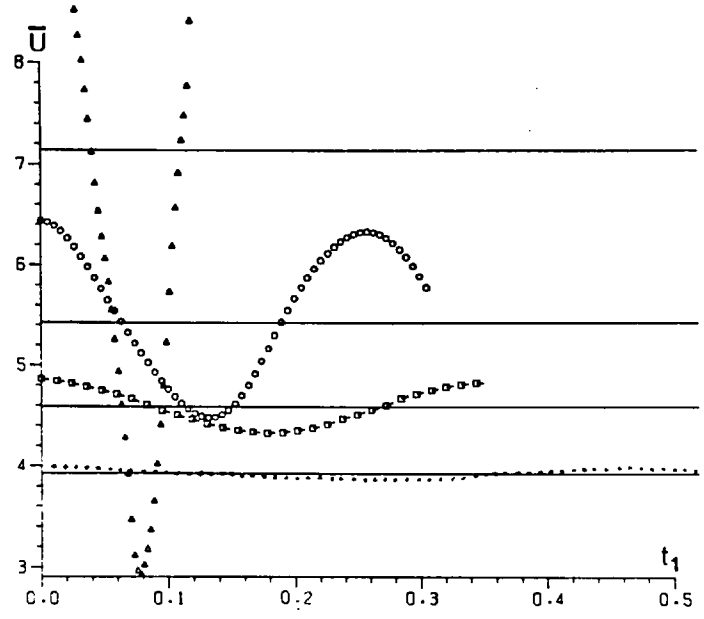

c

Figure 6.1. Plot of (a) variance $\Sigma(t_1)$ vs. t_1, (b) amplitude $B(t_1)$ vs. t_1 and (c) centroid velocity $\bar{U}(t)$ vs. t_1 for cases b/a = 0.2(Δ), 0.4(●), 0.6(□) and 0.8 (·). The solid lines in (C) give velocity $V_L(\frac{a+b}{2}, c_0, 1)$

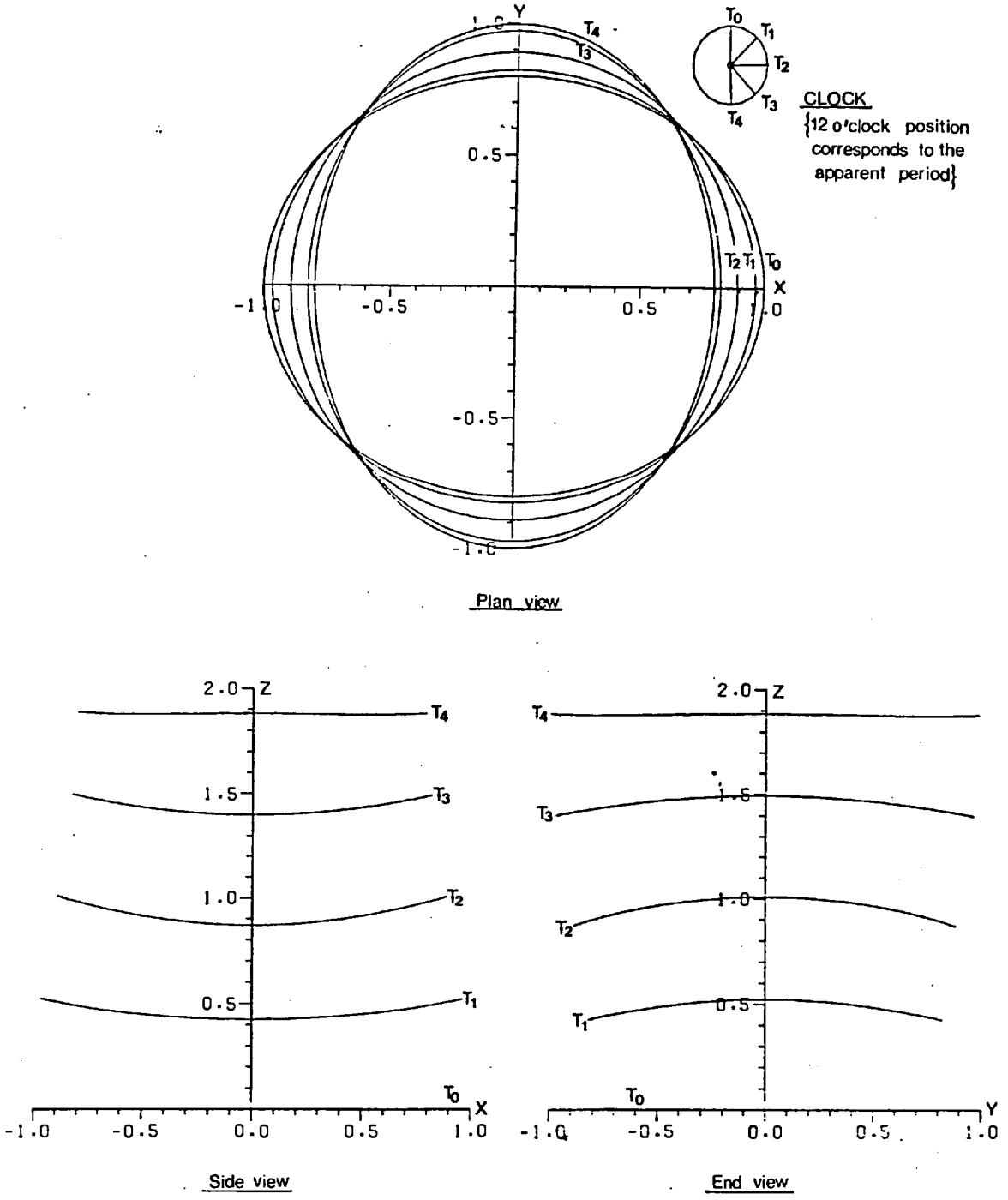

Figure 6.2. Evolution of the elliptic vortex ring of axes ratio 0.8.

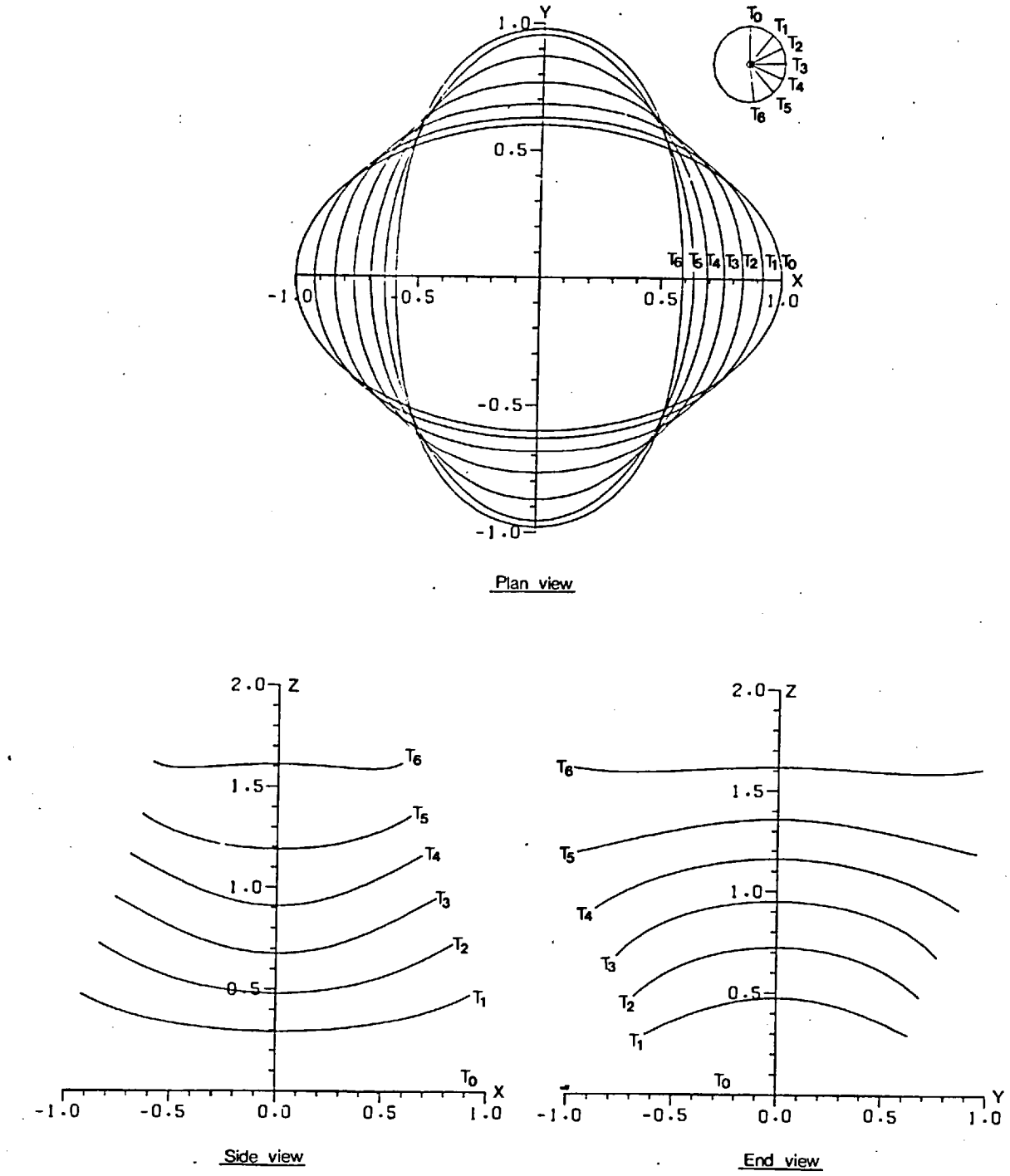

Figure 6.3. Evolution of the elliptic vortex ring of axes ratio 0.6.

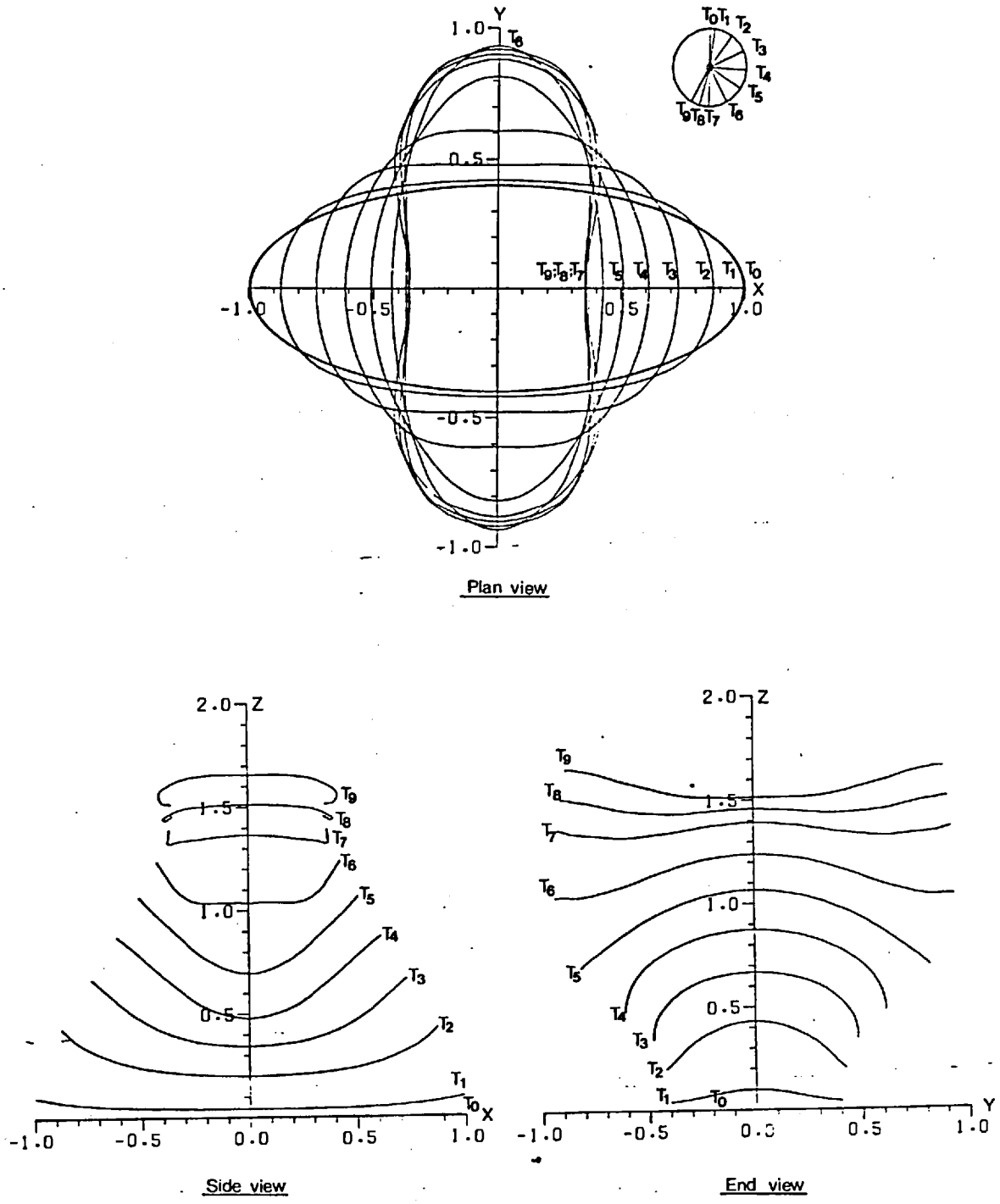

Figure 6.4. Evolution of the elliptic vortex ring of axes ratio 0.4.

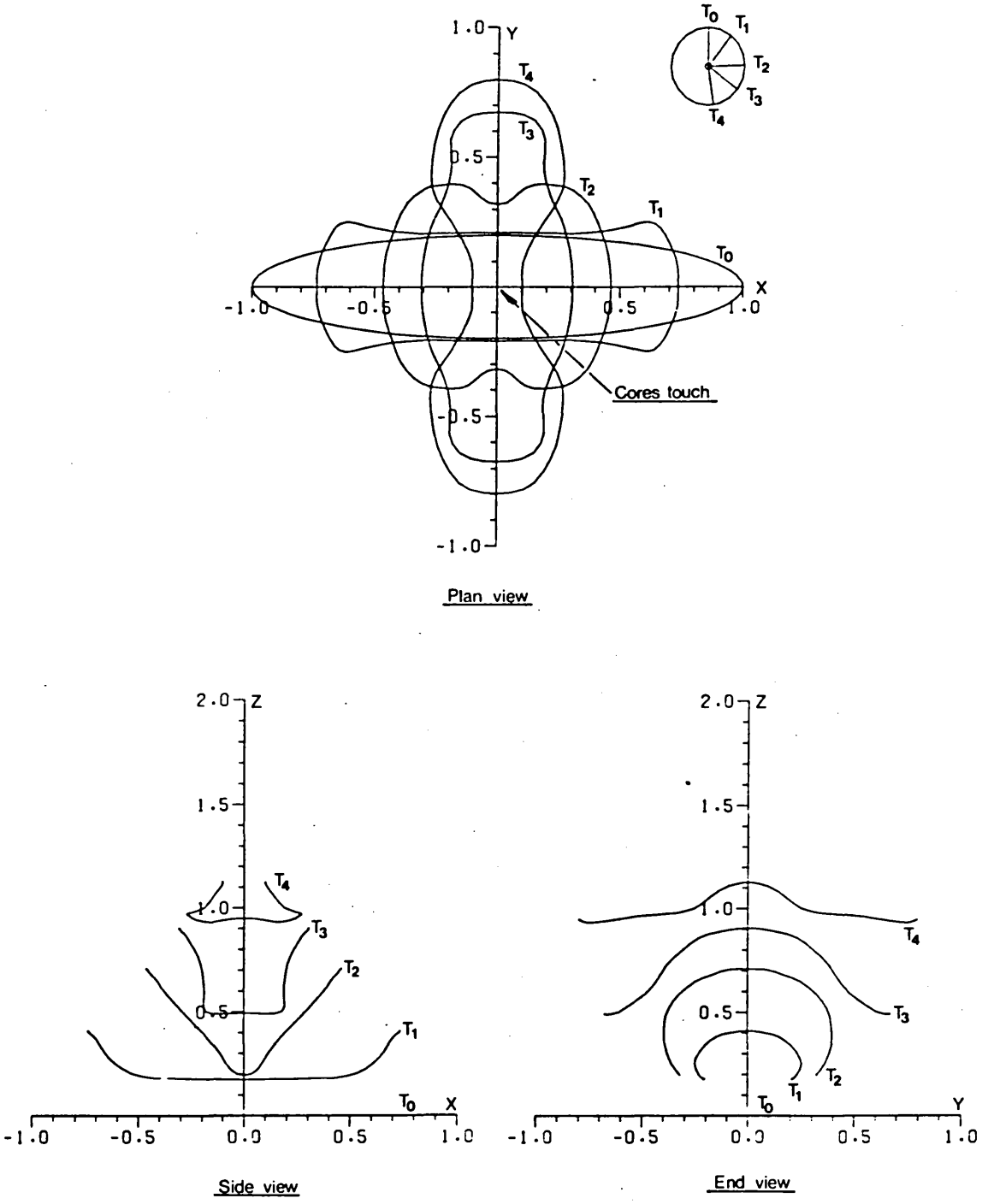

Figure 6.5. Evolution of the elliptic vortex ring of axes ratio 0.2.

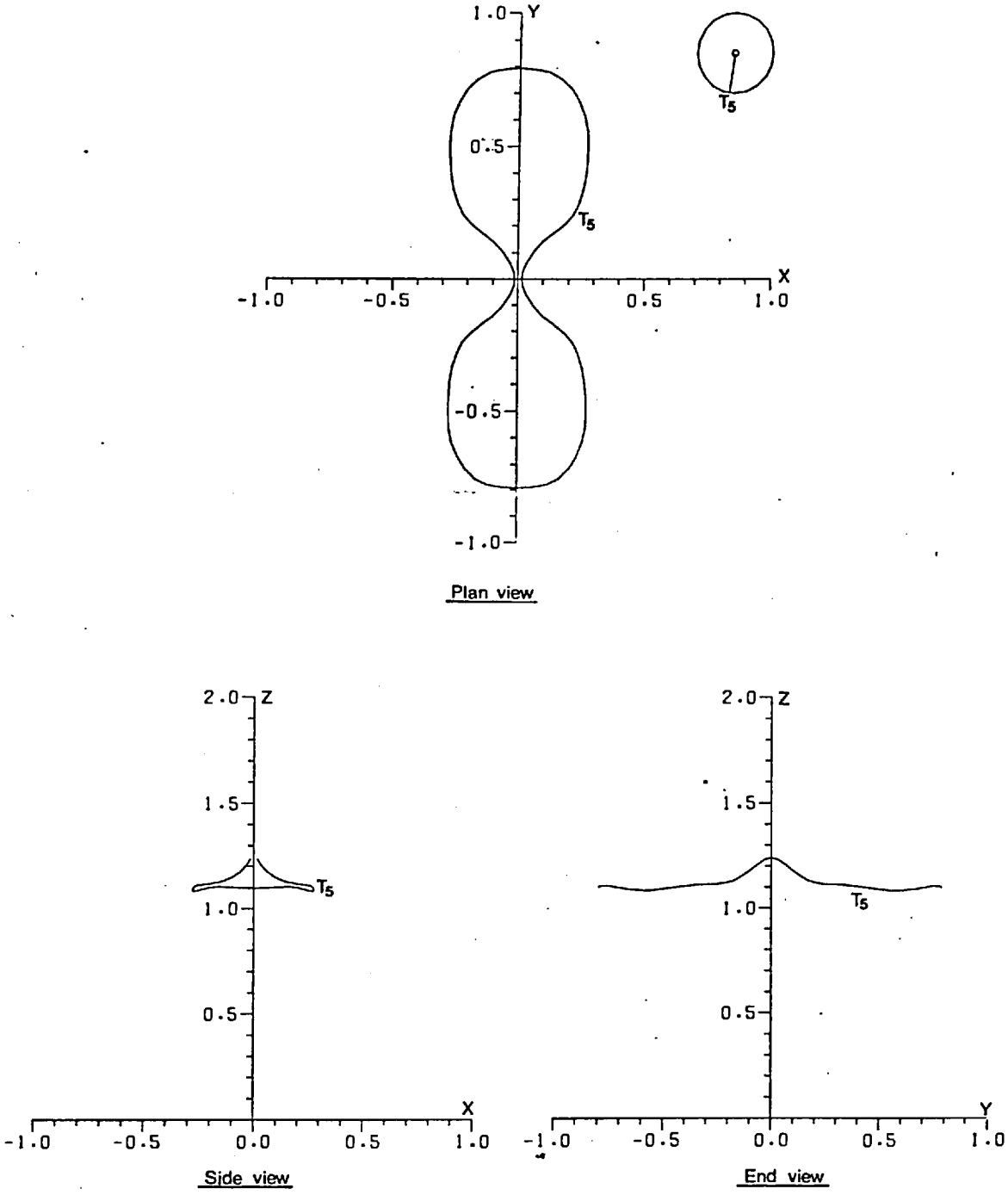

Figure 6.6. Shape of the vortex ring of case b/a = 0.2 at t_1 = 0.149 ($> \frac{1}{2}\tau_A$).

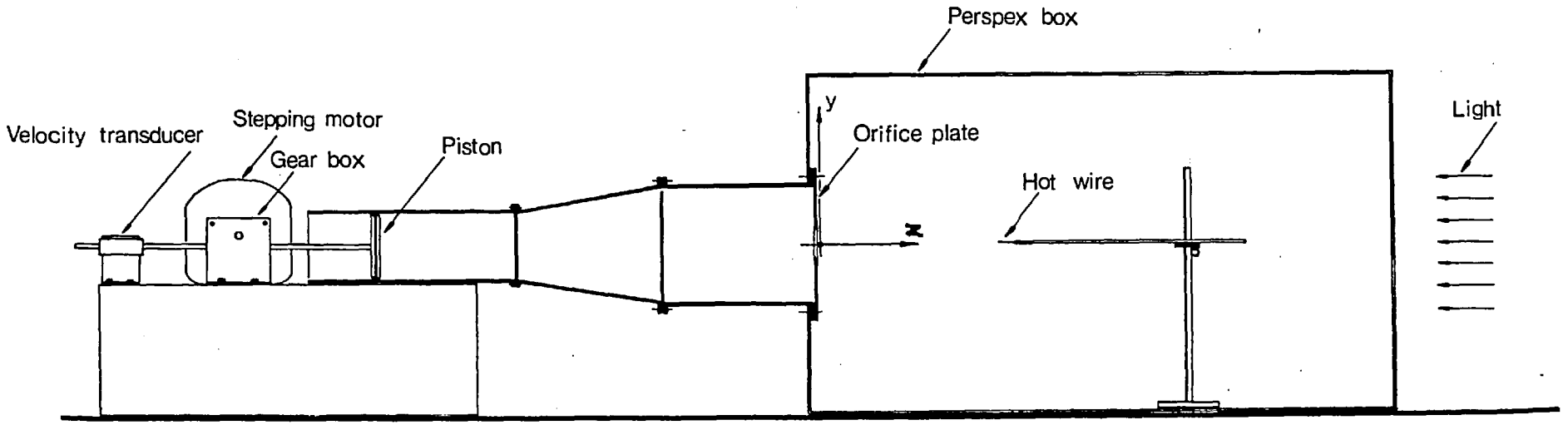

Figure 6.7. Experimental set-up.

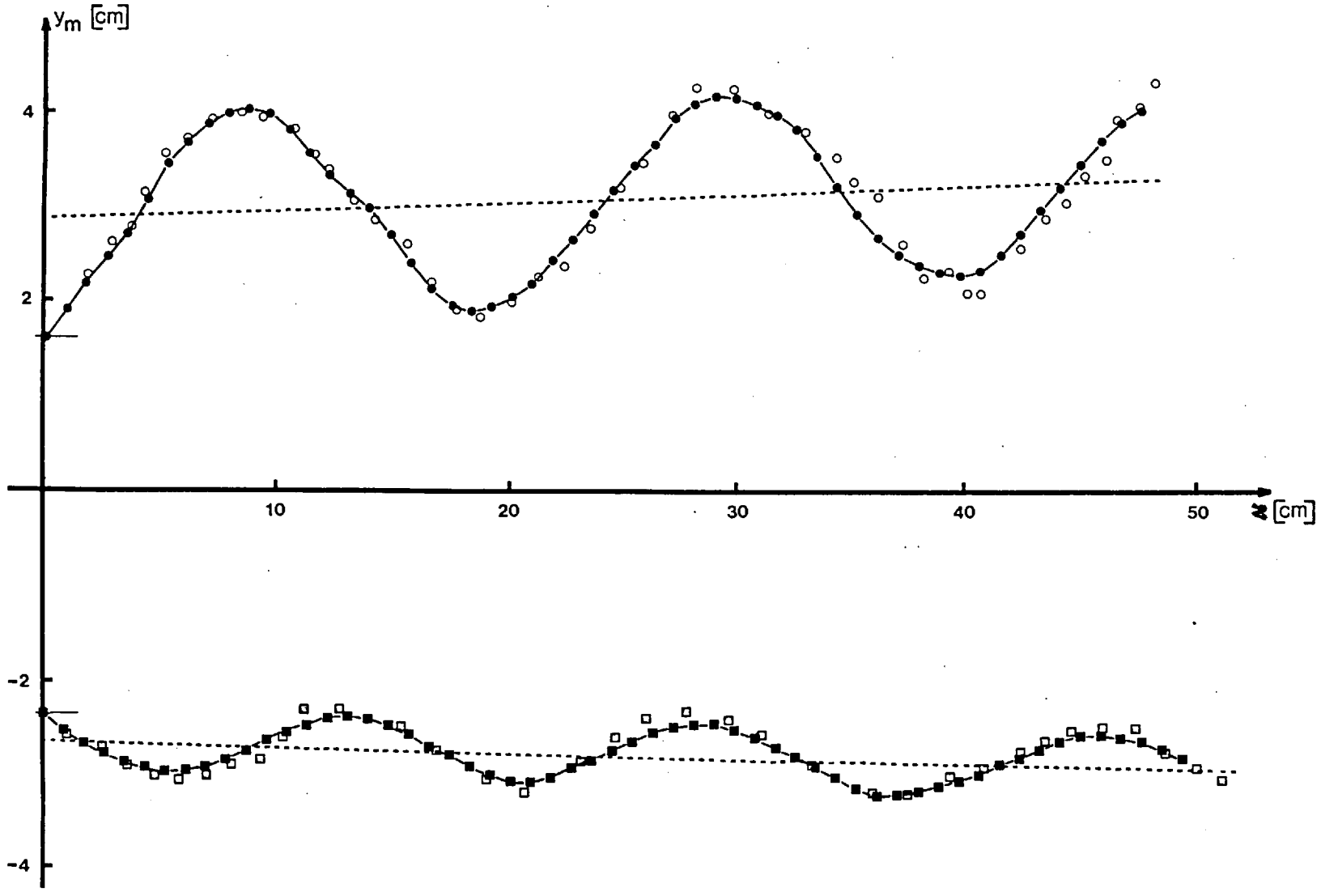

Figure 6.8. Plot of y_M vs. distance from the orifice. In the upper half positive y_M is plotted for b/a = 0.6 case and in the lower half negative y_M is plotted for b/a = 0.8 case. The unshaded symbols ○ and □ refer to values obtained from a single run while the corresponding shaded symbols refer to averaged values.

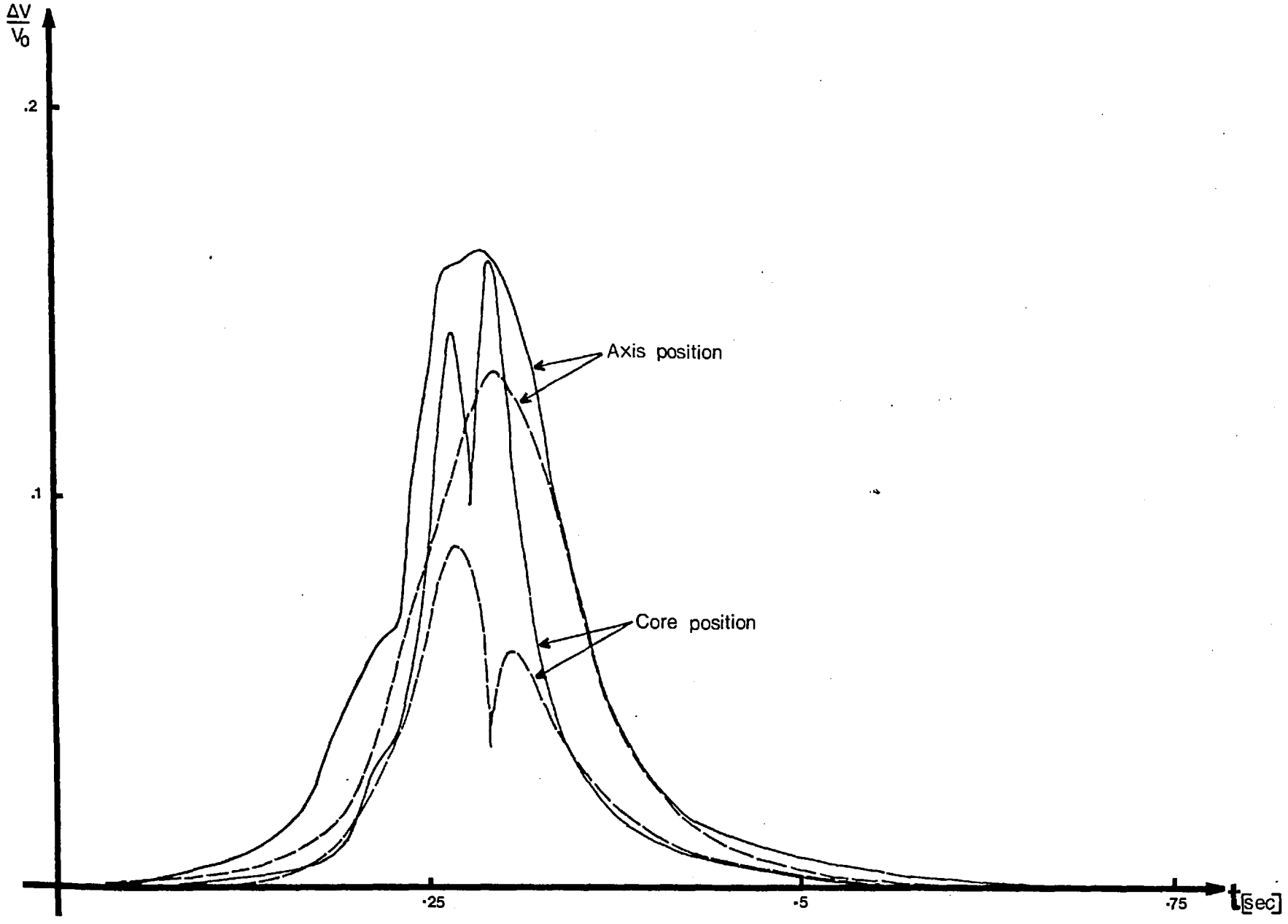

Figure 6.9. Non-dimensional voltage output from the hot-wire anemometer, placed 10 cm from the orifice, plotted against time. The ----- refers to b/a = 0.8 and ——— refers to b/a = 0.4 case.

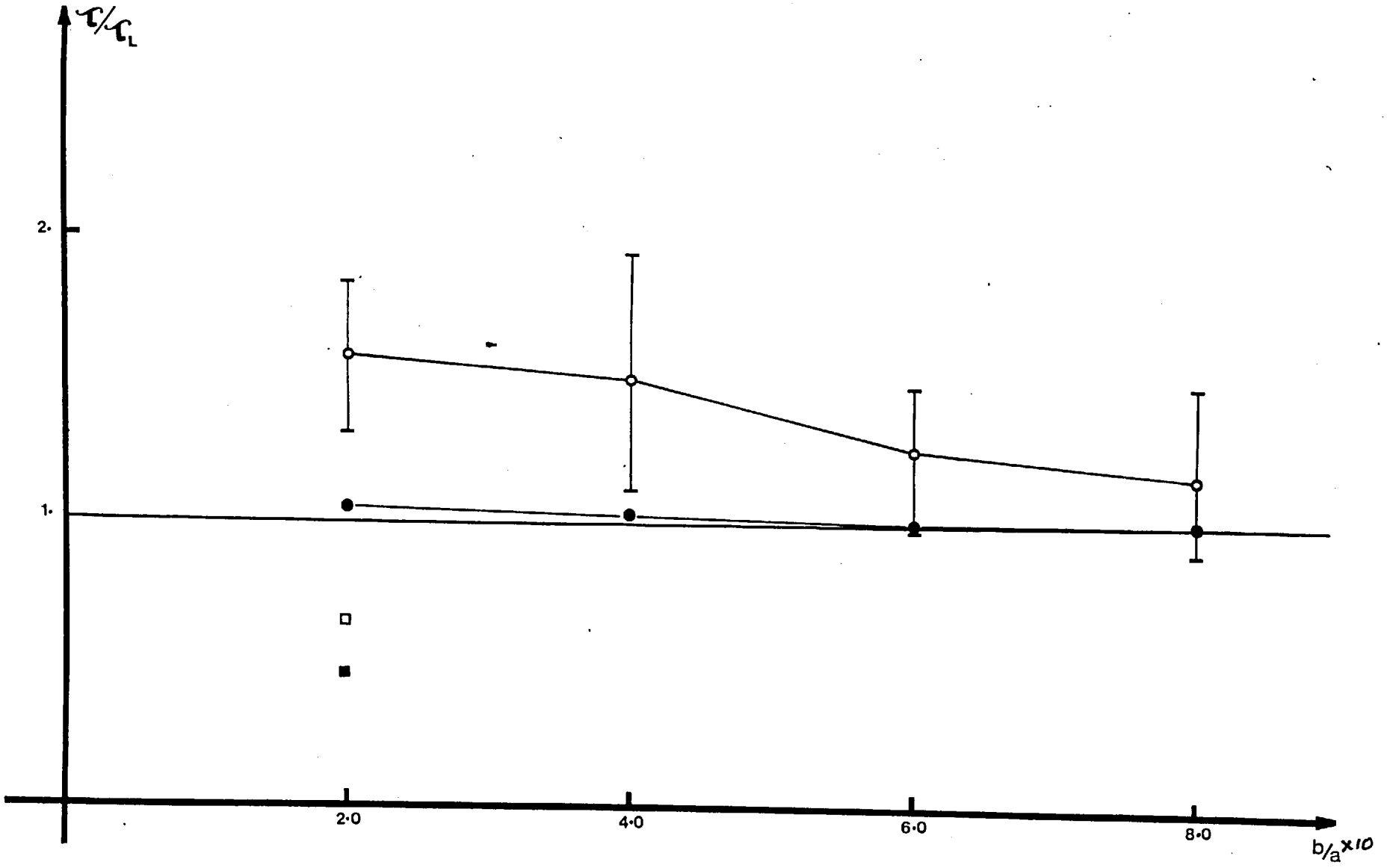

Figure 6.10. Plot of τ/τ_L against axes ratio b/a. The symbol O refers to $\tau_E/\tau_L(\frac{a+b}{2}, C_E, 1)$; the standard errors for these experimental values are also shown. The ● refers to $\tau_N/\tau_L(\frac{a+b}{2}, C_0, 1)$. For b/a = 0.2, the corresponding times of the break-up of the ring are shown by □ and ■ respectively.

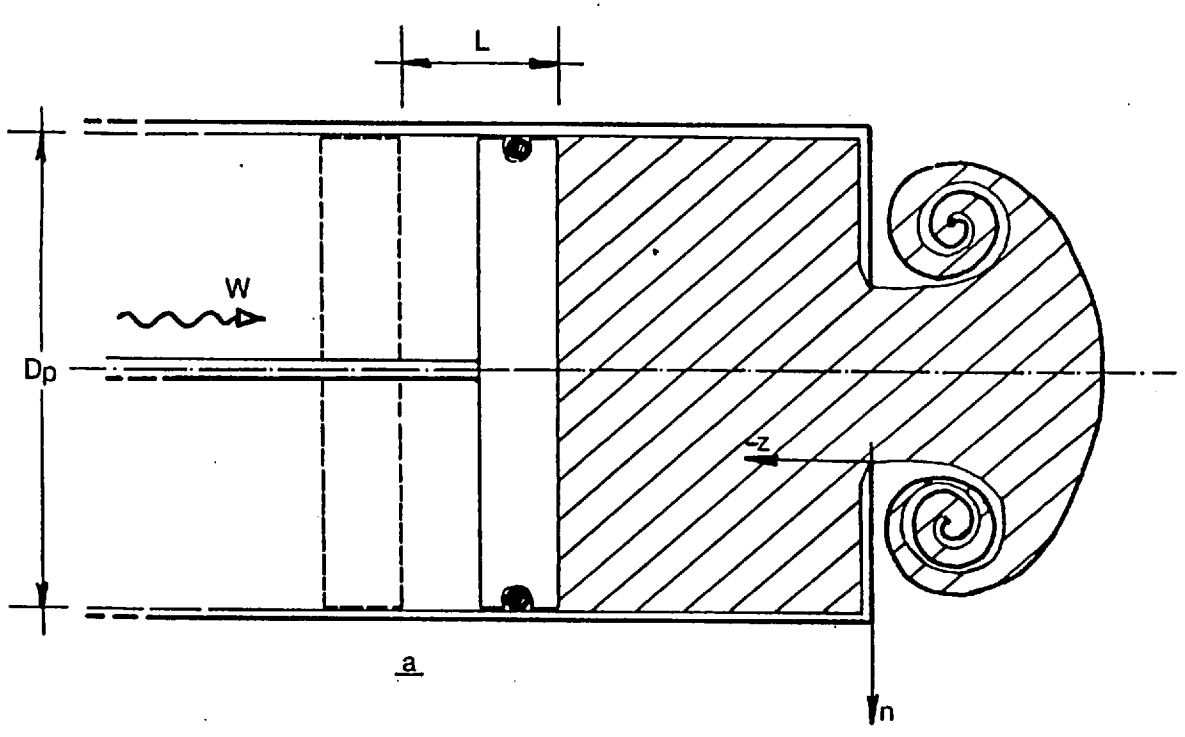

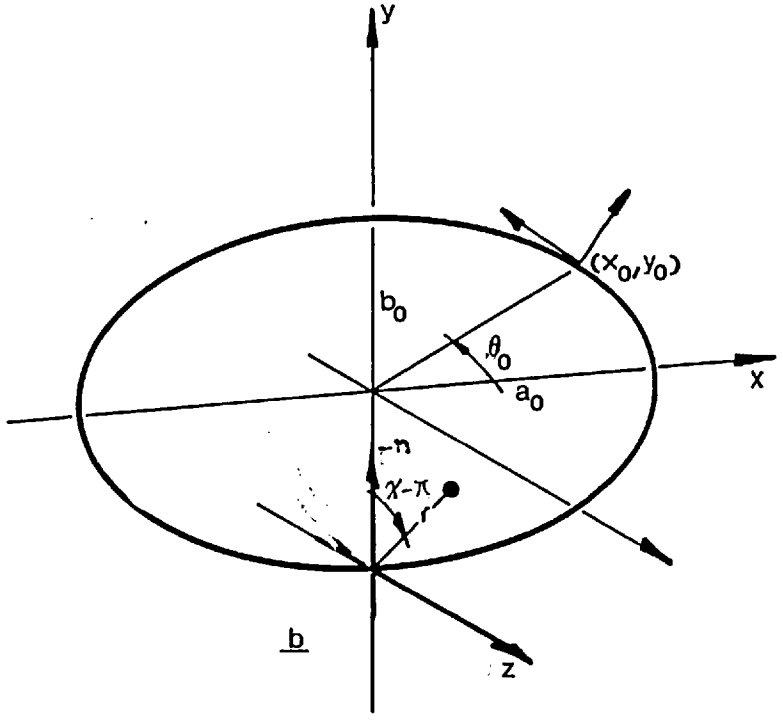

Fig. 6.11

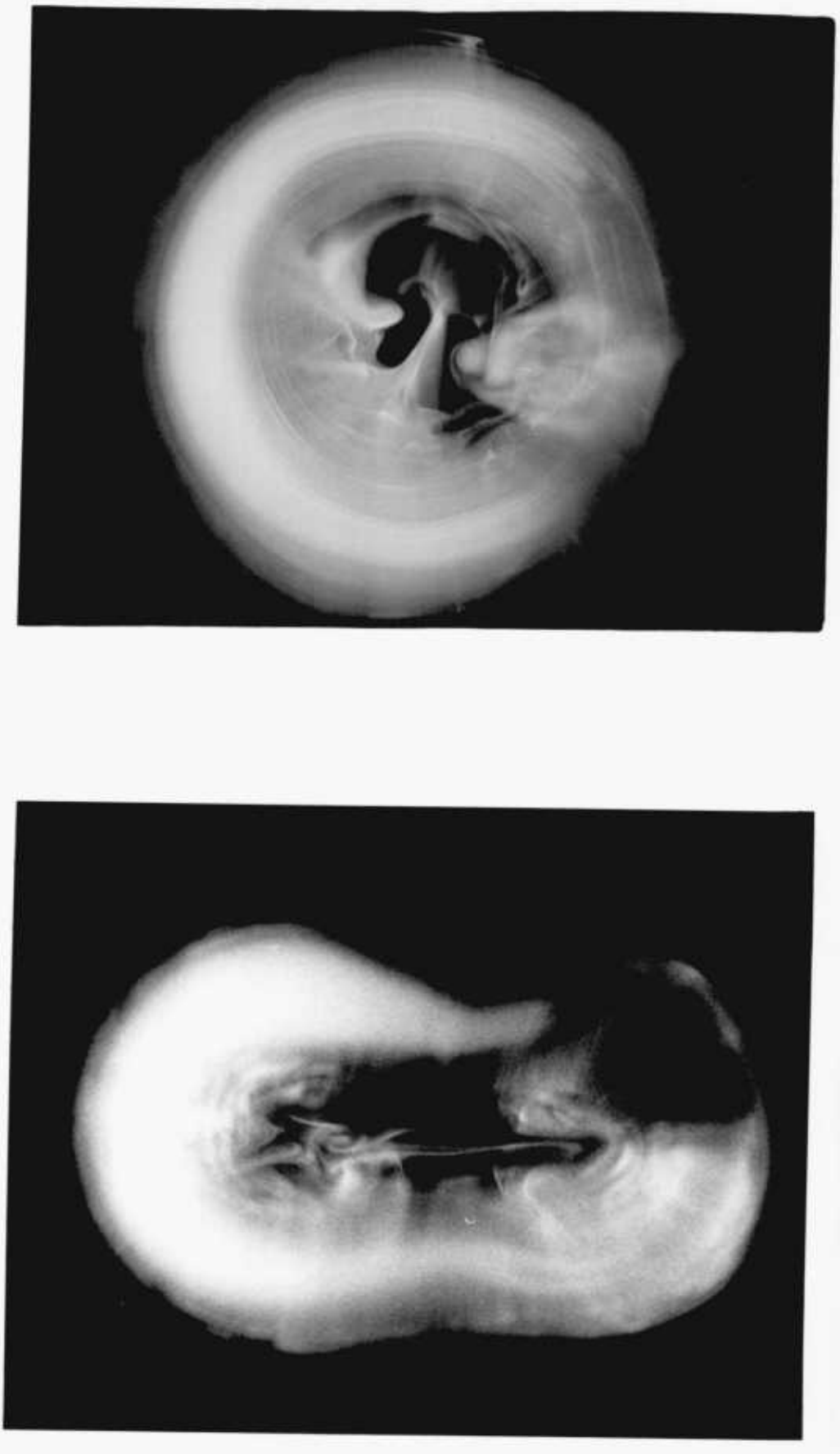

Plate 6.1. Comparison between an evolving vortex ring and a non-evolving vortex ring.

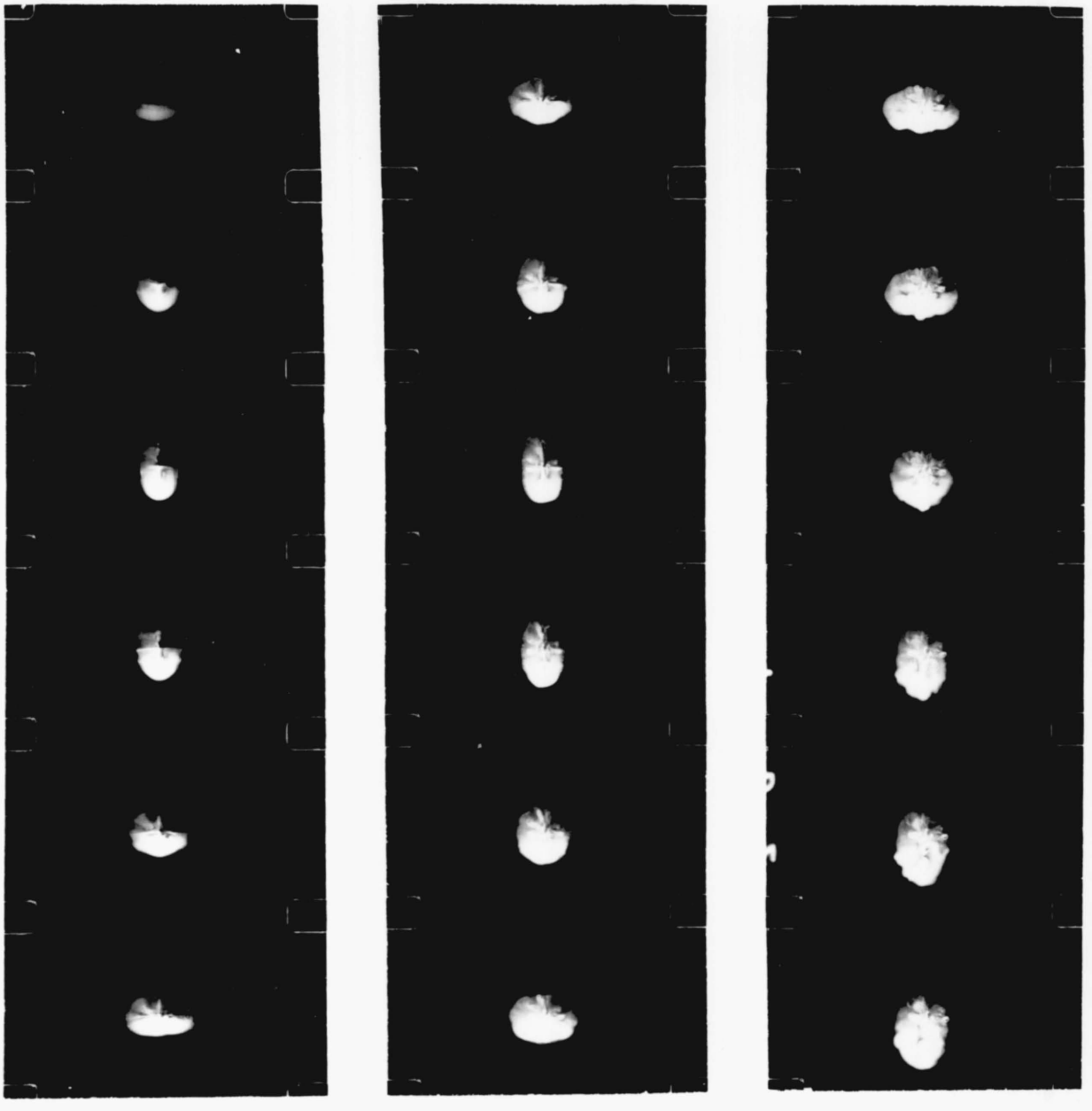

Plate 6.2. The plan view of the evolution of an elliptic vortex ring of axes ratio 0.4. The order of the sequence is from top to bottom and left to right. The top left-hand frame shows the vortex ring just forming. The major axis of the orifice is in the horizontal direction. The film sequence was taken at 32 frames/sec.

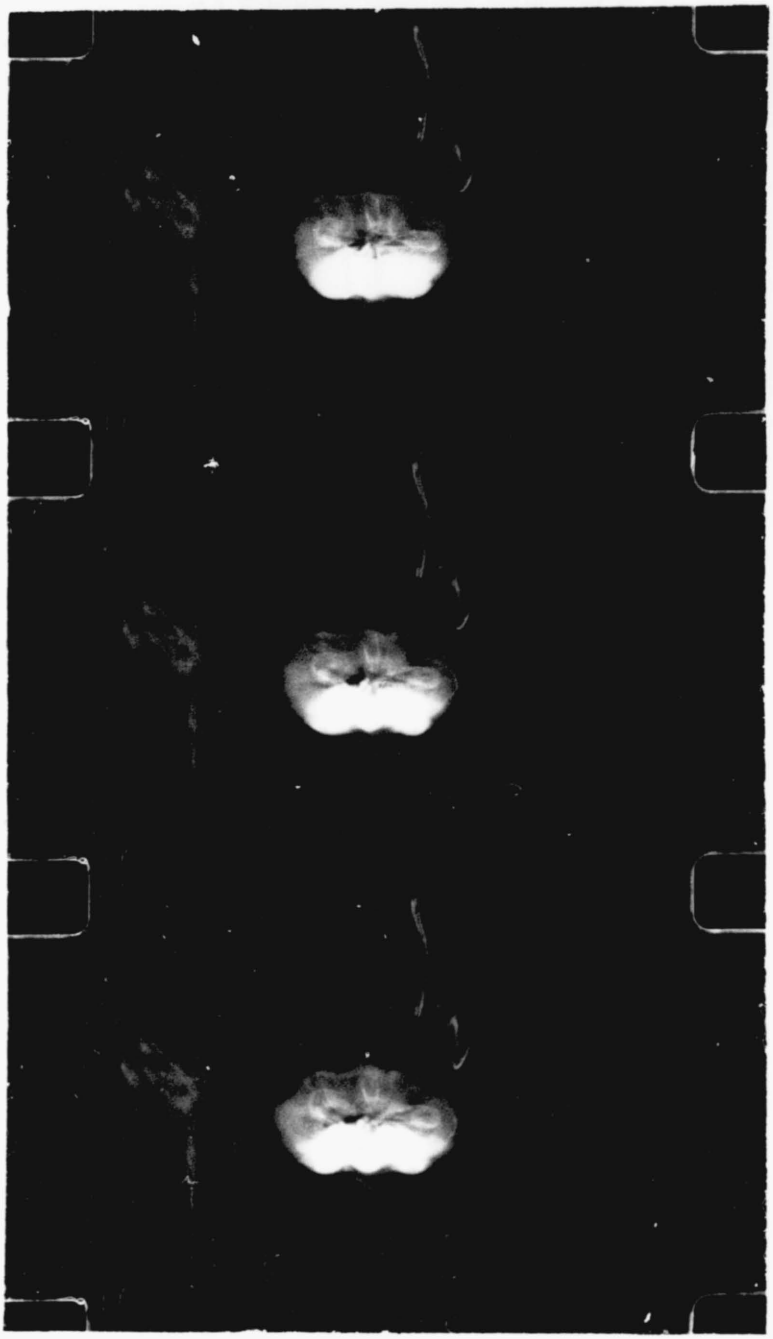

Plate 6.3. Vortex ring in the case b/a = 0.4 at the end of third oscillation showing short-wave instability. The sequence was taken at 32 frames/s.

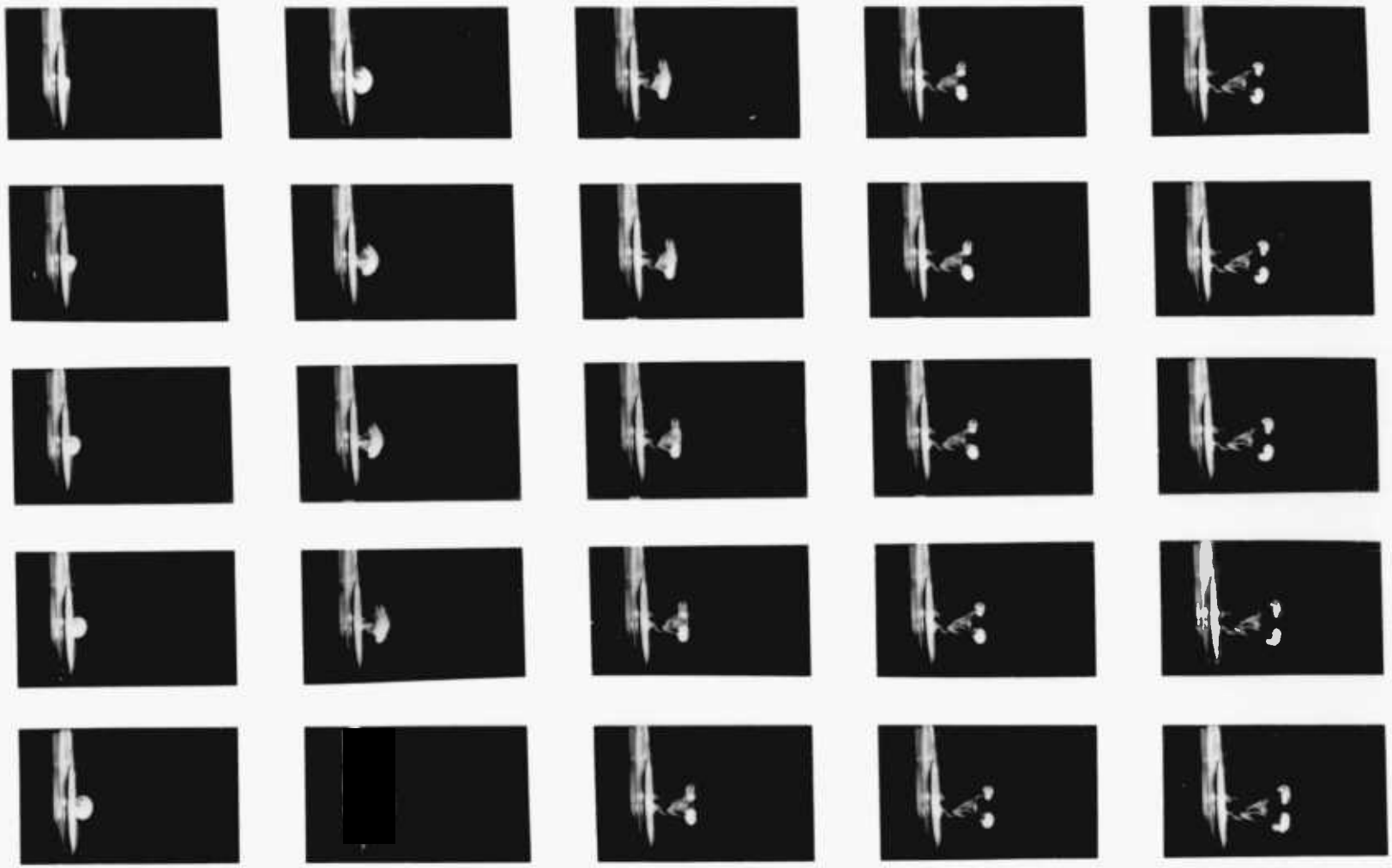

Plate 6.4. Side-view of the break-up process of the vortex ring in the case b/a = 0.2. The order of the sequence is as in Plate 6.2. The film sequence was taken at 32 frames/sec.

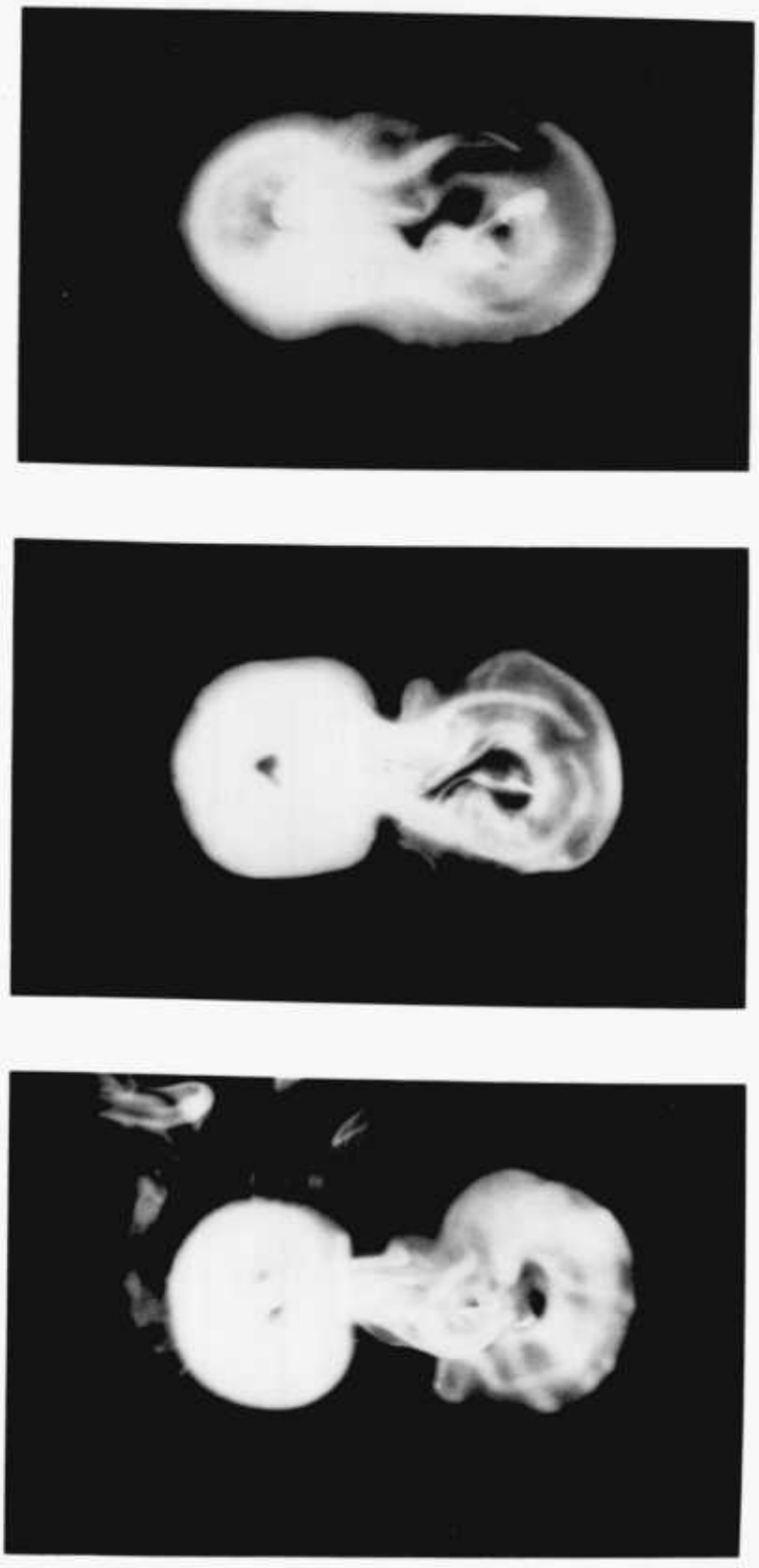

Plate 6.5. Detailed plan view of the break-up of the vortex ring in the case b/a = 0.2.

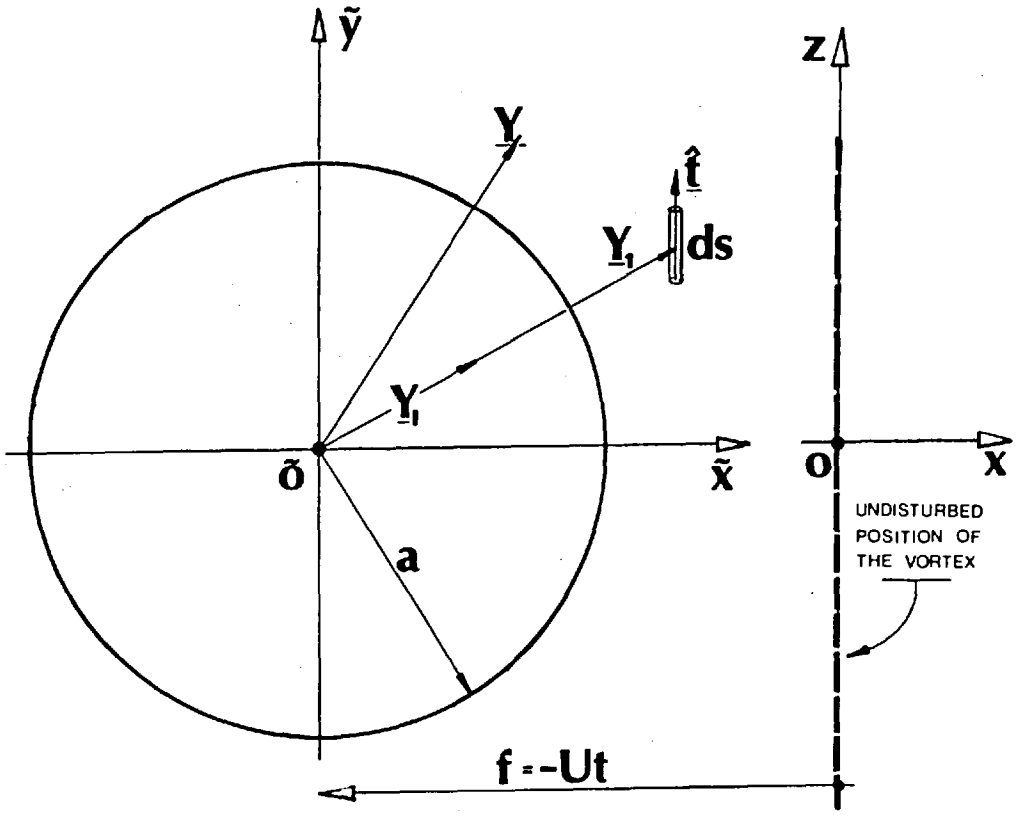

Figure 7.1 Coordinate system used in §§3,5.

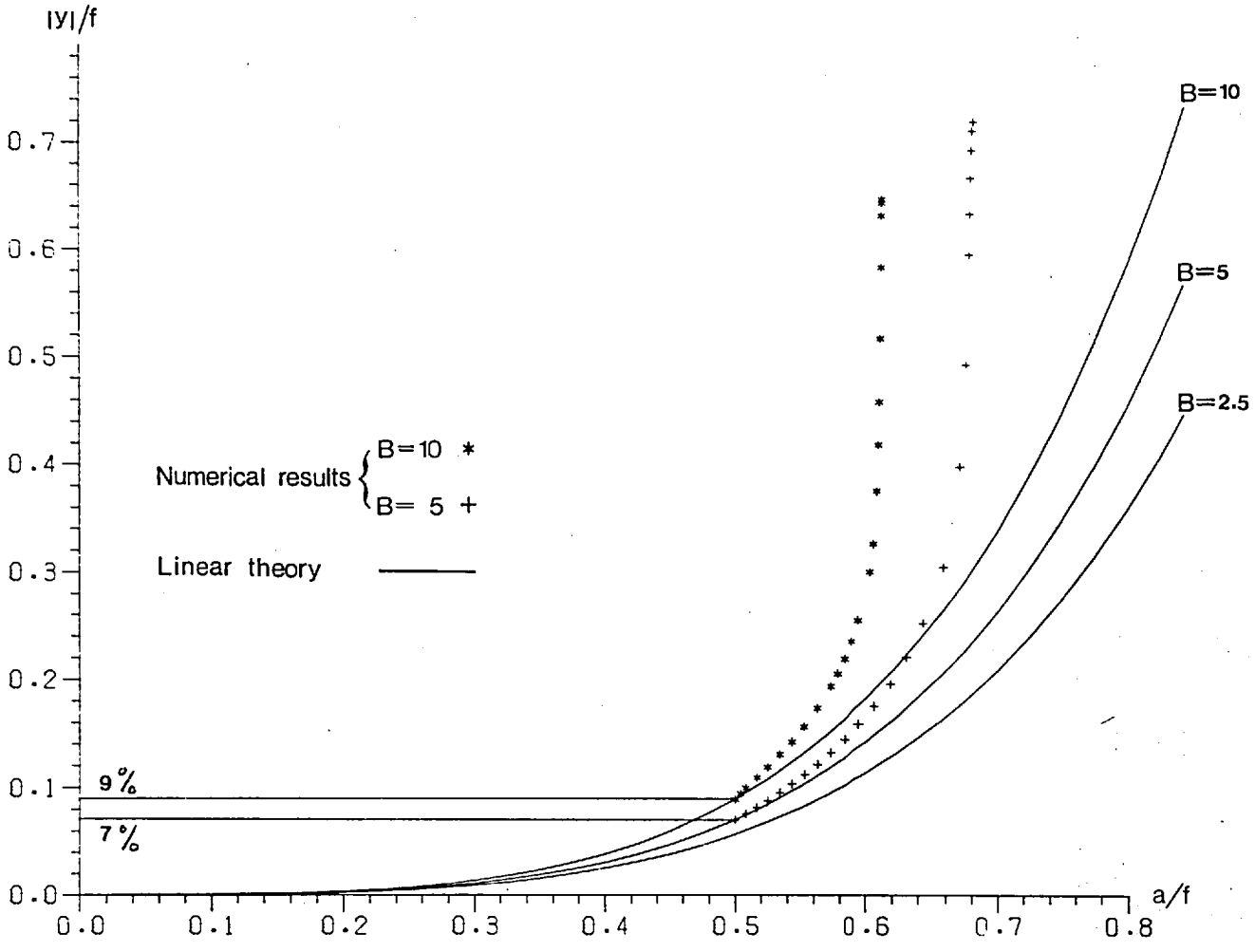

Figure 7.2 A plot of |y|/f vs. a/f.

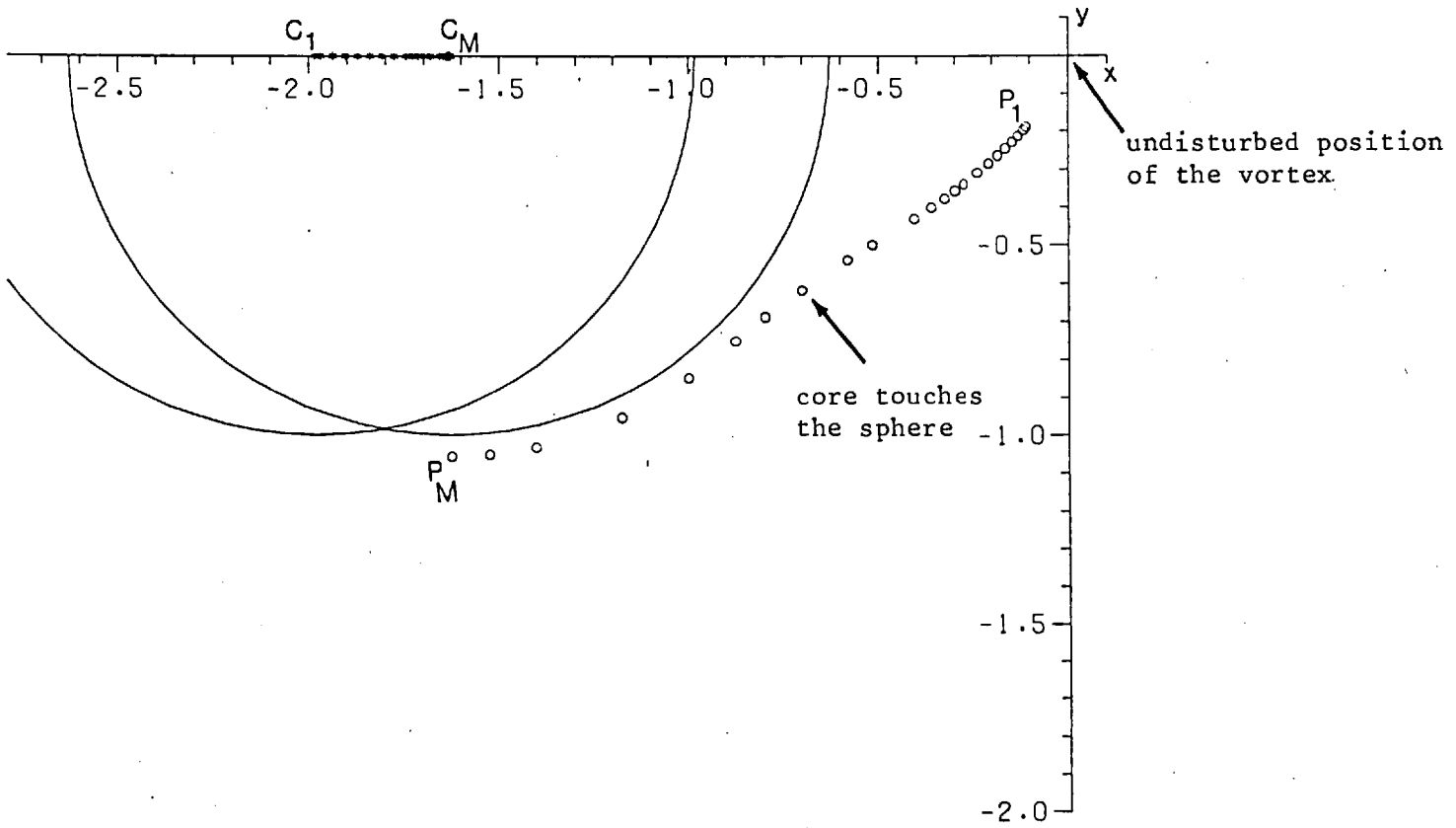

Figure 7.3 Track of $\xi = 0$ point of the vortex in the x-y plane for B = 10. C_1 and C_M are the positions of the centre of the sphere corresponding to the positions P_1 and P_M of the vortex. The sphere has been drawn in these two cases while for intermediate times only the centre of the sphere is shown. P_M is the position of the vortex at $t_1 = t_M$. The circulation of the vortex is in anti-clockwise sense.

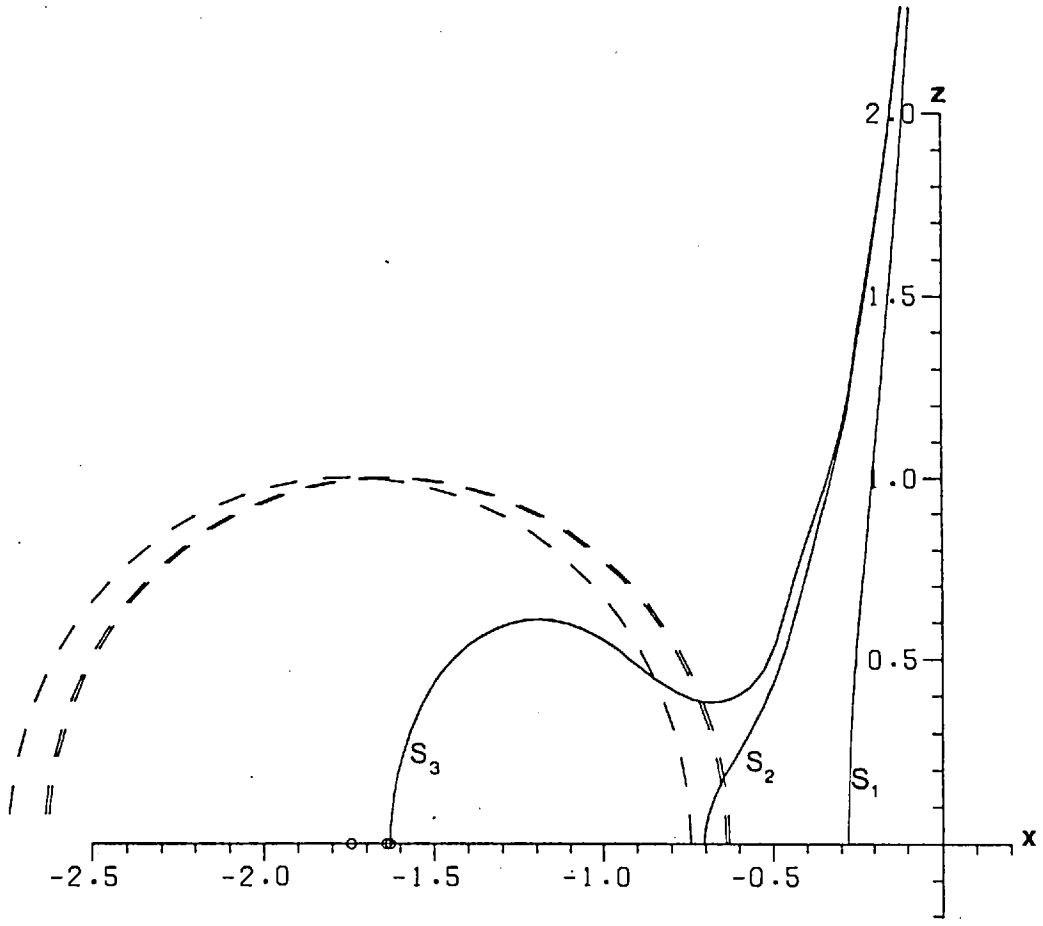

Figure 7.4 Side view of the evolution of the vortex at times $t_1 = 2.56$ (S_1), $t_1 = t_1^*$ (S_2) and $t_1 = t_M$ (S_3) for B = 10. o marks the position of the centre of the sphere at these times.

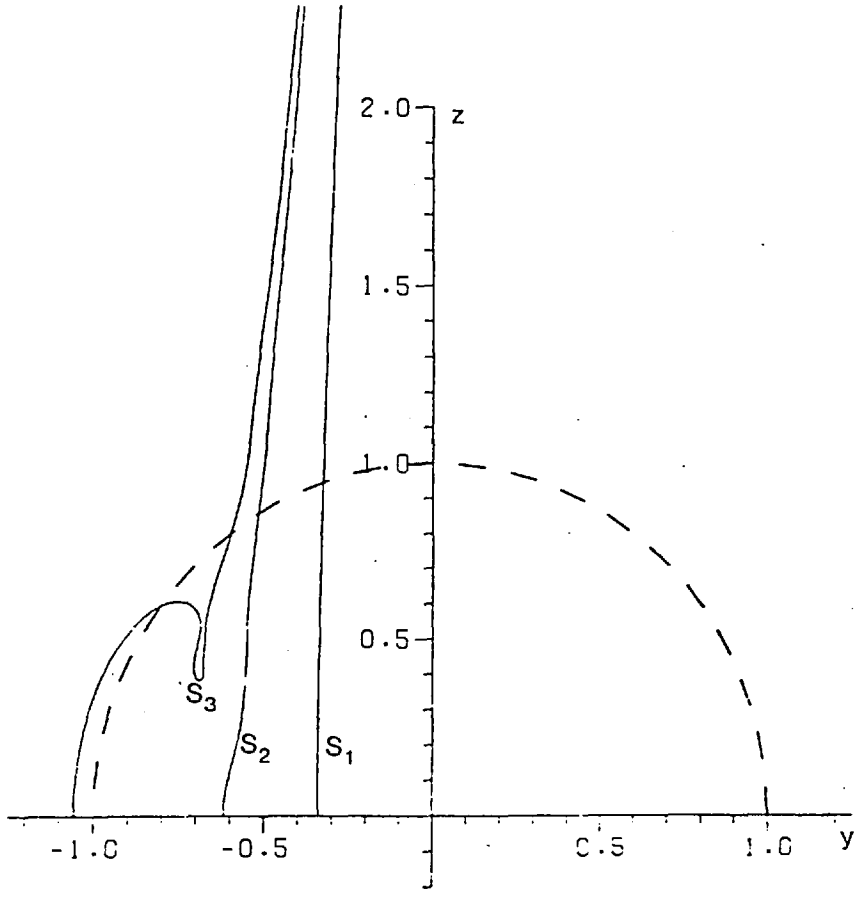

Figure 7.5 End view of the evolution of the vortex at times $t_1 = 2.56$ (S_1), $t_1 = t_1^*(S_2)$ and $t_1 = t_M$ (S_3) for B = 10.

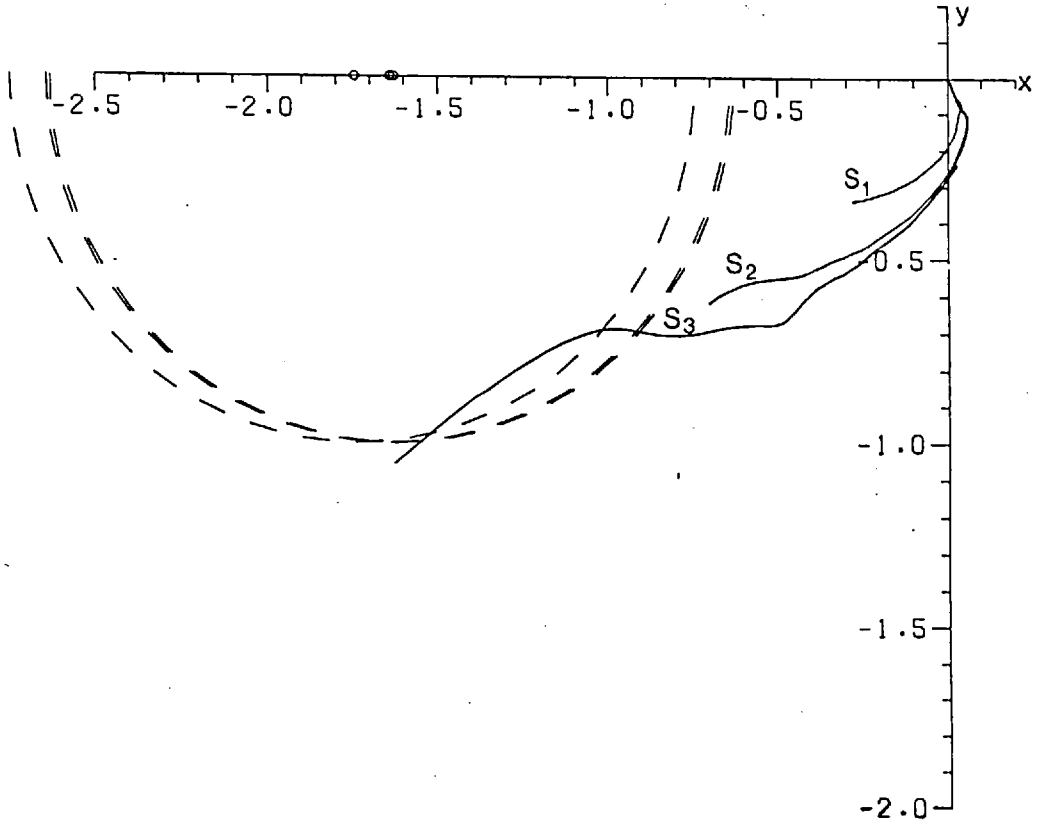

Figure 7.6 Plan view of the evolution of the vortex at times $t_1 = 2.56$ (S_1), $t_1 = t_1^*$ (S_2) and $t_1 = t_M$ (S_3) for B = 10. o marks the position of the centre of the sphere at these times.

REFERENCES

ARMS, R.J. & HAMA, F.R., 1965. Localized-induction concept on a curved vortex and motion of an elliptic vortex ring. Phy. Fluids, 8, 553.

BENJAMIN, T.B., BONA, J.L. & MAHONY, J.J., 1972. Model Equations for long waves in nonlinear dispersive systems. Philos. Trans. R. Soc. London, A272, 47.

BIRKHOFF, G., 1962. Helmholtz and Taylor instability. Proc. Symp. Appl. Math. Am. Math. Soc. 13, 55.

CROW, S.C., 1970. Stability theory for a pair of trailing vortices. AIAA J. 8, 2172.

CROW, S.C. & BARKER, S.J., 1977. The motion of two-dimensional vortex pairs in a ground effect. J. Fluid Mech. 82, 659

DIDDEN, N., 1979. On the formation of vortex rings. ZAMP, 30, 101.

DRÁZIN, P.G. & HOWARD, L.N. 1962. The instability to long waves of unbounded parallel inviscid flow, J. Fluid Mech., 14, 257.

FFOWCS WILLIAMS, J.E. & O'SHEA, S. 1970. Sound generation by hydrodynamic sources near a cavitated line vortex, J.Fluid Mech., 43, 675.

FINK, P.T. & SOH, W.K., 1974. Calculation of vortex sheets in unsteady flow and applications in ship hydrodynamics. Proc. 10th Symp. Nav. Hydrodyn. Cambridge, Mass., 463.

FOHL, T. & TURNER, J.S. 1975. Colliding vortex rings. Phys. Fluids, 18, 433.

FRAENKEL, L.E., 1970. On steady vortex rings of small cross-section in an ideal fluid. Proc. Roy. Soc. A316, 29.

GOLDSTEIN, S. 1938. Modern Developments in Fluid Dynamics, I, Dover, New York.

KIRCHOFF, G. 1876. Mehanik, Leipzig.

KOKSHAYSKY, N.V. Tracing the wake of a flying bird. Nature, 279, No. 5709, 146.

LAMB, H. 1932. Hydrodynamics, Dover, New York.

LEONARD, A. 1974. Numerical simulation of interacting, three-dimensional vortex filaments. Proc. of the 4th Int. Conf. Num. Meth. Fluid Dyn., 245. Berlin:Springer.

LIGHTHILL, M.J. 1956. The image system of a vortex element in a rigid sphere. Proc. Camb. Phil. Soc., 52, 317.

MANGLER, K.W., 1952. Improper integrals in theoretical aerodynamics. Aero Re. Coun., CP No. 94.

MOORE, D.W. & SAFFMAN, P.G., 1971. Structure of a line vortex in an imposed strain. Aircraft Wake Turbulence, ed. Olsen, J.H., Goldberg, A., Rogers, M., p.339, New York: Plenum.

MOORE, D.W. & SAFFMAN, P.G., 1972. The motion of a vortex filament with axial flow. Philos. Trans. R. Soc. London. Ser. A272, 403.

MOORE, D.W., 1972. Finite amplitude waves on aircraft trailing vortices. Aeronaut. Q., 23, 307.

MOORE, D.W. & GRIFFITH-JONES, R. 1974. The stability of an expanding circular vortex sheet. Mathematika 21, 128.

MOORE, D.W. 1976. The stability of an evolving two-dimensional vortex sheet. Mathematika 23, 35.

MOORE, D.W. (referred to as (M)) 1978. The equation of motion of a vortex layer of small thickness. Stud. Appl. Math., 58, 119.

MUSHKELISHVILI, N.I., 1953. Singular Integral Equations. Erven P. Nordhoff, NV, Gronigen, Netherlands.

NORBURY, J., 1973. A family of steady vortex rings. J. Fluid Mech., 57, 417.

OLVER, F.W.J., 1961. Proc. Camb. Phil. Soc., 57, 790.

PULLIN, D.I. 1978. The large-scale structure of unsteady self-similar rolled-up vortex sheets. J. Fluid Mech. 88, 401.

RAYLEIGH, LORD. 1896. On the stability or instability of certain fluid motions. In "Scientific Papers", Vol. 3, Camb. Univ. Press, London.

RAYNER, J.M.V. 1979. A vortex theory of animal flight. Part 2. J. Fluid Mech., 91, 731.

ROSENHEAD, L. 1930. The spread of vorticity in the wake behind a cylinder. Proc. R. Soc. A, 127, 590.

SAFFMAN, P.G. 1970. The velocity of viscous vortex rings. Stud. App. Math., 49, 371.

SAFFMAN, P.G. 1974. The structure and decay of trailing vortices. Arch. Mech., 26, 423.

SAFFMAN, P.G. 1978. The number of waves on unstable vortex rings. J. Fluid Mech., 84, 625.

SAFFMAN , P.G. & BAKER, 1979. Vortex interactions. Ann. Rev. Fluid Mech., 11, 95.

SALLET, D.W. 1975. Impulsive motion of a circular disk which causes a vortex ring. Phys. Fluids, 18, 109.

SALLET, D.W. & WIDEMAYER, R.S. 1974. An experimental investigation of laminar and turbulent vortex rings in air, Z. Flugwiss, 22, 207.

SHEFFIELD, J.S. 1977. Trajectories of an ideal vortex pair near an orifice. Phys. Fluids, 20, 543.

TAYLOR, G.I. 1953. Formation of a vortex ring by giving an impulse to a circular disc and then dissolving it away. J. Appl. Phys., 24, 104.

WEISS, P. 1944. On hydrodynamical images. Arbitrary irrotational flow disturbed by a sphere. Proc. Camb. Phil. Soc., 40, 259.

WIDNALL, S.E. & SULLIVAN, J.P. 1973. On the stability of a thin vortex ring of constant vorticity. Proc. R. Soc. London. A322, 335.

WIDNALL, S.E. & TSAI, C.Y. 1977. The instability of a thin vortex ring of constant vorticity. Philos. Trans. R. Soc. London. Ser A287, 273.

ZAKHAROV, S.B. 1977. The stability of plane vortex sheets in ideal fluid. Fluid Mech. -Soviet Research, 6 (2), 1.